The role of xanthophores in the stripe pattern formation of Zebrafish, *Danio rerio*

Dissertation

der Mathematisch-Naturwissenschaftlichen Fakultät

der Eberhard Karls Universität Tübingen

zur Erlangung des Grades eines

Doktors der Naturwissenschaften

(Dr. rer. nat.)

Vorgelegt Von

Prateek Mahalwar

Aus Meerut

(Indien)

Tübingen

2016

Gedruckt mit Genehmigung der Mathematisch - Naturwissenschaftlichen Fakultät
der Eberhard Karls Universität Tübingen.

Tag der Mündlichen Qualifikation: 06:12:2016

Dekan:	Prof. Dr. Wolfgang Rosenstiel
1. Berichterstatter	Prof. Dr. Christiane Nüsslein-Volhard
2. Berichterstatter	Prof. Dr. Alfred Nordheim

To my family & friends

Contents

Abstract

Animals have evolved a fascinating diversity in their color patterns, which serves as an essential component of their survival strategies. Color pattern formation in zebrafish (*Danio rerio*) is a great model system to study general pattern formation involving different cell types. The conspicuous pattern of alternating blue and yellow/silver stripes displayed by adult zebrafish is composed of three kinds of pigment cells - black melanophores, yellow xanthophores, and silvery iridophores. It is known that almost all vertebrate pigment cells originate during early embryogenesis from the neural crest, a vertebrate-specific transient population of multipotent migratory cells giving rise to the peripheral nervous system, some craniofacial structures, pigment cells and others. Mutants specifically lacking one class of pigments cells show that color pattern formation in zebrafish requires interactions among all three kinds of pigment cells. Uncovering the origin and behaviors of these individual cell types is of great interest for researchers studying the mechanism of color pattern formation in zebrafish. In particular, very little is known about the origin, role and behavior of xanthophores during the process.

By employing genetic tools, such as the Cre-LoxP and the Gal4-UAS system, in combination with high-resolution live imaging techniques, I examined the cellular identity of the progenitor cells during metamorphic stages of development. The analysis of pigment cell dynamics during stripe pattern formation *in vivo* had led to the discovery of several novelties about xanthophores. Firstly, with the help of genetic cell ablation and long term imaging of clonal xanthophores, I confirmed the notion of a dual cellular origin of adult xanthophores: while most adult xanthophores originate from existing larval xanthophores, others come from multipotent postembryonic progenitors. Secondly, xanthophores are the first cells to cover the entire skin during metamorphosis, and iridophores and melanophores induce local reorganizations of xanthophores. Xanthophores disperse in response to melanophores in the dark stripe regions, whereas they compact their shapes and densely cover the metamorphic iridophores in the light stripe regions. These local cellular reorganizations of xanthophores, repulsion by

melanophores, and attraction by iridophores, lead to a sharpening and coloration of the striped pattern.

Lastly, I explored the *in vivo* mechanisms of these xanthophore behaviors, and found that local, heterotypic interactions with dense iridophores regulated xanthophore cell shape transition and density in the light stripe. Genetic analysis revealed a cell-autonomous requirement of gap junctions composed of Cx41.8 and Cx39.4 in xanthophores for an iridophore-dependent cell shape transition and increase in density. Initial melanophore-xanthophore interactions are independent of these gap junctions; however, they are subsequently required to induce the stellate shapes of xanthophores in the dark stripes. In conclusion, the color pattern formation in zebrafish involves a novel mechanism of patterning, dependent on cell shape transitions of xanthophores and iridophores. These shape transitions are dependent on local cell-cell interactions, and are mediated by gap junctions. This analysis of stripe pattern formation gives us an insight into the origins and interactions of diverse cell-types in a genetically tractable vertebrate system.

Zusammenfassung

Im Tierreich ist durch die Evolution eine faszinierende Vielzahl von Farbmustern mit großer Bedeutung für die Überlebensstrategien der verschiedenen Arten entstanden. Die Bildung des Farbmusters beim Zebrafisch (*Danio rerio*) stellt ein hervorragendes Modellsystem dar zur Untersuchung von Musterbildungsprozessen, an denen mehrere Zelltypen beteiligt sind. Das auffällige Farbmuster aus dunkelblauen und gelblich/silbernen Längsstreifen, das ausgewachsene Zebrafische aufweisen, wird von drei verschiedenen Typen von Pigmentzellen gebildet schwarzen Melanophoren, gelben Xanthophoren und silbernen Iridophoren. Es ist bekannt, dass fast alle Pigmentzellen bei Wirbeltieren von der Neuralleiste abstammen. Bei der Neuralleiste handelt es sich um eine Wirbeltier-spezifische transiente Population von Zellen, die sich im Embryo verteilen und zu unterschiedlichen Geweben beitragen, z.B. zum peripheren Nervensystem, zu Knochen und Knorpeln im Kopfbereich oder zur Pigmentierung. Zebrafischmutanten, bei denen spezifisch eine Klasse von Pigmentzellen fehlt, haben gezeigt, dass für die Musterbildung alle drei Typen von Zellen miteinander interagieren müssen. Ein detaillierteres Wissen über die Herkunft und die zellulären Verhaltensweisen der Pigmentzellen ist von großem Interesse für Forscher, die den Mechanismus der Pigmentmusterbildung beim Zebrafisch untersuchen. Insbesondere über den Ursprung, die Rolle und das Verhalten der Xanthophoren in dem Prozess der Musterbildung ist bislang recht wenig bekannt.

Mit Hilfe moderner genetischer Methoden, wie dem Cre-LoxP und dem GAL4-UAS System, und hoch-auflösender 4D-Mikroskopie an lebenden Objekten habe ich das Zellverhalten während der sogenannten Metamorphose, dem Entwicklungszeitraum, in dem das Streifenmuster entsteht, untersucht. Die *in vivo* Analyse des Verhaltens der Pigmentzellen während der Streifenbildung führte zu neuen Erkenntnissen über die Xanthophoren. Zuerst konnte durch Zell-Ablationsexperimente und Langzeitbeobachtungen der duale Ursprung der Xanthophoren bestätigt werden: Während die meisten adulten Xanthophoren sich direkt aus larvalen Xanthophoren entwickeln, stammen andere von postembryonalen multipotenten Vorläuferzellen ab. Außerdem konnte ich zeigen,

dass Xanthophoren die ersten Pigmentzellen sind, die während der Metamorphose die gesamte Oberfläche bedecken; sie werden anschließend lokal von Iridophoren und Melanophoren in ihrem Verhalten beeinflusst: in den dunklen Streifen, als Antwort auf die Anwesenheit von Melanophoren, verteilen sich die Xanthophoren, während sie in den hellen Streifen, über den dichten Iridophoren, kompakter werden. Diese lokalen Veränderungen der Xanthophoren, die Abstoßung durch Melanophoren und die Anziehung durch Iridophoren, führen dazu, dass das Pigmentmuster schärfer und kontrastreicher wird.

Zum Schluss habe ich den *in vivo*-Mechanismus untersucht, der das Verhalten der Xanthophoren steuert; dabei konnte ich zeigen, dass lokale, heterotypische Interaktionen mit den dichten Iridophoren in den hellen Streifen sowohl die Zellformveränderungen der Xanthophoren als auch ihre Packung bestimmen. Weiterführende genetische Untersuchungen zeigten, dass Gap Junctions aus Cx41.8 und Cx39.4 zellautonom in den Xanthophoren benötigt werden, damit diese Iridophoren-abhängig ihre Zellform und –Packung verändern können. Die anfänglichen Interaktionen zwischen Melanophoren und Xanthophoren sind unabhängig von diesen Gap Junctions; später werden sie jedoch auch hier gebraucht, damit die Xanthophoren ihre für die dunklen Streifen charakteristische sternförmige Gestalt annehmen können. Zusammenfassend lässt sich sagen, dass es sich bei der Bildung des Pigmentierungsmusters beim Zebrafisch um einen neuen Mechanismus der Musterbildung handelt, der auf Zellformveränderungen bei Xanthophoren und Iridophoren basiert. Diese zellulären Verhaltensweisen beruhen auf lokalen Zell-Zell-Interaktionen, die durch Gap Junctions vermittelt werden. Diese Untersuchungen zur Pigmentmusterbildung beim Zebrafisch erlauben einen Einblick in den Ursprung und die Interaktionen von mehreren verschiedenen Zelltypen, und dies in einem Wirbeltier, das sehr gut genetisch untersucht werden kann.

List of publications in the thesis

Mahalwar, P., Walderich, B., Singh, A. P. and Nüsslein-Volhard, C. (2014). Local reorganization of xanthophores fine-tunes and colors the striped pattern of zebrafish. *Science*

Walderich, B., Singh, A. P., **Mahalwar, P.** and Nüsslein-Volhard, C. (2016). Homotypic cell competition regulates proliferation and tiling of zebrafish pigment cells during colour pattern formation. *Nature Communication*

Mahalwar, P. [#]**,** Singh, A.P., Nüsslein-Volhard, C. and Irion, U. [#] (2016). Connexin-mediated organization of xanthophores in zebrafish light stripes. *Development, Biology Open*

Singh, A.P., Dinwiddie, A., **Mahalwar, P.**, Schach, U., Linker, C., Irion, U. and Nüsslein-Volhard, C. (2016) Pigment cell progenitors in zebrafish remain multipotent through metamorphosis. *Developmental Cell*

Corresponding author

CHAPTER 1

Introduction

1.1 Evolution of color pattern

In this world many natural aspects show an innate beauty, including the natural variation in skin color patterns of various species in the animal kingdom. Well known examples include white and bold black stripes of zebra, flatfish that can change coloration on the upper side of their body to blend into the surrounding environment, *Melanitis* butterflies that are pigmented only one half of their body and even alter their appearance. This great variation, and the ease of observing it, has attracted the attention of researchers for many years. In the past few decades, our understanding of the formation of color pattern in model and non-model organisms has advanced via the use of genetics, molecular and cell biological approaches. However, basic underlying questions remain elusive, what is the function of these color patterns and how are they formed*?* Interestingly, many animals employ these conspicuous external features, which are ethologically relevant with respect to concealment, warning of toxicity, mimicry, sexual selection, thermoregulation and salinity tolerance (Roulin, 2004). Moreover, one of the important aspects of animal social behaviour is kin recognition that allows individuals to respond adaptively to the presence of genetic relatives, with familiarity and phenotype matching being the most common mechanisms (Hamilton, 1964). Color patterning might play a role in kin recognition, whereby kin evokes remembrance of early interactions in life on the basis of differing color pattern and other characteristics (Spence et al., 2008). In particular, cave animals may not have the adaptive functions mentioned above, for example the loss of pigmentation in *Astyanax mexicanus* (cavefish), where pigmentation cannot provide typical functions like UV protection, concealment

from predators and mate choice. However, one of the theories for pigmentation loss is non-selective advantage because of the dark environment (Culver, 1982). All of these possible functions give us some ideas of the evolutionary prospects underlying the great diversity in coloration and patterning in the animal kingdom. Recent developments of genetic and molecular biology tools have made it possible to move beyond observation and approach answers to these questions including: how are these variable color patterns formed? What genes are playing a major role in the development of color patterning? What is the cellular identity of pigment cells? What type of mutations cause phenotypic changes?

Model- and non-model organisms have been used for many years to study coloration differences. Genetic methods like selective breeding were used in China for more than thousand years ago to generate different coat colors of goldfish. In the past several years extensive work on coloration has been performed on various model species including the fly *Drosophila melanogaster* (Wittkopp et al., 2003), the mouse *Mus musculus* (Bennett and Lamoreux, 2003), and the zebrafish *Danio rerio* (Irion et al., 2016). Large-scale mutagenesis screens identified several genes and pathways in color pattern formation. Different animals use different strategies for generating color patterns. In *D. melanogaster*, epidermal cells produce and secrete pigments giving brown color to its body and black bristles generating dark abdominal stripes. Mice color pattern is produced with the help of dorsal-root ganglion-derived melanocytes and a further genetic switch between eumelanin and phaeomelanin, whereas in basal vertebrates like zebrafish, color pattern is produced by the combination of several chromatophores: black melanophores, silvery iridophores and yellow xanthophores.

1.2 **Neural-crest and pigment cells**

The neural-crest (NC) is a population of multipotent cells and a source of a large variety of vertebrate innovations (Gans and Northcutt, 1983). NC cells are induced at the border between the epidermis and the neural plate of a developing embryo. In accordance with their anterior-posterior position within an embryo the NC can be subdivided into 5 major populations: cranial, trunk, cardiac, vagal and sacral NC (Hall, 2009). Neural-crest cells are considered to be multipotent cells,

and after being specified they delaminate from the neural tube and migrate through the whole organism, differentiating in a wide variety of the cell types, including skin pigment cells, cartilage cells, neurons, adrenal gland, heart, glial cells (Green et al., 2015). The NC-derived pigment cells are ancestrally diverse within amphibians, fish and reptiles (Kelsh, 2004). Majorly three model systems, chick, mouse, and zebrafish, have been used to study the basics of the molecular mechanism underlying the pigment cell lineage specification from NC in vertebrates. This development of NC shows an evolutionarily highly conserved pattern (Noden, 1983). The mechanism for pigment pattern formation exclusively produced by melanocytes in chick and mouse is quite simple compared to the zebrafish, in which it is generated by a combination of three different cell types, melanophores, iridophores and xanthophores. In mouse and chick, NC cells that migrate in the space between the somites and the neural tube (ventral pathway) give rise to neuronal and glial cells, whereas those that migrate between the somite and the non-neural ectoderm (dorsolateral pathway) differentiate into pigment cells – melanocytes. In zebrafish, the migratory pathways of these three cell types are differentially regulated and this contributes, in part, to their pigment pattern. Thus, iridoblasts utilize predominantly the medial pathway, xanthoblasts migrate on and spread out within the lateral migration pathway and melanoblasts migrate on both the ventral and lateral pathways. In the past few years the mechanism how these pigments cells form color pattern in zebrafish has become a model system to study the problem of general pattern formation (Kelsh et al, 2004)

1.3 Zebrafish as color pattern model system

Zebrafish as a model system has been established in the last 25 years as an organism for vertebrate development, most notably by researchers in Eugene (Oregon, USA), Tübingen (Germany), and Boston (USA). The major advantage of the zebrafish as a model organism is the combined application of embryological methods; e.g. transplantation of cells, *in-vivo* observations are easy to perform, as zebrafish embryos are very robust and cell movements can be monitored due to a total transparency of embryos (Westerfield et al, 1999). Several large-scale mutagenesis screens using the chemical mutagen N–ethyl-N-nitrosourea (ENU) and extensive screening for developmental defects have been

performed (Driever et al., 1996; Haffter et al., 1996b). These screens can be done efficiently, as zebrafish embryos can be obtained in large numbers, have a rather short generation time of three months and adult fish are maintained in relatively small facilities (Haffter et al., 1996a). Moreover, gain-of-function and transient gene knockdown analysis can be efficiently performed by mRNA overexpression and injection of antisense morpholino oligonucleotides, respectively (Nasevicius et al, 2000). Furthermore, due to the transparency of zebrafish embryos, expression analysis by *in situ* hybridization and cell tracing using transgenic fluorescent reporter lines can be performed. Most importantly, in zebrafish, novel genes controlling functionally important developmental processes can be identified and functionally characterized.

1.4. Color pattern formation in larva and adult zebrafish

1.4.1. Larval pattern

Zebrafish have not just one, but two pigment cell patterns, an early larval pigment pattern and a subsequent adult or post-metamorphic pattern. Early larval pigment patterns among fishes and even amphibians are highly conserved as compared to the variable ones of the adults. However, the initial mechanism for pigment cell progenitors migrating away from the neural tube is conserved between all vertebrates (Kelsh et al, 2004). However, the cellular and molecular underpinnings of lineage specification of the different zebrafish pigment cell types from pigment cell progenitors and their interactions with the extracellular environment before adopting the specific lineage are incompletely understood. Large-scale mutagenesis screens in zebrafish have yielded important information about the variety of genes that are involved in development of each of the three pigment cell types. For example, *mitfA* (*nacre* mutant) is essential for melanophore development and is expressed by melanophore precursors well before overt differentiation (Lister et al., 1999). NC cell lineage analyses in chick and mouse have indicated that the initial specification of distinct sub-lineages may come considerably before the initial expression of identified marker genes that are expressed in a sub-lineage-specific manner (Henion and Weston, 1997). Pigment cells in the zebrafish embryo and early larva have lineages distinct from pigment cells in the adult.

1.4.2. The metamorphic and adult pattern

By replacing a much simpler larval pattern, the zebrafish acquires a striking stereotypic pattern of four to five longitudinal dark stripes and four light stripes during metamorphosis - a period between approximately 3 and 6 weeks of development (Kelsh, 2004). The dark stripes consist of melanophores covered by a thin layer of iridophores and xanthophores; whereas light stripes are composed of iridophores covered by xanthophores. The metamorphic and adult pigment cells arise from a pigment progenitor population that can be recognized in the larval-to-adult transition and identified as connected with the peripheral nervous system. Iridophores and melanophores originate from a small set of stem cells located at the segmentally reiterated dorsal-root ganglia, but the origin of adult xanthophores had remained unknown until recently (Budi et al., 2011; Dooley et al., 2013; Singh et al., 2014). The regenerative capacity for pigment cells is likely to be explained by the persistence of pigment progenitor cells into adulthood. The dorsal-root ganglion association of pigment cell progenitors (Dooley et al., 2013) suggested the question whether all adult pigment cells arise from these progenitor cells. Although it had been suggested that adult xanthophores are derived from a different cell type, none of the pigment cell studies had been able to identify the origin of adult xanthophores.

At the onset of metamorphosis, iridophores appear in the skin at the region of the horizontal myoseptum that serves as a morphological prepattern (Frohnhöfer et al., 2013). The first light stripe is formed at the horizontal myoseptum by dense iridophores, whereas at the margins of the first light stripes, dense iridophores switch shape and spread dorsally and ventrally as loose iridophores in the skin of the juvenile fish by proliferation and migration. These two morphologically distinct shapes of iridophores, dense iridophores in light stripes and loose blue iridophores in dark stripes, are clonally related (Singh et al., 2014). Melanoblasts migrate along spinal nerves into the skin in the presumptive dark stripe regions, where they differentiate and expand in size to form the compact dark stripes (Budi et al., 2011; Dooley et al., 2013; Singh et al., 2014).

Mutants lacking one of the pigment cell types – the *nacre/mitfA* mutant lacks melanophores (Lister et al., 1999), the *pfeffer/csf1rA* mutant lacks adult

xanthophores (Parichy et al., 2000b), and the *shady/ltk, rose/ednrb1b*, and *transparent/mpv17* mutants have absent or strongly reduced iridophores (Krauss et al., 2014; Lopes et al., 2008; Parichy et al., 2000a) form an irregular residual striped pattern (Frohnhöfer et al. 2013). These genes are autonomously required in the respective cell types indicating that interactions among all three chromatophore types are necessary to generate the zebrafish striped pattern (Maderspacher and Nüsslein-Volhard, 2003; Parichy and Turner, 2003). Furthermore, analysis of single and double mutants missing one or two of the three cell types have revealed that iridophores play a leading role in stripe formation and interactions between all the three pigment cell types are absolutely necessary for emergence of the final striped colouration (Frohnhöfer et al., 2013; Irion et al., 2014a). Iridophores promote and sustain melanophores at a distance; furthermore, iridophores attract xanthophores, whereas between xanthophores and melanophores long-range activation and short-range inhibition has been observed (Frohnhöfer et al., 2013; Hirata et al., 2005). In the striped anal and tail fins, only melanophores and xanthophores participate in stripe formation indicating that the mechanisms of stripe formation in the trunk skin and the fins differ; mutants lacking iridophores form normal stripes in the fins (Singh et al., 2014; Patterson et al., 2014; Parichy et al., 2003). In adult *pfeffer* mutants, a number of stripes and interstripes, although irregular, are discernible in the body but not in the fins. The melanophore stripes break up into spots, dense iridophore regions invade the stripes, further ectopic melanophores are observed in the interstripe regions giving an irregular appearance to the blue and white spotted pattern. However, iridophores form a normal first interstripe in *pfeffer* mutants and melanophores appear in comparable numbers in the stripe region indicating that basic stripe formation is independent of xanthophores (Singh et al., 2014). *In vitro* studies of fin-derived pigment cells have suggested that xanthophores repel melanophores in a run-and-chase-manner leading to melanophore aggregation and thereby stripe pattern formation (Inaba et al., 2012). These and previous studies based on pattern regeneration and modelling proposed that xanthophores and melanophores act as 'diffusible factors' in a Turing-type self-organization model. According to this model, differences in the cell movement of melanophores and xanthophores during their contact-based interactions would lead to a striped organization of pigment cells (Nakamasu et al., 2009;

Yamaguchi et al., 2007; Yamanaka and Kondo, 2014). These models may hold for patterning in the fins but not for the body, as they are neither compatible with the *pfeffer* mutant phenotype nor do they take iridophores into account, a cell type which has been shown to be crucial for trunk stripe pattern formation (Frohnhöfer et al., 2013; Maderspacher and Nüsslein-Volhard, 2003; Singh et al., 2015). Therefore, one of the main goals of this thesis is to examine xanthophore behaviour *in vivo* to understand their role in colour pattern formation.

Mutants in which all chromatophore types are present, but in which stripe formation is impaired, indicates that the communication or interaction between the chromatophores might be affected. The genes identified in such mutants encode integral membrane proteins, for example, Seurat/Igsf11, a cell-adhesion molecule of the immunoglobulin superfamily (Eom et al., 2012), Obelix/Kir7.1, a rectifying potassium channel (Iwashita et al., 2006), and Dali/Tetraspanin 3c, a transmembrane-scaffolding protein (Inoue et al., 2014). *Leopard* (*leo*) is the best-known example from this class of mutants, where the stripes are broken up into a series of dark spots. Originally, it had been considered a separate *Danio* species (Frankel, 1979; Kirschbaum, 1975; Kirschbaum, 1977). Subsequently, several dominant alleles were identified in *Danio rerio* (Haffter et al., 1996a), and further, it has been shown that the *leo* phenotype is caused by a mutation in connexin 41.8 (Watanabe et al., 2006), which codes for a gap junction subunit.

1.5. Gap Junctions and zebrafish pigment pattern

Gap junctions are intercellular channels that allow the passage of small molecules and ions between neighbouring cells, and thus are responsible for their chemical and electrical coupling (Kar et al., 2012). They are formed by the juxtaposition of two hemi-channels (connexons), composed of six connexin subunits, in adjacent cells (Unwin and Zampighi, 1980). Connexins are integral membrane proteins with four transmembrane domains, two extracellular loops, one intracellular loop, and intracellular N- and C-termini (Milks et al., 1988). Hemi-channels can take multiple forms depending on the connexin expression pattern of the cell type. Hemi-channels made from a single connexin protein are termed homomeric. Mixtures of two or more connexins in a single hemi-channel are heteromeric. Apposing homomeric connexons are homotypic junctions and

apposing heteromeric connexons are heterotypic junctions. In addition to the subunit composition, gap junction conductivity is regulated by a number of different factors, for example, by the intracellular levels of Ca^{2+}, by polyamines, by the membrane potential, or by phosphorylation (Thevenin et al., 2013).

It has been reported that the function of the *leo* gene is required in two of the chromatophore types, the melanophores and the xanthophores, for homotypic and heterotypic cellular interactions (Maderspacher and Nüsslein-Volhard, 2003). The mutant forms of Cx41.8 artificially expressed in wild-type melanophores can lead to different variations of the stripe pattern (Watanabe and Kondo, 2012). This suggested that gap junctions are responsible for some of the short-range signals occurring within or between chromatophore types (Parichy and Turner, 2003; Inaba et al., 2012; Frohnhöfer et al., 2013).

Several alleles of *leopard* have been described so far. These alleles show a range of phenotypes from irregular, wavy and occasionally interrupted stripes over rows of spots to a complete loss of the pigment pattern, where isolated melanophores remain dispersed on a uniform background of dense iridophores and xanthophores. In one of the recessive *leo* allele, leo^{t1}, a spotted phenotype is due to the premature stop codon in Cx41.8 (Watanabe et al., 2006). A recent ENU mutagenesis screen has identified two dominant alleles of *luc*, encoding another connexin, Cx39.4, and loss-of-function of *luc* leads to a phenotype very similar to that of leo^{t1}. The loss of both connexins results in a stronger phenotype as compare to the one seen in homozygous mutants for the dominant alleles of *leo* or *luc* (Irion et al., 2015). However, the presence of spots and wavy irregular stripes suggest that there is still some patterning activity present leading to the phenotype. Other dominant alleles, leo^{tq270} and leo^{tw28}, are missense mutations leading to a much stronger phenotype (Haffter et al., 1996; Watanabe et al., 2006). The dominant phenotype of these alleles led to the suggestion that heterotypic as well as homotypic connexons containing Cx41.8 could be involved in pigment patterning, postulating the existence of other connexin partner(s) in the potential heterotypic channels (Watanabe et al., 2006). The homozygous leo^{tK3} phenotype is much stronger than other *leo* alleles, indicating that the mutant Cx41.8 protein present in leo^{tK3} cells has a dominant negative effect on some further component(s) involved in pigment pattern formation (Irion et al.,

2015, Maderspacher and Nusslein-Volhard, 2003). Altogether, analysis of *leo* mutants led to suggestions of models of a functional gap junction in the formation of the pigment pattern, where another connexin is involved in the formation of heteromeric gap junctions together with Cx41.8 (Watanabe et al., 2006, Irion et al., 2015). However, the roles of gap junctions in the mechanisms of interactions between different chromatophores remain unexplored. One of the goals of the thesis is to further understand the role of gap junctions in pigment pattern formation.

CHAPTER 2

Results

Publication 1

Mahalwar P, Walderich B, Singh AP, Nüsslein-Volhard C (2014). **Local reorganization of xanthophores fine-tunes and colors the striped pattern of zebrafish**. ***Science***, 345:1362-1364

Synopsis

The zebrafish owes its name to a striking stereotypic pattern of longitudinal dark and light stripes that develop over the duration of several weeks replacing a much simpler larval pattern. Long developmental time-windows, increasing body sizes, and limited imaging possibilities make it technically challenging to study the cell-cell interactions leading to the formation of an adult color pattern in vertebrates. As a result, a large body of work in vertebrate color patterning has focused on theoretical models (Kondo and Miura, 2010). These models suggest that adult zebrafish striping involves Turing-type reaction-diffusion interactions between xanthophores and melanophores. This paradigm is based on stripe regeneration experiments, as well as observed interactions between isolated pigment cells *in vitro*. The Turing-like models predict that xanthophores appear in the skin after melanophores, and induce melanophore aggregation into stripes by repelling them in a run-and-chase manner; importantly however, this work neither includes the third pigment cell type, iridophores, nor discusses the possibility of its role in stripe formation (Nakamasu et al., 2009; Takahashi and Kondo, 2008; Yamaguchi et al., 2007; Yamanaka and Kondo, 2014). Thus, *in vivo*

developmental analyses of all three cell types in wild-type zebrafish were required to uncover the process of stripe pattern formation. While long-term *in vivo* analysis of iridophores and melanophores had provided us with an improved and more comprehensive picture of their distinct cellular behaviors (Dooley et al., 2013; Frohnhöfer et al., 2013; Singh et al., 2014), the origin, organization, and cellular behavior of xanthophores remained unclear.

In order to observe xanthophores during stripe pattern formation *in vivo*, I used several combinations of transgenic lines that labeled xanthophores by expressing fluorescent proteins under the control of two promoters: NC-specific *sox10* and xanthophores-specific *fms*. These transgenes were previously shown to label xanthophores (Gray et al., 2011; Mongera et al., 2013).

In the first experiments, *fms*-positive cells were traced along the dorsal side of early zebrafish embryos (at 24 hpf). This *in-vivo* tracking confirmed the NC origin of xanthophores. It also showed that NC-derived xanthoblasts divide while traveling along the dorsolateral path during NC migration, and differentiate into larval xanthophores, which spread over the larval skin forming the simple larval pattern. Genetic lineage tracing, using the Cre-loxP system as well as transplantation experiments, further revealed that most of the metamorphic xanthophores arise from these larval NC-derived xanthophores.

My observations of the arrangement of xanthophores in the adult skin did not only confirmed the presence of xanthophores in the dark stripes (Hirata et al., 2003), but also showed that the organization of xanthophores, in terms of their cell shape and density, is different in the dark and light stripes. Xanthophores that are associated with the light stripe region are densely packed, expanded, have small filopodial protrusions, and display a bright orange pigment. In contrast, xanthophores in the dark stripe region display a net-like and loose organization. They are arborized, have long filopodial protrusions, and display faint yellow pigment.

Finally, to reveal the behavior of individual cells in stripe pattern formation, I used *Tg(sox10:Cre)* with the reporter line *Tg(UBI:loxp-EGFP-loxp-mCherry)*. Fish with patchy reporter labeling of xanthophore clusters were selected for long-term imaging to follow individual xanthophores. These experiments showed that

xanthophores are the first pigment cell type to cover the skin at the onset of metamorphosis, and that they undergo differential cellular reorganization depending on their location (dark or light stripes) along the adult trunk. My work led to the discovery of several xanthophore behaviors that were previously unknown:

1) There is no global reorganization of xanthophores.

2) Xanthophores locally proliferate.

3) Xanthophores have long filopodial extensions.

4) Short-scale movements of xanthophores sharpen the stripe-interstripe boundary.

5) When xanthophore and iridophores interact, xanthophores acquire a compact morphology; they retract their long filopodial projections and intensify their pigmentation.

6) Xanthophores repulse early melanophores.

7) Later, xanthophores rearrange themselves with the appearance of more melanophores in the dark stripes and spread out into a stellate shape with faint pigmentation.

8) When xanthophores and xanthophores interact, they create a net-like structure.

This study provides us with an improved understanding of xanthophore behaviors. In combination with previous pigment cell behavior studies (Frohnhöfer et al., 2013; Singh et al., 2014), it provides us with a more comprehensive picture of pigment cell interactions and their roles in the formation of the beautifully colored and striped adult zebrafish pattern.

Local reorganization of xanthophores fine-tunes and colors the striped pattern of zebrafish
Prateek Mahalwar, Brigitte Walderich, Ajeet Pratap Singh and Christiane Nüsslein-Volhard (August 28, 2014)
Science **345** (6202), 1362-1364. [doi: 10.1126/science.1254837]
originally published online August 28, 2014

Editor's Summary

Origin of fish pigment cell for pattern

Zebrafish stripes arise from the interactions of pigment cells: black melanophores, iridescent iridophores, and yellow-orange xanthophores. Melanophores and iridophores develop from nerve-associated stem cells, but the origin of xanthophores is unclear. Two studies now reveal that adult xanthophores originate from xanthophores in embryonic and larval fish, when they proliferate to cover the skin before the arrival of black and silver cells in a striped arrangement. Mahalwar *et al.* show that xanthophores change their final shape and color depending on their location. In black cells, xanthophores appear faint and stellate, but in silver cells, they are bright and compact. Precise superposition creates the blue and golden colors. McMenamin *et al.* observe the loss of pigment in embryonic xanthophores and the later reappearance in the adult. They show that redifferentiation depends on the thyroid hormone that also limits melanophore population expansion.

Science, this issue p. 1362 and p. 1358

Science (print ISSN 0036-8075; online ISSN 1095-9203) is published weekly, except the last week in December, by the American Association for the Advancement of Science, 1200 New York Avenue NW, Washington, DC 20005.

FISH PIGMENTATION

Local reorganization of xanthophores fine-tunes and colors the striped pattern of zebrafish

Prateek Mahalwar, Brigitte Walderich, Ajeet Pratap Singh,* Christiane Nüsslein-Volhard*

The pattern of alternating blue and golden stripes displayed by adult zebrafish is composed of three kinds of pigment cells: black melanophores, yellow xanthophores, and silvery-blue iridophores. We analyzed the dynamics of xanthophores during stripe morphogenesis in vivo with long-term time-lapse imaging. Larval xanthophores start to proliferate at the onset of metamorphosis and give rise to adult xanthophores covering the flank before the arrival of stem-cell–derived iridophores and melanophores. Xanthophores compact to densely cover the iridophores forming the interstripe, and they acquire a loose stellate shape over the melanophores in the stripes. Thus, xanthophores, attracted by iridophores and repelling melanophores, sharpen and color the pattern. Variations on these cell behaviors may contribute to the generation of color pattern diversity in fish.

Many animals have evolved diversity in their color patterns, which serve as an essential component of their survival strategy. Replacing a much simpler larval pattern (Fig. 1, A and B), the zebrafish acquires a stereotypic pattern of four to five longitudinal dark stripes and four light interstripes (Fig. 1C) during the metamorphic period [20 to 45 days postfertilization (dpf)]. The stripes consist of melanophores covered by a thin layer of iridophores and xanthophores, whereas interstripes are composed of iridophores covered by xanthophores (*1*–*4*). Iridophores come in two morphologically distinct shapes that are clonally related: dense iridophores in interstripes and loose blue iridophores in stripes. The first light interstripe is formed by dense iridophores emerging along the horizontal myoseptum that serves as a morphological prepattern (*3*). At the margins of the first interstripe, iridophores switch shape and spread dorsally and ventrally as loose iridophores in the skin of the juvenile fish by proliferation and migration. They form a coherent net of cells covering the flank of the fish and generate additional light stripes at a distance from the horizontal myoseptum by patterned aggregation into dense iridophores (*5*). Melanoblasts emerge at their future position between these interstripes along peripheral neurons innervating the skin; they differentiate and expand in size to form the compact dark stripes (*5*–*7*). Thus, the dark and light stripes are formed by different cellular routes. Xanthophores are thinly distributed over the dark stripes and densely cover the iridophores in light stripes giving them a yellow tinge (*1*, *2*, *4*). Adult iridophores and melanophores originate from a small set of stem cells located at the segmentally reiterated dorsal root ganglia (*5*, *7*), but the origin of adult xanthophores has remained unknown.

Analysis of mutants lacking one or two of the three pigment cell types has revealed that interactions between all the three cell types are absolutely necessary for emergence of the final striped coloration (*3*, *8*). Iridophores play a leading role in stripe formation and mutants lacking iridophores do not add stripes to a basic pattern, whereas mutants lacking xanthophores (*pfeffer/fms/csf1a*) or melanophores (*nacre/mitfa*) exhibit a residual striped pattern, albeit an irregular one (fig. S1) (*3*, *8*–*10*). *pfeffer* (*pfe*) encodes *csf1a/fms* that is expressed and required specifically in xanthophores (*3*, *8*, *11*, *12*). In adult *pfe* mutants, a number of stripes and interstripes, although irregular, are discernible: The

Max-Planck-Institut für Entwicklungsbiologie, Tübingen, Germany.
*Corresponding author. E-mail: ajeet.singh@tuebingen.mpg.de (A.P.S.); christiane.nuesslein-volhard@tuebingen.mpg.de (C.N.-V.)

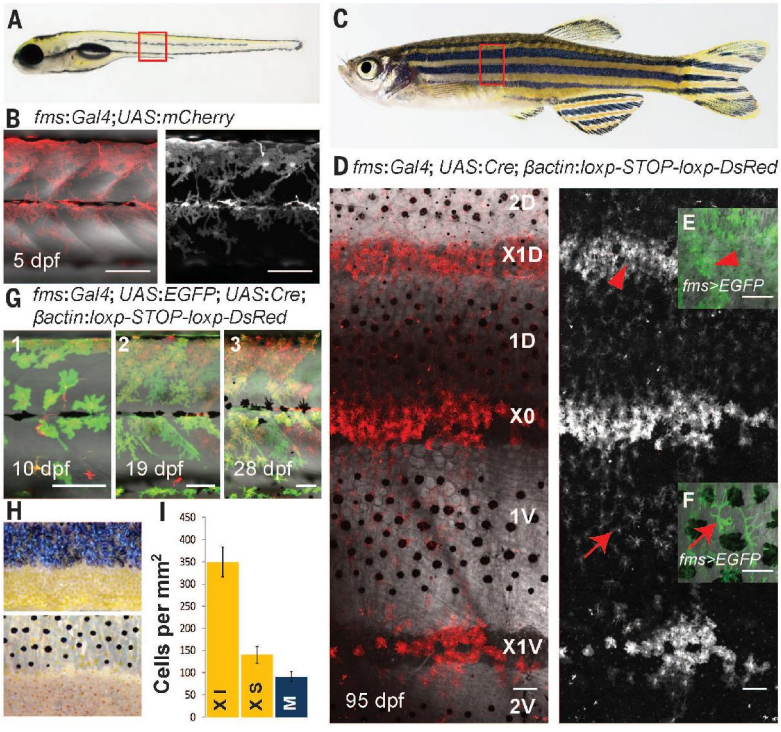

Fig. 1. Distribution of xanthophores in larval, metamorphic, and adult zebrafish. Pigmentation pattern and xanthophores of the (**A** and **B**) larva and (**C** and **D**) adult. Arrowhead, dense interstripe xanthophores; arrow, loose stripe xanthophores. Red boxes in (A) and (C) indicate approximate areas highlighted in (B) and (D), respectively. (**E** and **F**) Xanthophores at higher magnifications. EGFP, enhanced green fluorescent protein. (**G**, 1 to 3) Continuous development of xanthophores from larval to postmetamorphic stages. (**H**) Normal (top) and epinephrine-treated (bottom) zebrafish adult skin. (**I**) Density of interstripe xanthophores (XI), stripe xanthophores (XS), and melanophores (M) in adult zebrafish. Error bars denote SD. Scale bars, 100 μm.

melanophore stripes break up into spots; dense iridophore regions invade the stripes; and further, ectopic melanophores are observed in the interstripe regions. Introduction of xanthophore progenitor cells into *pfe* mutant embryos by blastomere transplantations restores a normal pattern indicating the importance of xanthophores in stripe sharpening and coloration (*8*, *11*). We examined xanthophore origin and behavior in vivo to establish their role in color pattern formation.

We used *Tg(fms:Gal4.VP16)* (*13*) in combination with appropriate UAS-reporter lines or *Tg(Pax7:GFP)* (GFP, green fluorescent protein) (see supplementary materials and methods) to label xanthophores from larval stages throughout metamorphosis (Fig. 1). Labeled cells were identified on the dorsal side of the embryo at ~24 hours postfertilization (movie S1). These cells migrate while dividing along the dorsolateral path of neural crest migration, differentiate into xanthophores and spread over the larval skin, ventrally decreasing in density (*1*) (Fig. 1, A and B). The larva at 5 dpf displays six to eight xanthophores per segment. In the adult fish, xanthophores are distributed over the stripes and interstripes all along the skin (Fig. 1, C and D). The xanthophores associated with the interstripe region were densely packed, expanded, possessed small filopodial protrusions, and displayed bright orange pigment (arrowheads in Fig. 1, D, E, and H, and fig. S2). In contrast, xanthophores in the stripe region displayed a netlike, loose organization; they were arborized, had long filopodial protrusions, and displayed faint yellow pigment (arrows in Fig. 1, D, F, H, and fig. S2). Xanthophore density was ~2.5 times higher in the interstripe region as compared with the stripe region (Fig. 1I and fig. S2). This indicates two distinct types of xanthophores: (i) compact and bright in the interstripes and (ii) stellate and faint in the stripes.

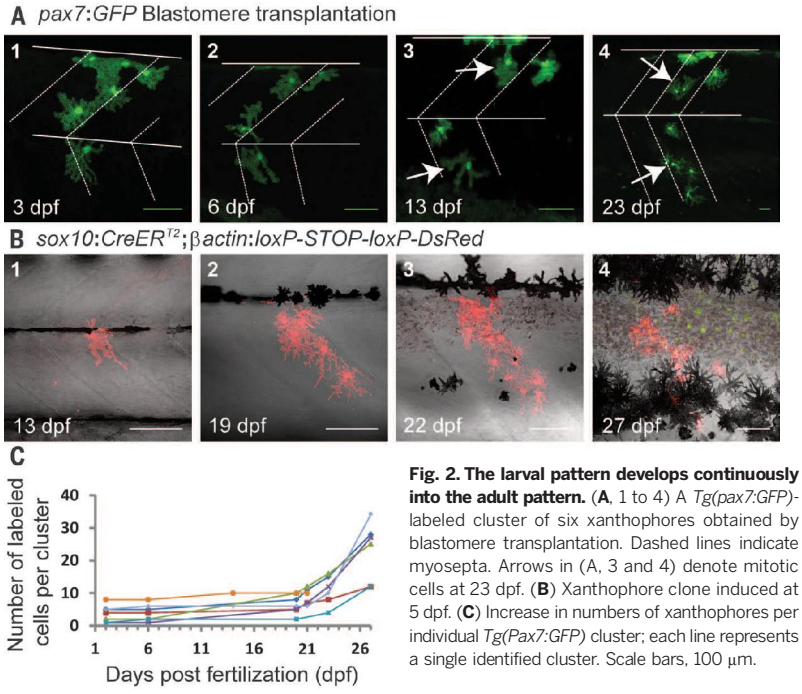

Fig. 2. The larval pattern develops continuously into the adult pattern. (**A**, 1 to 4) A *Tg(pax7:GFP)*-labeled cluster of six xanthophores obtained by blastomere transplantation. Dashed lines indicate myosepta. Arrows in (A, 3 and 4) denote mitotic cells at 23 dpf. (**B**) Xanthophore clone induced at 5 dpf. (**C**) Increase in numbers of xanthophores per individual *Tg(Pax7:GFP)* cluster; each line represents a single identified cluster. Scale bars, 100 μm.

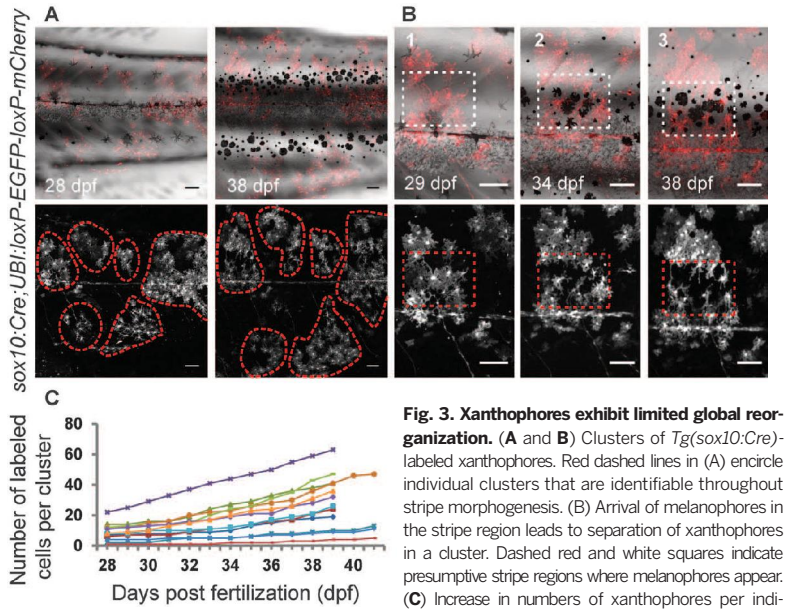

Fig. 3. Xanthophores exhibit limited global reorganization. (**A** and **B**) Clusters of *Tg(sox10:Cre)*-labeled xanthophores. Red dashed lines in (A) encircle individual clusters that are identifiable throughout stripe morphogenesis. (B) Arrival of melanophores in the stripe region leads to separation of xanthophores in a cluster. Dashed red and white squares indicate presumptive stripe regions where melanophores appear. (**C**) Increase in numbers of xanthophores per individual *Tg(sox10:Cre)*-labeled cluster; each line represents a single identified cluster. Scale bars, 100 μm.

Time-course analysis of xanthophores revealed that the larval xanthophores persisted, increased in number at the onset of metamorphosis, and finally covered the entire dorsolateral skin (Fig. 1G). To obtain labeled clusters of xanthophores for lineage analysis, we transplanted cells of *Tg(pax7:GFP)* embryos into wild-type hosts at the blastula stage (Fig. 2A). The xanthophore number remained constant until the onset of metamorphosis (~16 to 20 dpf), when xanthophores begin to divide and increase in number continuously with a doubling time of about 1 week (five fish, seven clusters of xanthophores) (Fig. 2C). Second, we analyzed xanthophore clones induced in *Tg(sox10:ER^{T2}-Cre)* larvae in which tamoxifen-inducible Cre was expressed under the *sox10* promoter (*14*). DsRed-labeled larval xanthophores in such clones gave rise to metamorphic xanthophores (six clones) (Fig. 2B). In contrast to previous studies (*10*, *15*), our in vivo analysis suggests that xanthophores, albeit barely visible by pigment content, are the first pigment cell type to cover the trunk skin before the appearance of metamorphic iridophores and melanophores (Figs. 1G and 2B and figs. S3 and S4).

We further analyzed the behavior of clusters (coherent groups of clones) of labeled xanthophores in *Tg(sox10:Cre)* (*16*) individuals throughout metamorphosis (Fig. 3A and fig. S5). The xanthophore clusters maintained their relative positions during the formation of the stripes and interstripes, whereas numbers of xanthophores in each cluster continuously increased throughout metamorphosis (Fig. 3C and fig. S6) by proliferation (fig. S7). Thus, there is no global reorganization of xanthophores during stripe morphogenesis (fig. S9). However, arrival of the iridophores during metamorphosis lead to a compaction of the overlaying xanthophores (fig. S4). Furthermore, upon arrival of melanophores in the stripe region, the xanthophores underwent

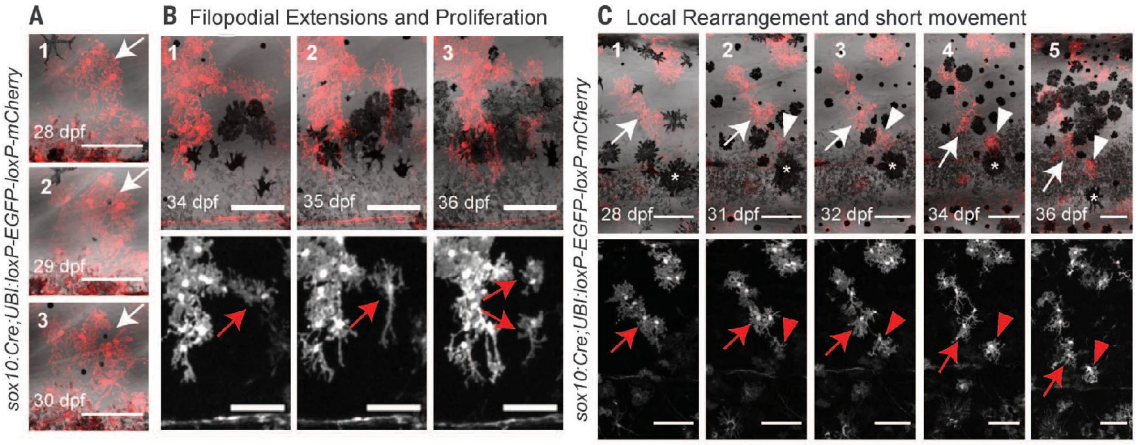

Fig. 4. Context-dependent changes in xanthophore behavior during stripe pattern formation. Time-lapse imaging of labeled xanthophores during metamorphosis. (**A**, 1-3) Xanthophores present in the presumptive stripe region give space (arrows) to an arriving melanophore. (**B**, 1-3) A xanthophore near the stripe-interstripe boundary extends filopodial protrusions (arrows) directed toward the interstripe and undergoes cell division. (**C**, 1-5) A xanthophore (arrows) locally reorganizes upon arrival of melanophores in the stripe region. Arrowheads indicate short movement of the xanthophore into the interstripe region. Asterisks indicate a melanophore that moves away from the interstripe upon encountering a xanthophore (arrowheads). Scale bars, 100 μm.

local rearrangement to accommodate the increasing number of melanophores (Figs. 3B and 4). Over the period of metamorphosis, more melanophores appeared in the skin and expanded, forming a compact stripe (*5*). This resulted in cellular reorganization and separation of the xanthophores and a decrease in xanthophore density (Figs. 1, D to I, and 3B and fig. S6B). Xanthophores of the stripe region reorganized their filopodia to give way to melanophores that appeared in their vicinity (Fig. 4A). The xanthophores spread out and became stellate with long filopodial extensions (arrows in Fig. 4, B and C) forming a netlike organization in the stripe region (figs. S8 and S9).

Xanthophores at the boundary of the developing stripes and interstripes often exhibited filopodial extensions directed toward the interstripe region, leading to cell division followed by integration of the proximal xanthophore into the interstripe (arrows in Fig. 4B) or a short-scale movement of the xanthophore into the interstripe region (arrowheads in Fig. 4C, and fig. S10). Limited local proliferation and context-specific local reorganization was the most prominent behavior exhibited by xanthophores (Fig. 4C). This is in contrast to iridophores, which exhibit extensive local proliferation combined with long-range dispersal along the dorsoventral axis and prefigure the stripe organization by patterned aggregation (*5*). Genetic analyses have indicated a role for xanthophores in sustaining melanophore numbers but also in sharpening the stripe-interstripe boundary by mutual repulsion (*3*, *8*, *11*). Xanthophores present in the first interstripe take part in elimination of the larval lateral stripe melanophores, as well as metamorphic melanophores that get trapped in the interstripe. In contrast, the stellate xanthophores of the stripes might be required for survival of melanophores and for compact stripe formation and maintenance. In summary, we found that the striped organization of pigment cells involves proliferation, local rearrangements, and short-scale movements of xanthophores in the skin of the fish.

Our observations do not support Turing-type models in their current form, which assume that stripe formation starts with a random distribution of melanophores and xanthophores that sort out by repulsion and attraction involving extensive cell movements (*15*, *17*–*19*). These models may hold for patterning in the fins [however, see (*20*)] but would require substantial modification for the body stripes to accommodate the cellular behaviors of xanthophores and melanophores observed in the present study, the *pfe* mutant phenotype, and the involvement of iridophores (*3*, *5*, *8*). Long-term imaging indicates that stripe melanophores barely move, whereas xanthophore movement is restricted to the boundary region between stripe and interstripe. The interactions between all the three kinds of pigment cells and their environment are crucial for stripe pattern formation (*3*, *8*, *10*). Xanthophores play a permissive role in the formation of the striped pattern by covering the skin of metamorphic fish, into which metamorphic iridophores and melanophores get integrated (schematic in fig. S11). The striped pattern is achieved by context-dependent cell shape changes occurring in both iridophores and xanthophores, which switch between loose and dense shapes. In both cases, the two forms are clonally related and depend on local cell-to-cell interactions. Melanophores in the stripes exist in only one shape. The precise superposition of the dense form of iridophores and xanthophores in the interstripe and the loose iridophores and xanthophores superimposed over the stripe melanophores produces a marked contrast between the golden and blue coloration of the pattern.

REFERENCES AND NOTES

1. R. N. Kelsh, *Pigment Cell Res.* **17**, 326–336 (2004).
2. M. Hirata, K. Nakamura, T. Kanemaru, Y. Shibata, S. Kondo, *Dev. Dyn.* **227**, 497–503 (2003).
3. H. G. Frohnhöfer, J. Krauss, H. M. Maischein, C. Nüsslein-Volhard, *Development* **140**, 2997–3007 (2013).
4. M. Hirata, K. Nakamura, S. Kondo, *Dev. Dyn.* **234**, 293–300 (2005).
5. A. P. Singh, U. Schach, C. Nüsslein-Volhard, *Nat. Cell Biol.* **16**, 607–614 (2014).
6. E. H. Budi, L. B. Patterson, D. M. Parichy, *PLOS Genet.* **7**, e1002044 (2011).
7. C. M. Dooley, A. Mongera, B. Walderich, C. Nüsslein-Volhard, *Development* **140**, 1003–1013 (2013).
8. F. Maderspacher, C. Nüsslein-Volhard, *Development* **130**, 3447–3457 (2003).
9. J. Krauss, P. Astrinidis, H. G. Frohnhöfer, B. Walderich, C. Nüsslein-Volhard, *Biol. Open* **2**, 703–710 (2013).
10. L. B. Patterson, D. M. Parichy, *PLOS Genet.* **9**, e1003561 (2013).
11. D. M. Parichy, J. M. Turner, *Development* **130**, 817–833 (2003).
12. D. M. Parichy, D. G. Ransom, B. Paw, L. I. Zon, S. L. Johnson, *Development* **127**, 3031–3044 (2000).
13. C. Gray *et al.*, *Thromb. Haemost.* **105**, 811–819 (2011).
14. A. Mongera *et al.*, *Development* **140**, 916–925 (2013).
15. G. Takahashi, S. Kondo, *Pigment Cell Melanoma Res.* **21**, 677–686 (2008).
16. F. S. Rodrigues, G. Doughton, B. Yang, R. N. Kelsh, *Genesis* **50**, 750–757 (2012).
17. M. Yamaguchi, E. Yoshimoto, S. Kondo, *Proc. Natl. Acad. Sci. U.S.A.* **104**, 4790–4793 (2007).
18. A. Nakamasu, G. Takahashi, A. Kanbe, S. Kondo, *Proc. Natl. Acad. Sci. U.S.A.* **106**, 8429–8434 (2009).
19. H. Yamanaka, S. Kondo, *Proc. Natl. Acad. Sci. U.S.A.* **111**, 1867–1872 (2014).
20. T. E. Woolley, P. K. Maini, E. A. Gaffney, *Pigment Cell Melanoma Res.* 10.1111/pcmr.12276 (2014).

ACKNOWLEDGMENTS

We thank A. Mongera and S. Alsheimer for providing transgenic lines before publication; U. Irion, C. Söllner, and P. Müller for comments on the manuscript; and S. Perathoner, H.-G. Frohnhöfer, A. Fadeev, U. Schach, H. Heth, and our fish facility, as well as C. Liebig and our light microscopy facility, for support. This work was funded by the Max-Planck Society. A.P.S. received a postdoctoral fellowship (EMBO-LTF) from the European Molecular Biology Organization.

SUPPLEMENTARY MATERIALS

www.sciencemag.org/content/345/6202/1362/suppl/DC1
Materials and Methods
Figs. S1 to S11
References (*21*–*31*)
Movie S1

15 April 2014; accepted 6 August 2014
Published online 28 August 2014;
10.1126/science.1254837

Publication 2

Walderich B, Singh AP, **Mahalwar P**, Nüsslein-Volhard C (2016). **Homotypic cell competition regulates proliferation and tiling of Zebrafish pigment cells during color pattern formation**. **Nature communications**, 1038/11462.

Synopsis

The striped pattern of adult zebrafish is composed of three types of pigment cells: melanophores, iridophores and xanthophores that are all arranged in superimposed layers in the skin. Recent studies, using long-term imaging, have shown that color pattern formation in zebrafish involves interactions between the different pigment cell types that will lead to migration and morphological changes of the cells (Mahalwar et al., 2014; Singh et al., 2014). *In vivo* analysis of both pigment pattern mutants, as well as chimeras generated between wild-type fish and mutants lacking one of the three cell types, emphasized the interactions among different pigment cell types (heterotypic interactions) in pattern formation (Maderspacher and Nüsslein-Volhard, 2003). *In vitro* observations of isolated pigment cells also found an interaction response between two different pigment cell types, melanophores and xanthophores (Inaba et al., 2012). However, neither of these studies uncovered any obvious interaction between cells of same type (homotypic interactions). Although genetic studies have indicated that there are homotypic interactions between pigment cells, very little was known about them (Maderspacher et al. 2003).

Therefore, in order to gain insight into the role of homotypic cell interactions in pigment pattern formation, labeled pigment cell progenitors (xanthophores - *pax7:GFP*, iridophores and melanophores - *TDL358:GFP; sox10:mRFP*) were introduced into mutants lacking a given cell type by blastomere transplantations in the early embryo. The fluorescently labelled cells were then followed via long-term *in vivo* imaging in larvae, and clones were followed-up through

metamorphosis. In all three cell types, we observed an increase in the rate of proliferation in the absence of endogenous cells. These results show us that the rate of pigment cell proliferation is likely controlled by competition between pigment cells of the same kind, and that the dorso-ventral spreading of chromatophores during stripe formation is a result of homotypic interactions.

To obtain more information on the regeneration and autonomous spreading behavior of iridophores and melanophores, drug-inhibition of the ErbB pathway in embryos carrying *Tg(sox10:mRFP)* were performed. Depletion of the ErbB pathway by a specific drug (PD168393) inhibits the formation of melanophore and iridophore stem cells leading to a large gap of these respective cells in the stripe region. mRFP-positive iridophores and melanophores were observed that had regenerated and were spreading to fill-in the large gaps. Interestingly, the iridophores and melanophores filled in the gaps with different dynamics. During spreading, chromatophores remain together, forming coherent sheets with normal density and spacing, rather than dispersing into regions devoid of the respective cell type. To test homotypic interactions in xanthophores, we performed genetic ablation experiments on larval xanthophores using nitroreductase-mediated cell ablation in *Tg(fms:gal4; UAS:nfsB-mCherry)* embryos. Segmental regeneration of xanthophores was observed in the follow-up of the ablated fish. The adult fish displayed a normal striped pattern, which indicated that xanthophores had fully recovered and spread across the skin. This observation supports the notion that in addition to the origin from larval xanthophores, adult xanthophores can also result from multipotent stem cells (Singh et al, 2014, 2016). Taken together, these findings suggest that there are contact-mediated (homotypic) interactions controlling the expansion and tiling of pigment cells. In all cases, donor-derived chromatophores locally restored the organization of the host chromatophores, which resulted in a normal pattern. In conclusion, this study showed that pigment cell proliferation and dispersal in the skin are predominantly regulated by homotypic competition, whereas changes in pigment cell morphologies during stripe formation are predominantly regulated by heterotypic interactions. These results provide crucial information, not only on a mechanistic level, but also for the formulation of mathematical models that describe the process of stripe pattern formation.

nature COMMUNICATIONS

ARTICLE

Received 9 Sep 2015 | Accepted 30 Mar 2016 | Published 27 Apr 2016

DOI: 10.1038/ncomms11462 OPEN

Homotypic cell competition regulates proliferation and tiling of zebrafish pigment cells during colour pattern formation

Brigitte Walderich[1], Ajeet Pratap Singh[1], Prateek Mahalwar[1] & Christiane Nüsslein-Volhard[1]

The adult striped pattern of zebrafish is composed of melanophores, iridophores and xanthophores arranged in superimposed layers in the skin. Previous studies have revealed that the assembly of pigment cells into stripes involves heterotypic interactions between all three chromatophore types. Here we investigate the role of homotypic interactions between cells of the same chromatophore type. Introduction of labelled progenitors into mutants lacking the corresponding cell type allowed us to define the impact of competitive interactions via long-term *in vivo* imaging. In the absence of endogenous cells, transplanted iridophores and xanthophores show an increased rate of proliferation and spread as a coherent net into vacant space. By contrast, melanophores have a limited capacity to spread in the skin even in the absence of competing endogenous cells. Our study reveals a key role for homotypic competitive interactions in determining number, direction of migration and individual spacing of cells within chromatophore populations.

[1] Max Planck Institute for Developmental Biology, Spemannstrasse 35, 72076 Tübingen, Germany. Correspondence and requests for materials should be addressed to C.N.-V. (email: christiane.nuesslein-volhard@tuebingen.mpg.de).

Colour patterns are widespread in the animal kingdom and not only protect against harmful radiation, but also serve as recognition signals in intra- and interspecies communication. The zebrafish, *Danio rerio*, has emerged as the vertebrate model organism to study the mechanisms underlying colour pattern formation[1–4]. The characteristic pattern of alternating horizontal dark and light stripes represents a system of three different pigment-cell types distributed in superimposed layers in the skin. In the dark stripes, black melanophores are covered by a middle layer of blue iridophores and a thin top layer of yellow xanthophores. In the light stripes, a compact layer of xanthophores covers silvery iridophores.

The adult pigmentation pattern is formed during metamorphosis, a period between ~3 and 6 weeks of development. Iridophores and melanophores are derived from stem cells located at the segmentally reiterated dorsal root ganglia (DRG) of the peripheral nervous system[5–7]. Iridophores emerge in the skin along the horizontal myoseptum; they proliferate and spread as densely connected cells forming the first light stripe. They spread further, dorsally and ventrally, as a loose net of cells into the regions where the dark stripes will form and then again undergo patterned aggregation to form new light stripes[5]. Melanoblasts migrate and proliferate along the peripheral neurons innervating the skin and emerge *in situ* in the skin where they differentiate and expand to fill in the dark stripes[5–7]. Most adult xanthophores arise from larval xanthophores, which begin to divide at the onset of metamorphosis and cover the entire body of the fish[8,9].

While each pigment-cell type is distributed in a single cell wide layer, xanthophores and iridophores display different morphologies depending on their position in the pattern: in the dark stripes stellate xanthophores form a net-like structure and loose iridophores appear blue, whereas densely packed, silvery iridophores are tightly associated with compact xanthophores in the light stripes[8,10–12]. The establishment of organized cell morphologies indicates close cell–cell communication between skin layers, and is essential for the sharpness and brightness of the striped pattern.

Mutants lacking one or more of the pigment-cell types are not able to produce the striped pattern correctly (for example, *nacre* (encoding Mitfa) mutants that lack melanophores, *pfeffer*/*fms* (encoding Csf1rA) mutants that lack xanthophores, and *shady* (encoding Ltk), *rose* (encoding Ednrb1Ba) and *transparent* (encoding Mpv17) mutants where iridophores are absent or strongly reduced)[13–17]. In all these cases the two remaining chromatophore types form an irregular, residual striped pattern. Supplementing the missing cell type in chimeric animals obtained by blastula transplantations can locally restore a normal pattern[12,17,18]. This indicates that heterotypic interactions between the three cell types are required to form a normal pattern. Analyses of mutants lacking one of the pigment-cell types, as well as ablation experiments, have suggested the presence of several attractive and repulsive signals between chromatophores, which act over long or short ranges during stripe formation[12,19,20]. In the absence of xanthophores, melanophore numbers are reduced, stripes break up into spots, and ectopic melanophores remain scattered in the light stripe region. In iridophore mutants, the number of melanophores is also strongly reduced, and only the first two dark stripes form broken into spots[5,12]. In the absence of two pigment-cell types, remaining iridophores (in *nacre*; *pfeffer* mutants) and xanthophores (in *shady*; *pfeffer*) cover the flank of the fish, whereas the melanophores in the absence of iridophores and xanthophores (*shady*; *pfeffer*) are reduced in number and scattered in lower than normal density[12]. These observations indicate a strong dependence of melanophore survival on interactions with the other cell types, whereas iridophores and xanthophores display a more autonomous behaviour.

Previous analyses of chimeras generated between wild type and mutants lacking one of the three cell types placed emphasis on the interactions among different pigment cells (heterotypic interactions)[12,18]. The role of homotypic interactions (between cells of the same type) remains poorly understood. *In vitro* observations of interactions between isolated pigment cells did not uncover any obvious response between cells of the same type, although an interaction response between melanophores and xanthophores has been detected[21]. Genetic analyses also have suggested that homotypic interactions exist among melanophores and xanthophores[18,22]. Here, we analyse the cell-level outcome of the homotypic interactions among the chromatophores *in vivo* through the generation of chimeric animals, and we corroborate our findings with results from regeneration experiments. We investigate the proliferation and spread of labelled chromatophore clusters in the presence or absence of endogenous cells within a layer. For all pigment-cell types, we observe an increase in the average size of clusters in environments lacking the respective cell type. This indicates that there is competition between pigment cells during normal development. Xanthophores and iridophores have an intrinsic tendency to proliferate and evenly fill the space in the skin, whereas melanophores have only a restricted potential to proliferate and spread in the skin. In addition, our observation that clusters of all three pigment-cell types filled the chromatophore-devoid region in their neighbourhood as coherent nets with normal density (rather than dispersing uniformly into all available vacant space), suggests that there are contact dependent homotypic interactions between chromatophores. In all cases, donor-derived chromatophores locally restored the organization of the host chromatophores, which resulted in a normal pattern. We conclude that, whereas changes in pigment-cell morphologies during stripe formation are regulated by heterotypic interactions[22,23], pigment-cell proliferation and dispersal in the skin are predominantly regulated by homotypic competition.

Results

Blastomere transplantations. We transplanted a small number of blastomeres to obtain single-labelled pigment-cell progenitors in wild type or mutant embryos. Using appropriate markers, we selected chimeric individuals for the presence of small clusters of donor-derived pigment cells at larval stages (5 days post fertilization (dpf)) or at the onset of metamorphosis (21 dpf) and traced their progeny to adulthood. Blastomere transplantations between wild-type embryos resulted in clusters of pigment cells that resemble Cre-induced clones[5] in shape and size, indicating that frequently a single progenitor cell had given rise to the clusters, and that in many cases the clusters were clonal. In experiments that allowed us to follow more than one type of pigment cell it became apparent that in most cases the donor cells gave rise to multipotent neural crest progenitors of all three cell types.

Homotypic interactions among xanthophores. The dynamics of xanthophore morphogenesis during stripe formation has been described previously[8]. To specifically track the xanthophores in normal development, chimeric animals were created by transplantation of cells from transgenic *Tg*(*pax7*:*GFP*)[8,24] blastula stage embryos into wild-type or *albino* hosts (Fig. 1a,d). In *albino* (Fig. 1d) melanophores are unpigmented[25], allowing for better visibility of donor-derived labelled xanthophores and pigmented melanophores. We followed the pattern development of individual

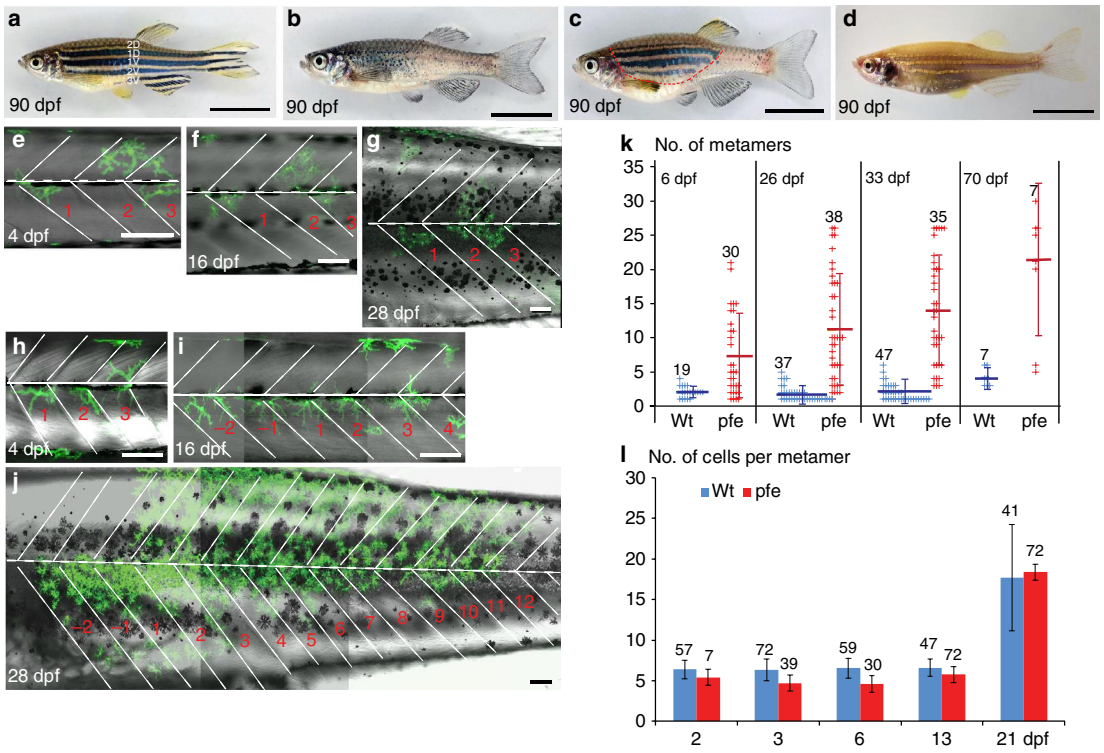

Figure 1 | Development of xanthophore clusters in wild type and *pfeffer*. (**a**–**d**) Stripe pattern in 3-month-old (**a**) wild-type zebrafish, (**b**) *pfeffer* mutant, (**c**) chimera obtained by blastomere transplantation of wild type (*Tg*(*pax7*:*GFP*)) into *pfeffer*; the area with donor xanthophores is demarcated by a red dashed line and (**d**) control (*albino*). In (**a**) the dark stripes nomenclature is depicted along the dorsoventral axis. Developmental profile of *Tg*(*pax7*:*GFP*)-labelled wild-type xanthophores (green) in a (**e**–**g**) control and (**h**–**j**) *pfeffer* chimera. Dashed white lines—vertical and horizontal myosepta. Scale bars, **a**–**d** = 1 cm; **e**–**j** = 100 μm. (**k**) Quantification of the number of metameres spanned by xanthophore clusters at larval stage (6 dpf) (wild type, $n = 19$ clusters, 12 fishes; *pfeffer*, $n = 30$ clusters, 18 fishes; $P \leq 0.0001$); 26 dpf (wild type, $n = 37$ clusters, 10 fishes; *pfeffer*, $n = 38$ clusters, 17 fish; $P \leq 0.0001$); 33 dpf (wild type, $n = 47$ clusters, 10 fishes; *pfeffer*, $n = 35$ clusters, 17 fishes; $P < 0.0001$); 70 dpf (wild type, $n = 7$ clusters, 4 fishes; *pfeffer*, $n = 7$ clusters, 7 fishes; $P = 0.0077$). The horizontal lines in dark blue (wild type) and red (*pfeffer*) indicate the mean value and the error bars represent standard deviation. We show that the differences between *albino* and *pfeffer* are significant at all time points investigated by using Student's *t*-test (Welsh corrected). (**l**) Number of xanthophores per metamere in wild type (blue) and *pfeffer* transplants (red). Numbers of metameres analysed are depicted in the graph, error bars represent standard deviation. No significant differences between wild-type fish (blue) and *pfeffer* transplants (red) according to Student;s *t*-test (Welsh corrected) were found for 2 dpf: $P = 0.1795$ and 21 dpf: $P = 0.6123$. Overall 3 dpf ($P = < 0.0001$), 6 dpf ($P = < 0{,}0001$) and 13 dpf ($P = 0.0042$) were shown to be significantly different.

fish with small clusters of 1–5 xanthophores in larvae (< 5 dpf) from the onset of metamorphosis until 70 dpf ($n = 47$ xanthophore clusters in 12 fishes) (Fig. 1e–g; Supplementary Fig. 1). Numbers of donor-derived xanthophores in the clusters remained constant during larval stages[8]. At the onset of metamorphosis between 16 and 20 dpf, the xanthophores began to divide as did the host xanthophores[8]. Subsequently the clusters spanned over 1–4 adjacent metameres (Fig. 1k) and across several light and dark stripes along the dorsoventral axis (Supplementary Fig. 1). The rate of division was variable between different clusters, averaging about one cell division per 10 days, as was previously observed in non-chimeric fish[8]. Labelled xanthophore clusters consisted of more or less loosely connected cells.

pfeffer mutants lack xanthophores in adults (Fig. 1b)[18]. The introduction of xanthophore progenitors into *pfeffer* hosts can lead to large patches of stripe rescue in chimeric animals indicating that xanthophores have the ability to divide rapidly and to spread into vacant space[18] (Fig. 1c). We analysed xanthophore clusters in chimeras obtained by transplantation of *Tg*(*pax7*:*GFP*) blastomeres into *pfeffer* mutant host embryos. The donor-derived xanthophores, in contrast to xanthophore clusters in wild-type hosts (Fig. 1h–k), already divided during larval stages and occupied larger areas in the skin during metamorphosis. The numbers of segments occupied by xanthophores in *pfeffer* hosts continually increased starting in larval stages (Fig. 1k). The analysis of *pfeffer* chimeras ($n = 38$ clusters of xanthophores in 18 fishes) revealed that the clusters spread on average over 6 metameres during larval stages (by 6 dpf) and by the age of 70 dpf they had spread over 21 metameres (Fig. 1k). Comparing the number of xanthophores per metamere in wild-type fish and *pfeffer* chimeras (Fig. 1l) revealed that the donor-derived xanthophores eventually fully restored the xanthophore number. This indicates that in normal development competition between xanthophores limit their rate of proliferation and spreading. Recently, it has been suggested that xanthophore proliferation and differentiation is triggered by thyroid hormone stimulation at the onset of metamorphosis[9]. Our data indicate that the reduction in xanthophore cell density is the critical cue that alone can trigger xanthophore proliferation.

Closer analysis revealed that the donor-derived xanthophores divided rapidly in the *pfeffer* hosts at a rate of more than two cell divisions per 10 days, and spread in all directions, most commonly along the myosepta both horizontally and vertically (Fig. 2a–c,d,e). The xanthophores at the border of the clusters collectively migrated into neighbouring regions devoid of xanthophores, thus increasing their coverage (Fig. 2d,e). In several cases individual clusters fused and covered the fish completely. When donor xanthophores encountered host iridophores in the light stripe, they changed in shape to become compact (as in wild type) (Fig. 2c). In *pfeffer* mutants, melanophores form small spots; however, when they encountered donor xanthophores, the melanophores increased in number and locally restored the striped pattern through local migration out of the light stripe region and accumulation in the dark stripe region (Fig. 2f–k). Ectopic melanophores in the mutant areas devoid of xanthophores disappeared on arrival and compaction of donor-derived xanthophores (Fig. 2f–k).

Our observations show that donor-derived xanthophores, in the absence of residual xanthophores in *pfeffer* hosts, begin to proliferate during embryonic stages. We confirmed this through live-imaging of xanthophore behaviour in both wild type and *pfeffer* chimeras during late embryogenesis at 48–60 hpf; (Fig. 3; Supplementary Movies 1–3). Xanthophores in wild-type environments extended dynamic filopodia that allowed them to contact and continually probe each other (Fig. 3a–f: filopodial retraction—yellow arrow, filopodial extension—red arrow; Supplementary Movie 1). Similarly, donor-derived xanthophores rarely changed their location or underwent cell division when transplantated into wild-type embryos (Supplementary Movie 2). In contrast, donor xanthophores in *pfeffer* hosts underwent cell divisions (arrowheads in Fig. 3g–l) and extended dynamic filopodia (arrows in Fig. 3g–l) to explore their environment, and they moved into regions devoid of xanthophores (Fig. 3g–l; Supplementary Movie 3).

To test if the absence of xanthophores in *pfeffer* can also influence melanophore spreading, we transplanted wild-type cells labelled with *Tg*(*pax7:GFP*) into *pfeffer*;*brass* mutants, which lack xanthophores and have unpigmented melanophores[26,27]. This allows a clear distinction between donor- and host-derived xanthophores and melanophores. Melanophore clusters did not spread farther than 4 metameres (see below), whereas the xanthophores spread along the anterior–posterior (AP) axis as described above (Fig. 2l). This suggests that the spreading is cell-specific to xanthophores rather than a general property of the *pfeffer* mutation.

These results indicate that the proliferation rate of xanthophores is regulated by competitive homotypic interactions. The xanthophores expand in areas devoid of xanthophores by cell proliferation and by short-scale cell movement. In hosts lacking xanthophores the donor-derived clusters expand in all directions as a coherent net, maintaining normal distances and close contact between cells, rather than dispersing into the space devoid of xanthophores. This indicates mutual interaction and attraction between xanthophores.

Homotypic interactions among melanophores. We analysed the melanophores in normal development using the dark melanin pigmentation, lacking in *albino* recipient fish, as a marker (Fig. 4a). Transplantation of blastomeres labelled with *Tg*(*βact:GFP*) into *albino* hosts yielded 22 melanophore clusters in nine fishes, which were followed into adulthood. Along the AP axis the clusters spread 2–4 segments on average. At the margins of the cluster, the donor-derived black melanophores intermingled with the unpigmented melanophores of the host. Clusters of donor-derived melanophores contributed to several dark stripes along the dorsoventral body axis as described before[6] (Supplementary Fig. 2). Melanophore clusters in a number of cases (7/28) contributed to all four stripes including the scales, and dorsal and anal fins, whereas 16 clusters contributed to between 1–3 stripes at the age of 3 months (Supplementary Fig. 4). Four clusters of melanophores appeared exclusively in the caudal fins of the fish. These observations are consistent with the known behaviour of melanophores and their origin in a wild-type context.

Blastomere transplantation into *nacre*[13] allowed us to track melanophores in the absence of endogenous melanophores (Fig. 4b). A total of 57 clusters of black, donor-derived melanophores were followed in 20 *nacre* fishes up to 3–4 months. As observed in the control (*albino*) chimeras, the donor-derived melanophores contributed to several dark stripes along the dorsoventral body axis (Fig. 4c; Supplementary Fig. 3). In 6 cases out of 57, we found melanophore clones contributing to all four dark stripes as well as pigmentation in scales and anal and dorsal fins. The clusters on the body, although larger than in wild-type chimeras (*albino*; Fig. 4a), remained restricted along the AP body axis, spanning 6 metameres on average (Fig. 4c–e), which is not statistically different from wild-type (*albino*) transplants. As observed previously[12,17,18], in *nacre*, the stripes were completely restored in chimeric areas, with a dense sheet of donor-derived melanophores, strictly separated from light stripe regions (Fig. 4c). Intriguingly, clusters started shrinking after 35 dpf and by 4 months, 64% of all clusters in *albino*, and 33% of the clusters in *nacre* disappeared (Fig. 5, cluster in *nacre*). The reason for the late death of donor melanophores in chimeras is unknown. It suggests that in the chimeras the stem cells providing a regular replacement of melanophores have not been maintained.

In *nacre* transplants, a series of larval melanophores on the ventral (30% of all clusters) and the dorsal side (24% of all clusters) of the fish were frequently observed (Fig. 5a–g). These clusters spanned on average 12 metameres and were present from early larval stages through 35 dpf when they started to disappear (Fig. 4d). Figure 5 shows an example of the development of melanophore clusters, labelled with *Tg*(*TDL358:GFP*; *sox10:mRFP*) in *nacre*. *Tg*(*TDL358:GFP*) labels iridophores, whereas *Tg*(*sox10:RFP*) labels all neural crest-derived tissue. On 13 dpf, streaks of larval melanophores were present both dorsally and ventrally (Fig. 5a), and a confocal scan on the same time point shows the presence of a *sox10:mRFP*-labelled DRG (Fig. 5b). At 27 dpf adult red fluorescent protein (RFP)-labelled melanophores appeared flanking the horizontal myoseptum (Fig. 5c,d), along with donor-derived xanthophore and iridophore clusters (Fig. 5d). At 35 dpf the first dark stripes 1 dorsal (D) and 1 ventral (V) were formed (Fig. 5e). In contrast to the melanophore cluster that spreads over 6 metameres, the xanthophore and iridophores clusters remained restricted to 1–2 metameres (Fig. 5f). On 58 dpf the larval melanophore streaks on the dorsal and the ventral side started to disappear, whereas the melanophores in stripes 1D and 1V persisted (Fig. 5g). At 83 dpf all melanophores have disappeared leaving empty areas between intact light stripes (Fig. 5h).

In summary, we observe that host melanophores have little influence on the dispersal of donor-derived melanophores, and that, in contrast to xanthophores, melanophore clusters in the adult pattern rarely spread laterally over more than six segments. Instead, donor-derived melanophores remain together, and form prominent stripes of normal melanophore density despite being surrounded by regions devoid of melanophores. This indicates that in the absence of residual melanophores, an increased number of melanophores reach the skin, and that melanophores attract each other.

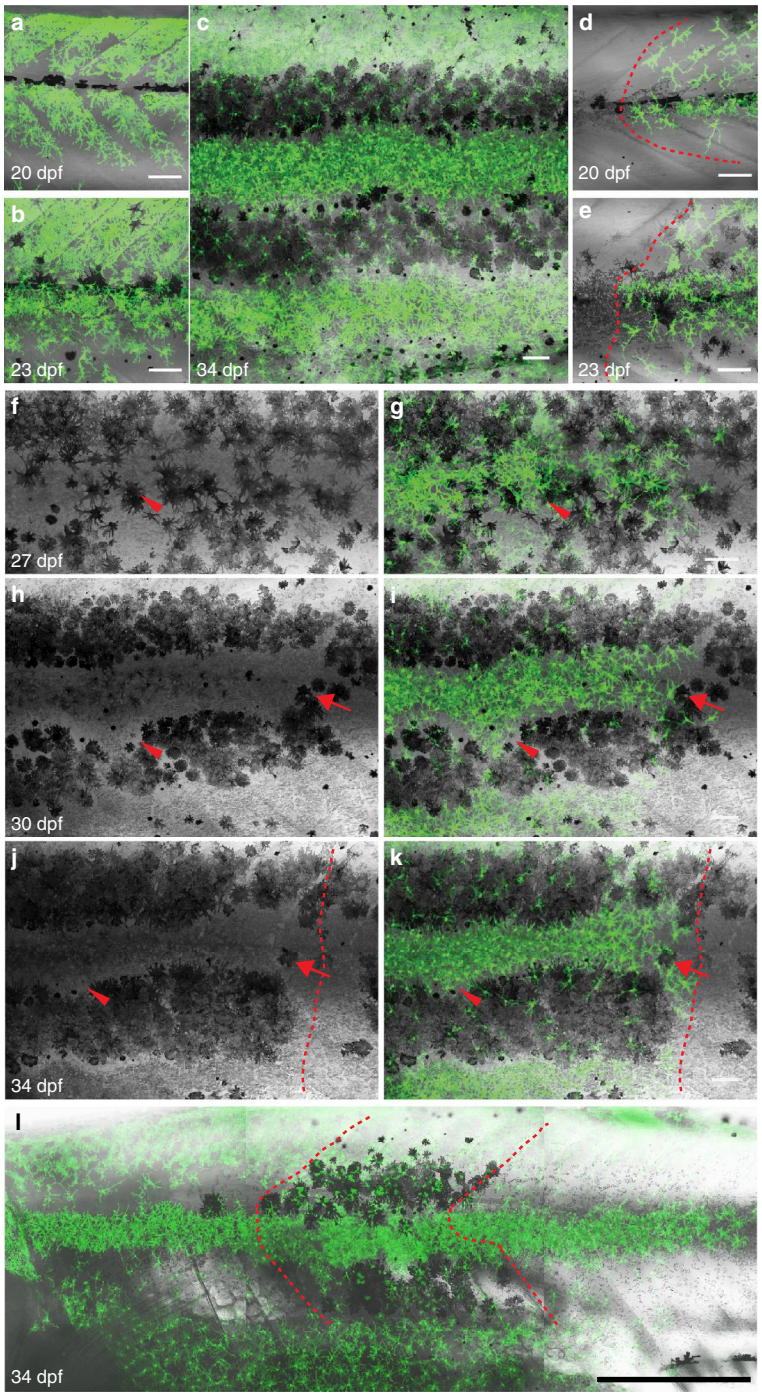

Figure 2 | Local rescue of xanthophore numbers and organization by xanthophores in *pfeffer* hosts. (**a**–**c**) Restoration of normal number and organization of xanthophores in *pfeffer*. (**d**,**e**) Xanthophores spread into neighbouring xanthophore-devoid segments as coherent net. Dashed red line: border of transplanted cluster. (**f**–**k**) Restoration of the striped pattern by interactions between the xanthophore cluster and the host melanophores. (**f**–**k**) Widely distributed melanophores (black) become organized into stripes on increase in number of xanthophores and their compaction in the light stripe region. Red arrow: a cluster of melanophores that is cleared over time; red arrowhead: xanthophores retracting from dark stripe region. Dashed red line: border of the cluster showing xanthophores-positive area with rescued pattern on the left, no rescue on the right. (**l**) Chimera obtained by transplantation of *Tg*(*pax7:GFP*) *into pfeffer;brass*. The xanthophore cluster covers 17 metamers, whereas the melanophores cluster covers 4 metamers. Xanthophores—green, *Tg*(*pax7:GFP*). Dashed red line: border of melanophores cluster. Scale bars, **a**–**k**: 100 μm, **l**: 250 μm.

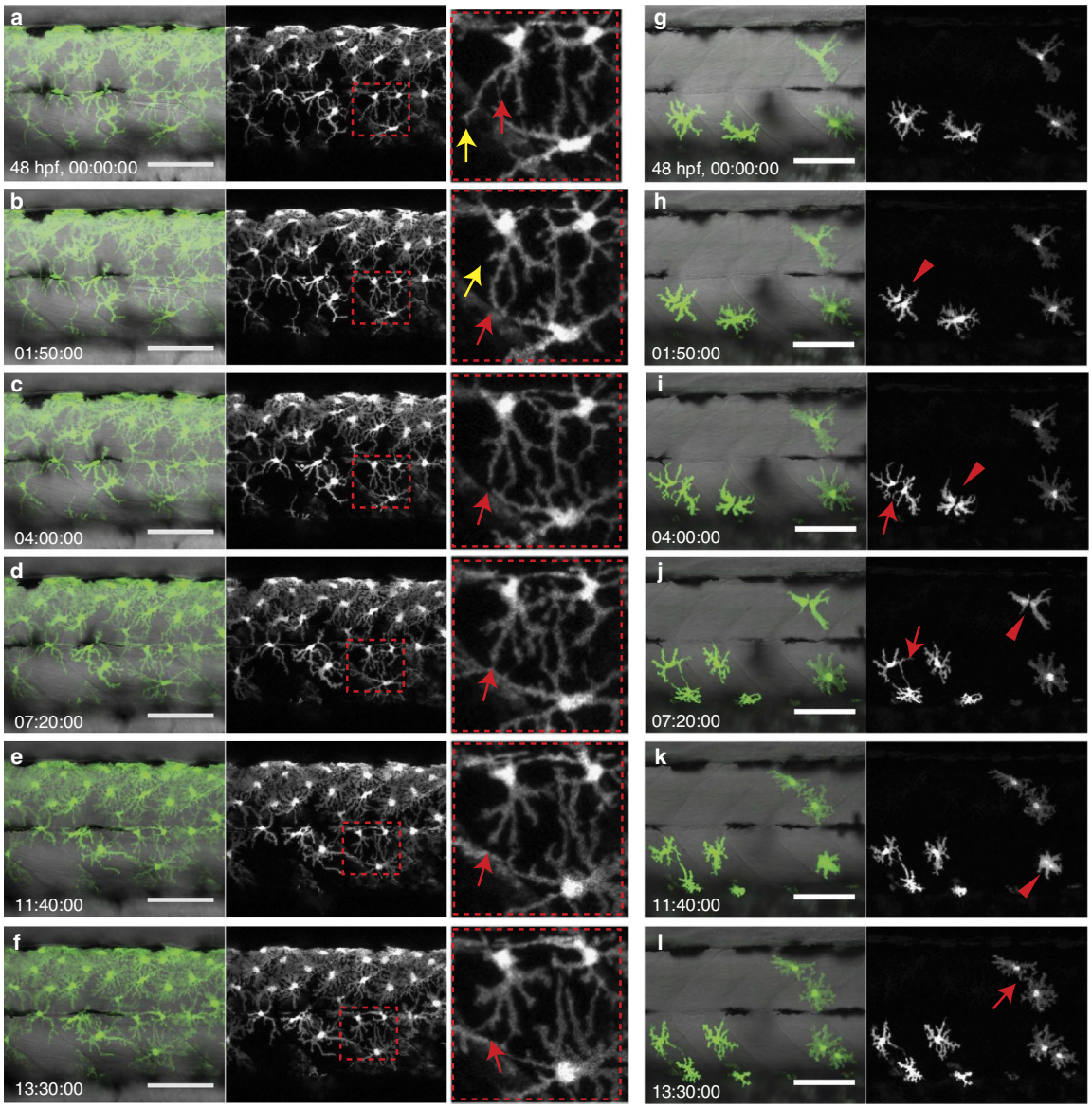

Figure 3 | Interaction of xanthophores in larval stage. (**a**–**f**) Live-imaging of wild-type xanthophores—green; *Tg*(*pax7:GFP*), shows that cell numbers remain constant during larval development. (Same images in grey scale). Magnification of red dotted boxes: dynamic cell-cell contacts occur by extension (red arrows) and retraction (yellow arrows) of filopodia. (**g**–**l**) Live-imaging of xanthophores—green; *Tg*(*pax7:GFP*) in *pfeffer* chimera. Transplanted xanthophores divide, for better visibility same image in grey scale (red arrowheads) and extent filopodia to each other (red arrow). Scale bars, **a**–**l**: 100 µm.

Homotypic interactions among iridophores. The labelling of donor cells with *Tg*(*βact:GFP*) allowed the simultaneous detection of iridophore- and melanophore clusters in chimeric animals in *albino* hosts (Fig. 6a–c). Iridophore clusters displayed a dorsoventral orientation contributing to several light stripes, much like the Cre-induced Sox10 clones previously analysed[5]. In these chimeras progenitors of melanophores as well as iridophores have been transplanted. Transplanting *Tg*(*TDL358:GFP*; *sox10:mRFP*) into wild-type hosts revealed that iridophore clusters begin divisions after the onset of metamorphosis (19–21 dpf). They formed the first light stripe together with the xanthophores (Fig. 6d–g). We followed six clusters through metamorphosis until 40 dpf, showing that the clusters spread over 1–4 metamers and the cell number of the clusters increased from 1–2 cells up to 300 cells within 17 days, which represents a doubling of cell numbers every 3–4 days.

Due to low survival rates of *shady* chimeras, only few clusters of iridophores developing in the *shady* mutant[16], which lack adult iridophores, could be followed over longer time periods. In the absence of host iridophores, donor-derived iridophores were able to spread laterally, in one case the cluster spanned 10 metameres at 35 dpf, which was never observed in wild type (Fig. 6h-l). This clone showed around 600 mature iridophore cells, whereas iridophore clones in wild type had only around 100 cells at the same time point.

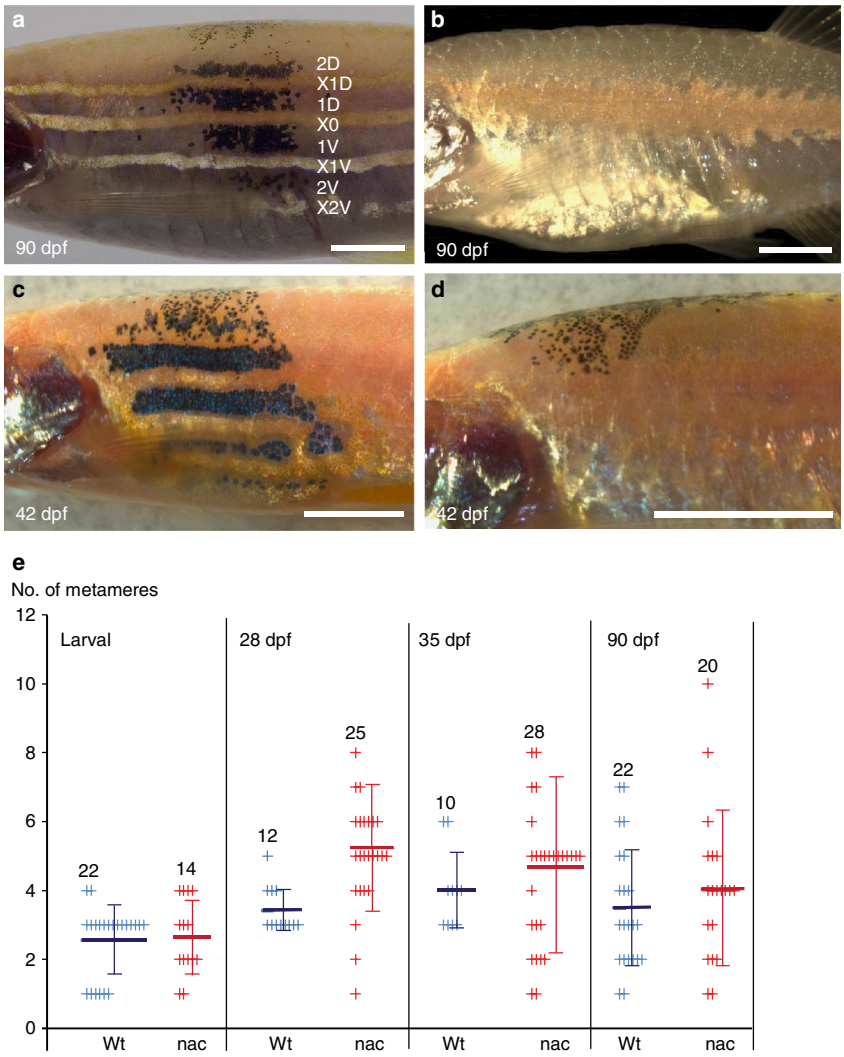

Figure 4 | Transplanted melanophore clusters in control (*albino*) and *nacre* chimeras. The organization of wild-type melanophores (black) in (**a**) *albino* and (**c**,**d**) *nacre* hosts. Adult *nacre* fish lacking melanophores (**b**). Scale bars, **a**–**d**: 250 µm. (**e**) Quantification of the number of metamers occupied by wild-type melanophores in the body stripes in *albino* control (blue) and *nacre* (red) hosts. The number of clusters analysed is depicted in the graph. Student's *t*-test (Welsh corrected) revealed significant differences between the size of wild type and *nacre* melanophore clusters at 28 dpf: (wild type, $n=12$ clusters, 7 fishes; *nacre*, $n=25$ clusters, 17 fishes, $P\leq0.0002$), at larval stages: (wild type, $n=22$ clusters, 10 fishes; *nacre*, $n=14$ clusters, 20 fishes, $P=0.7892$), 35 dpf: (wild type, $n=10$ clusters, 6 fishes; *nacre*, $n=28$ clusters, 17 fishes, $P=0.2512$ and adult (>90 dpf): (wild type, $n=22$ clusters, 9 fishes; *nacre*, $n=20$ clusters, 17 fishes, $P=0.3840$) no significant difference could be shown. Horizontal lines in dark blue (wild type) and red (*nacre*) indicate the mean value and the error bars represent standard deviation. Student's *t*-test (Welsh corrected) was used to determine the *P*-value.

Regeneration of chromatophores after stem cell depletion. Analysis of homotypic interactions among iridophores was hampered by a low survival rate of *shady* chimaeras. Other iridophore mutants, such as *rose* and *transparent*, have residual iridophores and hence are not suitable for our analysis. To obtain more information on the autonomous behaviour of iridophores and melanophores, we disrupted the formation of melanophore and iridophore stem cells by inhibiting the erb-b2 receptor tyrosine kinase (ErbB) pathway. ErbB signalling is required to establish the DRGs during the migration of neural crest cells in the early embryo[6,28]. To reduce ErbB3 activity in a temporally controlled manner, we used the small molecule inhibitor PD168393 at a concentration that results in the absence of several of the DRG-located stem cells of melanophores and iridophores causing gaps in the striped pattern[6,28]. This allowed us to study the behaviour of surviving iridophores and melanophores during the regeneration of the striped pattern in the gaps.

In many of the drug-treated fish, gaps in the striped pattern were observed at 21 dpf: they displayed regions with a reduced number of larval melanophores, and absence of dense iridophores forming the first light stripe at the horizontal myoseptum extending between 3 and 12 metameres (Fig. 7a,f; Supplementary Fig. 5). Fish with gaps in the stripes were followed

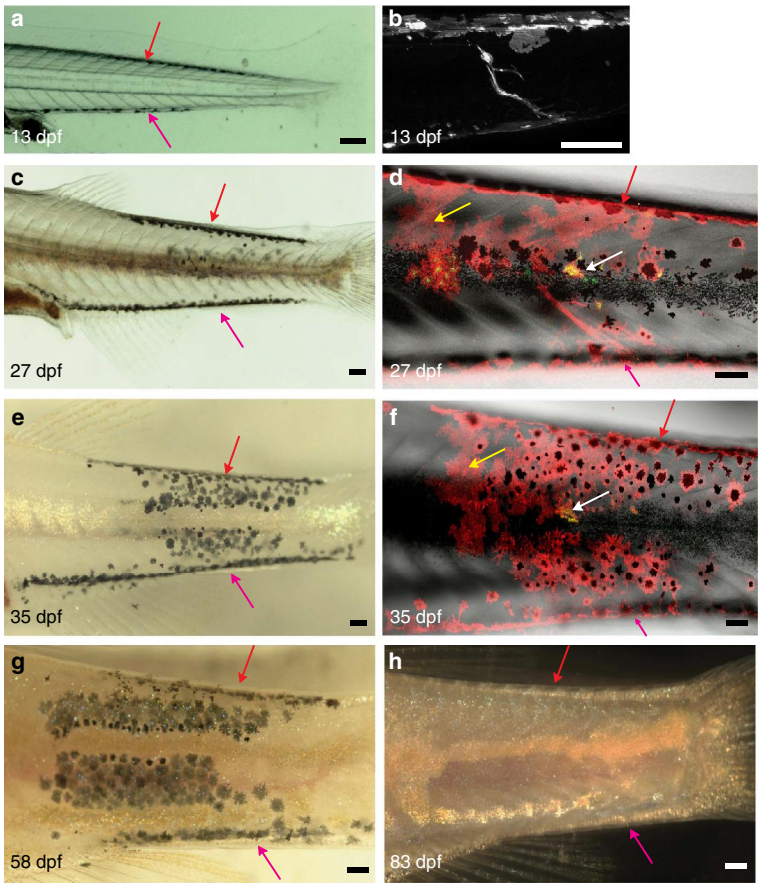

Figure 5 | Behaviour of melanophore clusters in *nacre* host. Clusters of wild-type melanophores (*Tg*(*TDL358:GFP; sox10:mRFP*)) in *nacre* followed through metamorphosis by (**a**,**c**,**e**,**g**,**h**) bright-field microscopy and (**b**,**d**,**f**) confocal imaging. (**a**–**h**): Dorsal and ventral streaks of melanophores are visible (red and pink arrows). These melanophores gradually disappear. (**e**–**g**) On 13 and 27 dpf confocal microscopy shows a DRG labelled within the melanophore cluster. (**b**,**d**) *Sox10:mRFP* labels clusters of xanthophores (yellow arrows), (**d**,**f**) *TDL358:GFP* labels iridophores (white arrows). (**e**–**g**) The melanophore cluster extends over about six segments. (**h**) At 83 dpf these melanophores disappear completely leaving a ghost dark stripe pattern surrounded by light stripes. Green plus red: iridophores, red only: xanthophores, red plus black: melanophores. Scale bars, **a**–**h**: 100 μm.

from 21 dpf every 3–4 days until 34 dpf (Fig. 7). We observed that 4–6 segment large gaps were completely filled by iridophores coming from adjacent segments (Fig. 7a–e) and the pattern regenerated within 7–10 days (quantification in Fig. 7k). Large gaps ($\sim$10 metameres on 21 dpf) were also filled in by spreading iridophores, but the recovery took longer (Fig. 7f–k). The striped pattern was not repaired perfectly resulting in wavy light and dark stripes on 34 dpf. In some cases ($n=7$) we observed that iridophore clusters appeared in the middle of the gaps (white arrows in Fig. 7g–i) spreading in all directions and resulting in a broader light stripe. In smaller gaps the cell number of melanophores in metameres recovered fully within 10 days yielding between 30 and 35 melanophores per metamere, the same number as compared to the control (the striped regions outside the gap) (Fig. 7l fish 1, 8; Supplementary Table 1), whereas in the bigger gaps on 34 dpf the melanophore number was still lower ($<$10 melanophores per metamere Fig. 7l, fish 2, 3 and 4; Supplementary Table 1). In these larger gaps, only the segments adjacent to the striped region recovered significantly.

To visualize the behaviour of surviving iridophores and melanophores during pattern regeneration, we performed drug-mediated ErbB inhibition on animals carrying *Tg*(*sox10:mRFP*) and imaged metamorphic fish (Figs 8, 9; Supplementary Fig. 5). Iridophores at the margins of the gaps migrate laterally, occupying iridophore-devoid regions of the prospective first light stripe (arrowheads in Fig. 8). Thus by proliferation and lateral dispersal, iridophores closed the gaps of 4–6 metamers completely within 10–12 days (graph in Fig. 7k). Iridophores at the margins of the gaps displayed the morphology of loose iridophores, and proliferated and migrated (Fig. 9a–c). Iridophores that are behind the migratory iridophores became densely packed and acquired the morphology of light stripe iridophores. In animals developing with large gaps ($\sim$10 segments), occasionally regenerating iridophores could be seen in the middle of the gaps (Fig. 7g-i; Supplementary Fig. 5). These iridophore clusters were similar in size to iridophore clones originating from stem cells[5], suggesting a regeneration potential for the progenitors.

Melanophores also regenerated from the margins of the gaps. Although a few melanophores displayed lateral movement (yellow arrow in Fig. 8c–g), most melanophores appeared *de novo*. This suggests that the new melanophores originate from unpigmented melanoblasts, which are regenerated by stem cells in the segments at the margins of the gaps. The melanophores exhibited limits in movement; in Fig. 8, three melanophores

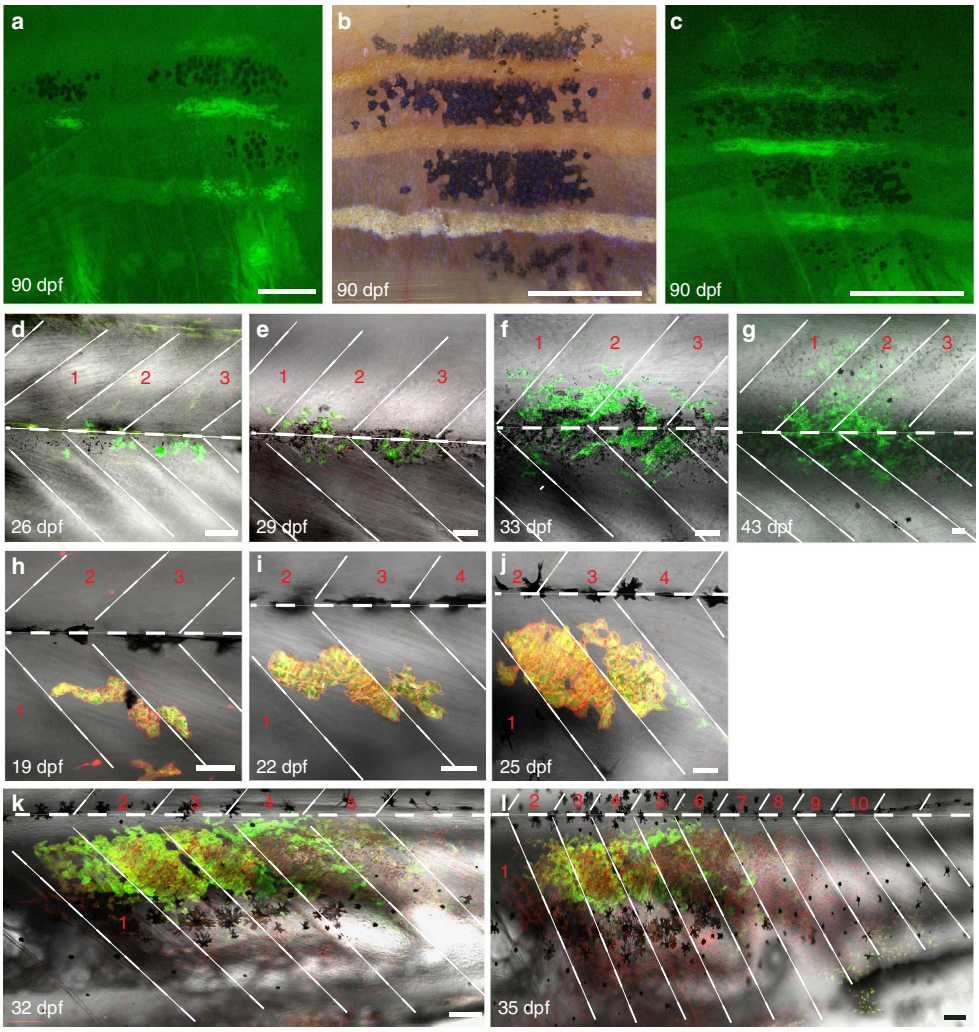

Figure 6 | Behaviour of iridophores in control (*albino*) and iridophore-deficient (*shady*) hosts. (**a**–**c**) Iridophore and melanophores clusters (derived from *Tg*(ß-*act:GFP*)) in control (*albino*) analysed with fluorescence (**a**,**c**) and bright-field microscopy (**b**): at 90 dpf iridophores and melanophores cover several stripes spanning between 1 and 4 metameres. (**d**–**g**) Confocal images of (*Tg*(*TDL358:GFP*))-labelled iridophore clusters in control (*albino*): iridophores appear in three adjacent metameres at 26 dpf and multiply within the same metameres. (**h**–**l**) (*Tg*(*TDL358:GFP*; *sox10:mRFP*)) cluster in *shady* covers 10 metameres at 35 dpf. Dashed white lines indicate vertical and horizontal myosepta. Red numbers indicate metameres. Scale bars, **a**–**c**: 250 µm, **d**–**l**: 100 µm.

situated along the horizontal myoseptum (blue arrows in Fig. 8a–d), displayed short-scale movement towards the dorsal stripe region on the arrival of iridophores in the adjacent light stripe region. The ErbB inhibition did not affect xanthophores (Supplementary Fig. 5).

A closer analysis of developing animals that had a gap in the first light stripe, allowed us to study the formation of an interrupted stripe pattern (Fig. 9d–k). In an animal with an initial gap of six segments, five segments were filled by lateral migration of iridophores within 10 days (Fig. 9d–i). Interestingly, a break in the first light stripe X0 corresponded to a break in newly forming light stripe X1V (red arrowheads in Fig. 9i). This is consistent with a clonally-related origin of iridophores along the dorsoventral axis[5]. Some larval melanophores persisted in the gaps (red arrows in Fig. 9d–h), however, the melanophore numbers did not recover as fast as iridophores, leading to a melanophore-deprived region in the dark stripe (Fig. 9d,e). Subsequently, this melanophore-deprived region was invaded by iridophores from the first (X0) and the newly forming (X1V) light stripes, leading to interruptions of the dark stripe by light stripe regions (Fig. 9i-k). We conclude that the lateral spreading of the melanophores, in contrast to that of the iridophores is constrained.

Regeneration of xanthophores after cell-specific ablation. To test the regenerative potential of xanthophores, we ablated larval xanthophores at 5 dpf by nitroreductase-mediated cell ablation[29] in *Tg*(*fms:gal4*; *UAS:nfsB-mCherry*) larvae. To efficiently trace the xanthophores, they were carrying *Tg*(*pax7:GFP*) (which also labels muscle stem cells). Following metronidazole treatment for 24 h, nitroreductase expressing xanthophores were efficiently ablated without affecting the surrounding architecture

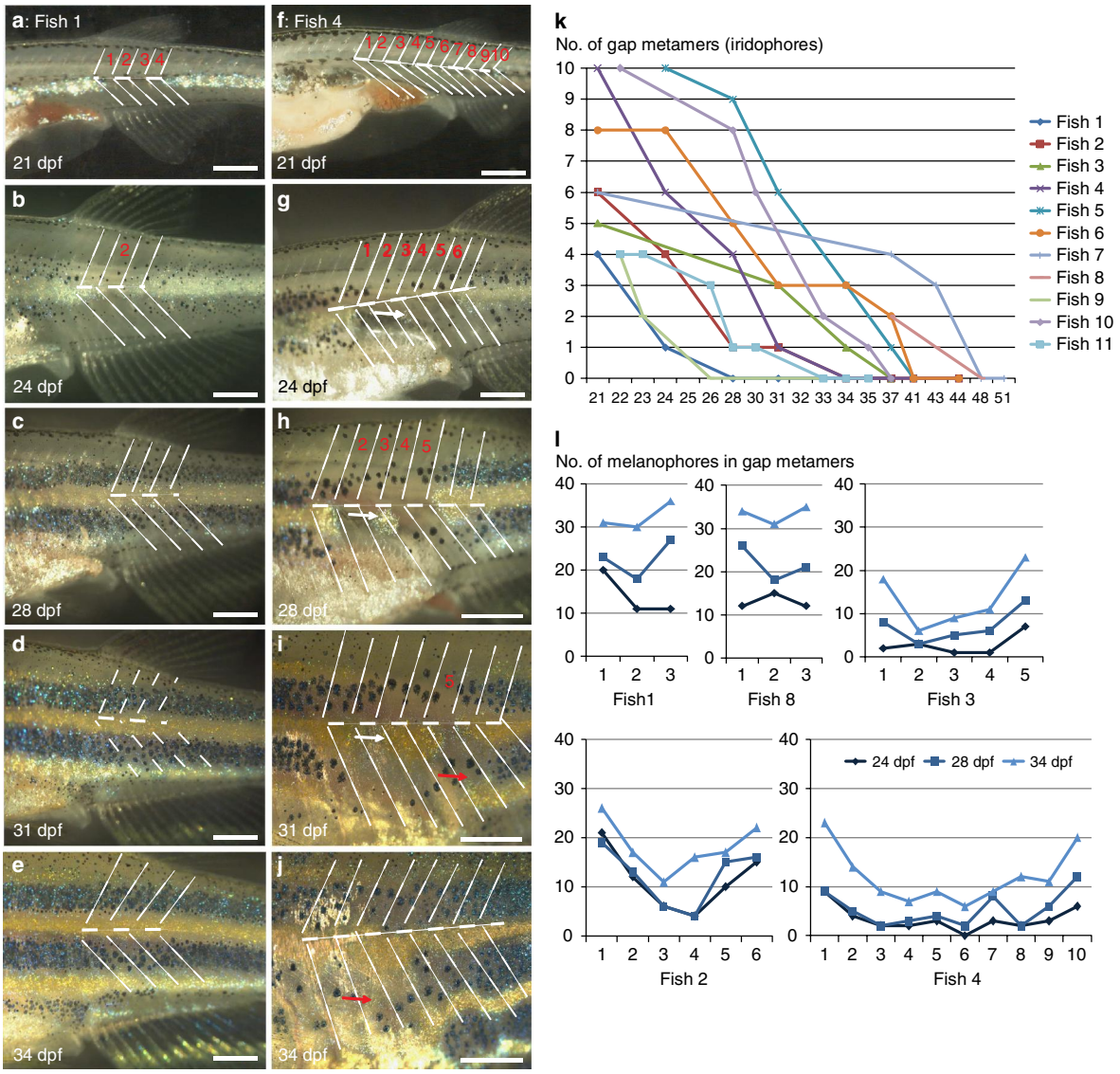

Figure 7 | Regeneration of iridophores and melanophores after ErbB inhibition. Treatment with PD168393 during embryogenesis (see methods) results in (**a**–**j**) gaps of different sizes (1–12 metamers) in the striped pattern of metamorphosing fish. Overall 15 fishes carrying gaps between 3 and 12 metamers were imaged through metamorphosis. Red numbers (**a**–**i**) indicate the segments that are devoid of iridophores at the onset of bright-field imaging. Dashed lines indicate vertical and horizontal myosepta. On 24 dpf (**g**) a spot of regenerating iridophores appears in the middle of the gap and it expands laterally (white arrow in **g**,**h**,**i**). (**k**) Time (in days) taken to fill the gaps of variable sizes in the stripe pattern. (**l**) Increase in numbers of melanophores in individual fish ($n=5$) during regeneration of gap metamers at three different time points, 24, 28 and 34 dpf. Scale bars, **a**–**j**: 250 μm.

(Fig. 10 a–l). To visualize the extent of xanthophore regeneration, we tracked the ablated regions using confocal microscopy. By 10 dpf regenerated green fluorescent protein (GFP)-labelled xanthophores could be observed in each segment. However, unexpectedly, regenerated xanthophores did not show the *fms:gal4*-mediated *nfsB-mCherry* expression, suggesting silencing of the transgene. When grown to adulthood, fish displayed a normal formation of the striped pattern indicating that xanthophores were fully restored (Fig. 10m). We suggest that the regeneration occurs from xanthophores originating from multipotent iridophore/melanophore stem cells[5].

Discussion

The formation of the striped colour pattern in zebrafish involves several cell behaviours, including pigment-cell proliferation, dispersal and spatially controlled cell-shape transitions in the skin[1,5,8,23]. In this study, we find a role for homotypic competition in regulating pigment-cell proliferation, dispersal and tiling in the skin for all three chromatophore types. In the absence of competing cells within a layer in the skin, donor-derived clusters of xanthophores and iridophores proliferate at a faster rate than in their normal surrounding and cover larger regions of the skin. Mutant analysis indicates that

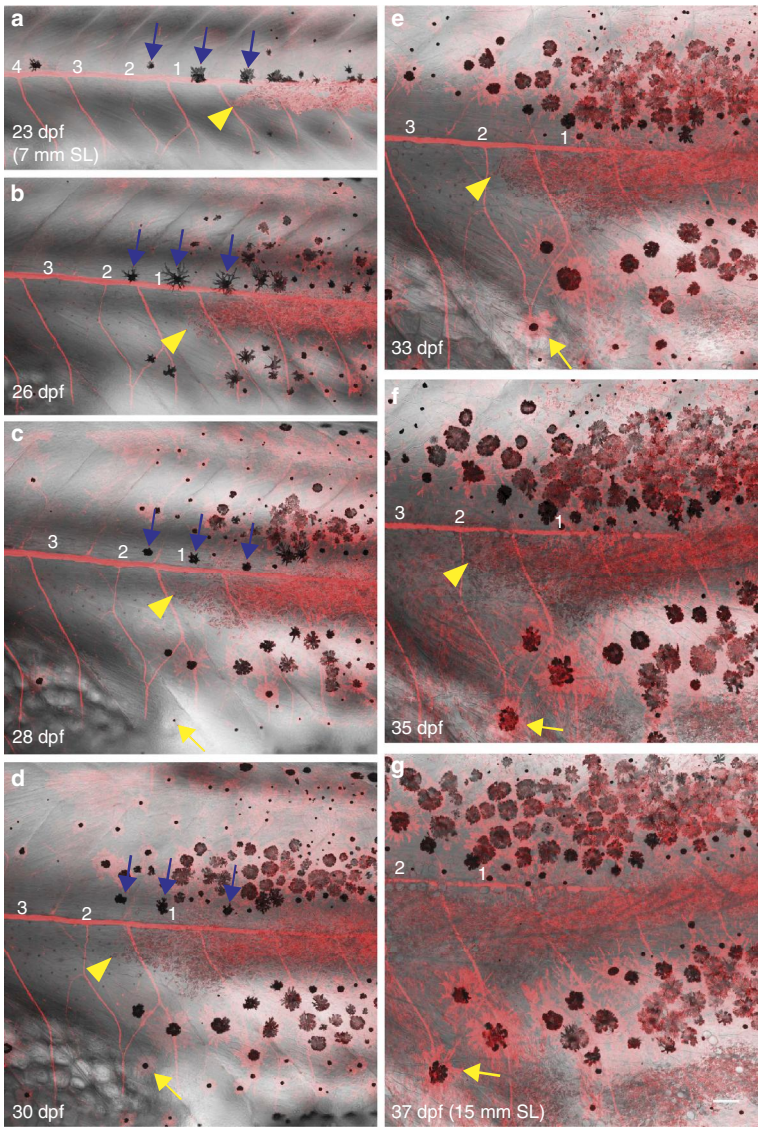

Figure 8 | Behaviour of iridophores and melanophores during pattern regeneration after ErbB inhibition. (**a**–**g**) Confocal images of *Tg*(*sox10:mRFP*) animal developing with a gap (indicated by number 1–4) in the stripe pattern. Existing iridophores (yellow arrowheads) extend laterally into the prospective light stripe region that is devoid of iridophores and fill the region. New melanophores appear near the margins of the gap and locally restore the pattern. Occasionally, melanophores display short-scale movement (yellow arrows). Blue arrows: melanophores situated along the horizontal myoseptum that move dorsally to join dark stripes on regeneration of the light stripe by iridophores. Iridophores—red (*Tg*(*sox10:mRFP*). SL, standard length of fish. Scale bars,100 μm.

specification, proliferation and maintenance of pigment cells depend on individual receptor–ligand systems; Kit signalling for melanophores, Ednr and Ltk signalling for iridophores, and Csf1r signalling for xanthophores[12,14–16,30–32]. Whereas the pigment cells express the respective receptor, the ligands are presumably functioning as trophic factors produced by surrounding tissue. Competition for the ligands may in part be responsible for the regulation of pigment-cell proliferation in normal development.

Competitive interactions among pigment cells result in an overall directionality in the pigment-cell migration that determines the dorsoventrally orientated clonal expansion of the pigment cells. During normal development, in the presence of pigment cells of the same type, clusters of all three pigment-cell types spread in dorsoventral direction as the fish grows ((ref. 5); Fig. 6a–c; Supplementary Figs 1, 2). The clusters contributed to most if not all stripes in a narrow patch along the dorsoventral axis. Spreading along the anteroposterior direction was less pronounced, and the clusters contributed to between 1 and 4 adjacent segments. This reveals that in normal development, the pattern is stitched together by adjacent clones derived from stem cells at the DRG of neighbouring metamers (iridophores and melanophores), and from larval xanthophores.

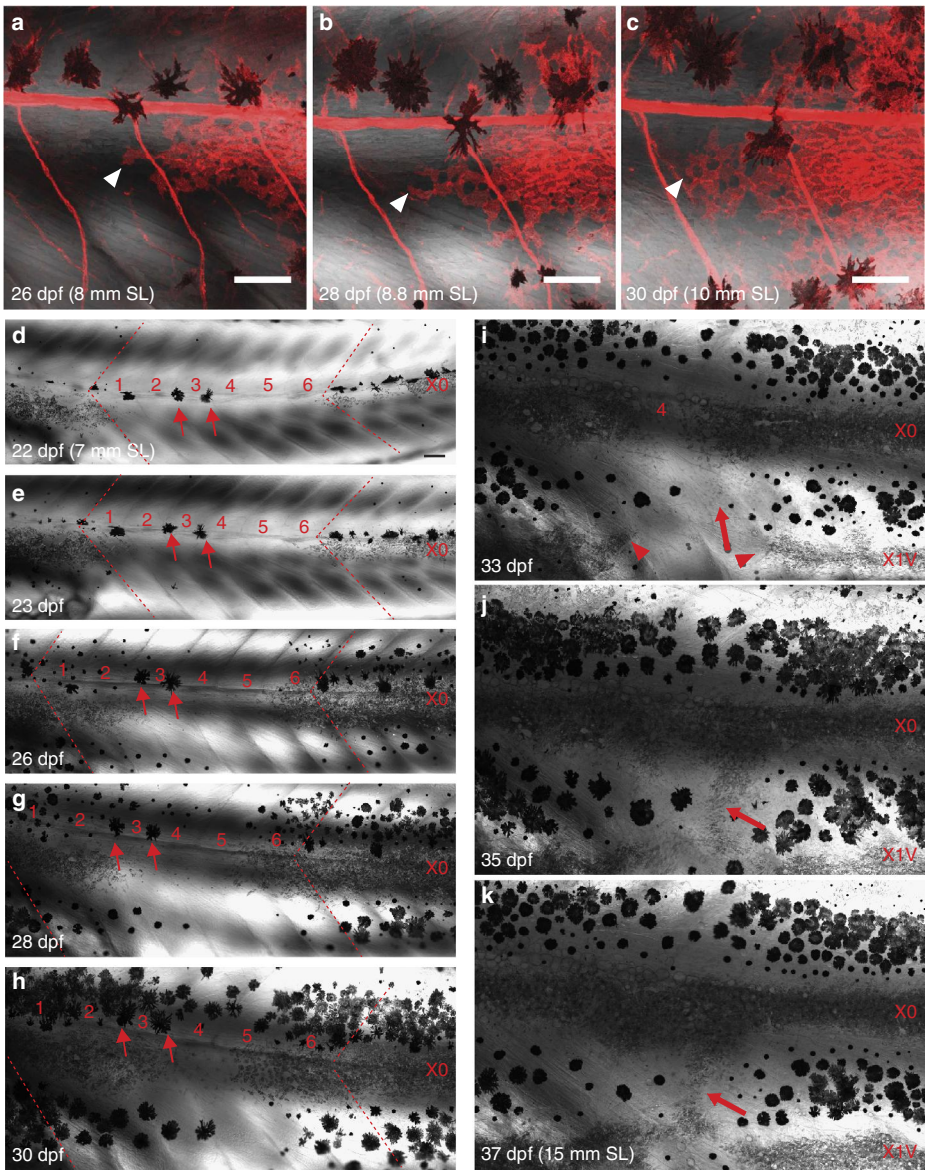

Figure 9 | Iridophore disperse laterally to occupy iridophore-devoid regions. (**a**–**c**) Iridophores (white arrowheads, *Tg*(*sox10:mRFP*)) extend to the empty segment on the left and increase in number. (**d**–**k**) Gap closure in an animal lacking iridophores in six segments at 22 dpf (numbered 1–6). Red dashed lines indicate the original borders of the gap. Small arrows in **d**–**h**: larval melanophores remain stable within the gap. (**e**) Iridophores that are present outside the gap begin to invade the iridophore-devoid segments and within a day, iridophores can be seen in segment 1 and 6. (**f**–**h**) By lateral movement, iridophores recover in segments 1–3 and 5–6, only the segment 4 remains devoid of iridophores. (**i**) The first light stripe, X0 lacks iridophores in the segment 4 and remains interrupted. Corresponding region in the newly formed light stripe also lacks iridophores (red arrowheads). The dark stripe region does not develop sufficient melanophores and subsequently iridophores begin to migrate vertically (big red arrow) invading the dark stripe region. (**j**,**k**) Vertically migrating iridophores lead to interruption of the dark stripe region by the light stripe region. SL, standard length of fish. Scale bars,100 μm.

The lateral extension of the clones is restricted by homotypic competition. Thus, the dorsoventral orientation of the pigment-cell clones observed in normal development is the result of competitive interactions between cells from neighbouring segments and not the product of a hypothetical, morphogen-based directed migration.

As reported earlier[12,18], the introduction of the missing cell type into mutants lacking a given pigment-cell type locally restores a normal pattern. The incoming cells in the spreading clusters induce cell-shape changes in the adjacent cell layers such that a normal stripe pattern is formed while the clusters grow. This involves extensive shape changes in the pigment cells of the host as well as the donor. Our high-resolution images confirm that there is a constant adjustment with mutual interactions between the three cell types during stripe formation. In conclusion, heterotypic interactions between the three layers

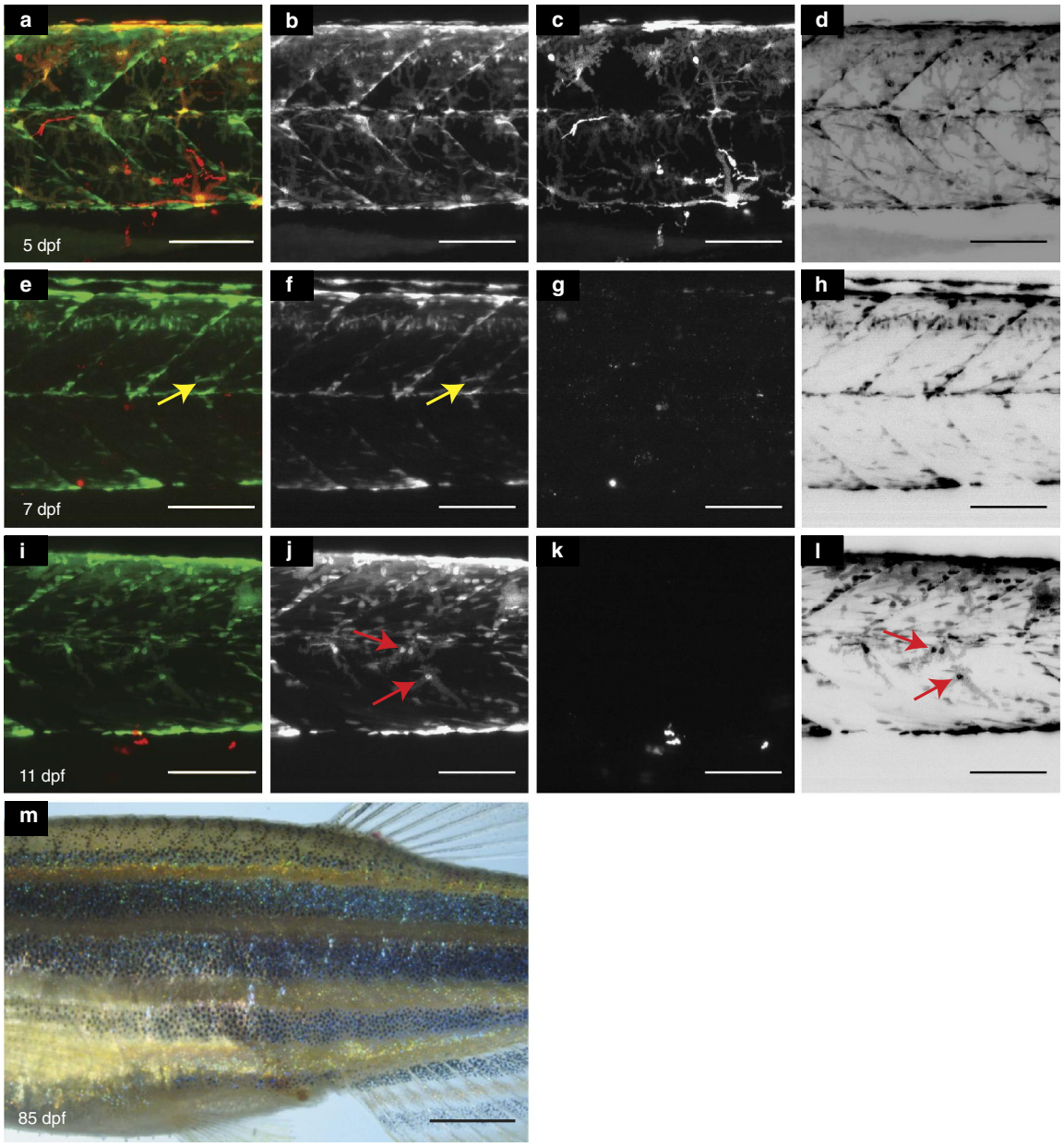

Figure 10 | Xanthophore regeneration following drug-mediated ablation. (**a**–**d**): Larva at 5 dpf, xanthophores: green (*Tg*(*pax7:GFP*) and red: *Tg*(*fms:Gal4, UAS:nfsB-mcherry*). (**e**–**h**): The same region after ablation at 7 dpf: yellow arrow: (*Tg*(*pax7:GFP*) labels muscle tissue and their precursors[24]. (**i**–**l**): same region at 11 dpf. Red arrow: regenerated xanthophore. (**a**,**e**,**i**): merge; (**b**,**f**,**j**): (*Tg*(*pax7:GFP*) in grey scale; (**c**,**g**,**k**): *Tg*(*fms:Gal4, UAS:nfsB-mcherry*) in grey scale; (**d**,**h**,**l**): (*Tg*(*pax7:GFP*) in inverted grey scale. (**m**): Adult fish after ablation displaying a normal pattern. Scale bars, **a**–**l**: 100 µm, **m**: 250 µm.

regulate cell-shape transition, whereas the homotypic interactions we observe regulate pigment-cell dispersal in a coherent two-dimensional sheet within one layer.

Strikingly, in adult chimeras, the patches of donor-derived pigment cells are coherent and have normal densities. This indicates that there is an intrinsic tendency for pigment cells to remain together observing normal distances, rather than dispersing into regions devoid of their cell type. We suggest that the cell–cell interactions are mediated by direct cellular contacts. Live-imaging of the behaviour of xanthophores in larvae (Fig. 3) shows that xanthophores maintain a dynamic contact with one another, and proliferate in the absence of neighbouring xanthophores. The xanthophore filopodia are highly dynamic actin-rich protrusions[33], which may allow xanthophores to probe their environment and contact neighbouring xanthophores, thus maintaining a sheet-like xanthophore cover in the skin through cell division and migration into xanthophore-devoid regions. In the growing skin, increasing the distances between neighbouring

xanthophores may trigger cell divisions such that a regular spacing is maintained.

Iridophores spreading in *shady* chimeras, or laterally migrating into gaps devoid of iridophores also acquire a loose migratory shape but stay in direct contact with one another rather than dispersing. This behaviour is also observed in normal development in which iridophores during metamorphosis populate the skin as a loose net of interconnected cells spreading dorsally and ventrally[5].

The melanophores in stripes formed in *nacre* chimeras also maintain normal distances to one another. In normal development, melanophores extend long cytoplasmic protrusions allowing them to contact each other while filling in the dark stripe region[5]. This suggests that the spacing of melanophores in the stripes is mediated by direct cell contacts between melanophores. Mutant analyses, however, indicate in addition a strong dependence of melanophore spacing on heterotypic interactions, in particular with xanthophores, whereas iridophores and xanthophores display a more autonomous behaviour[12].

The responses of pigment cells to homotypic interactions, in particular those observed in xanthophores and iridophores, resemble that of neural crest cells, which undergo collective cell migration and display co-attraction despite contact inhibition of locomotion[34]. Contact inhibition of locomotion is a long-established phenomenon observed in cultured cells *in vitro*[35–38], and more recently *in vivo*[39–41]. It is suggested that co-attraction and contact inhibition of locomotion act in concert orchestrating collective migration of neural crest cells—contact inhibition of locomotion alone would lead to dispersal of the group into single cells[40]. Co-attraction, in combination with contact inhibition of locomotion allows maintenance of appropriate cell density, local homotypic cell–cell interactions and efficient response to external cues. We hypothesize similar interactions between pigment cells of the same kind during pattern formation—clusters of wild-type xanthophores do not disperse into single cells in absence of xanthophores in the neighbourhood. Instead, these cells maintain appropriate local cell density while the cluster grows by local proliferation and short-scale movement. This is also true for iridophores and melanophores suggesting co-attraction and contact inhibition of locomotion may underlie pigment-cell coverage by homotypic interactions in the skin. Our knowledge of the molecular bases of cell contact-mediated interactions during colour pattern formation is still rudimentary. At the molecular level, interactions between chromatophores have been shown to depend on integral membrane proteins including connexins and potassium channels, suggesting that physical cell contacts between chromatophores are involved and that the directed transport of small molecules or bioelectrical coupling are important for these interactions[21,22,42]. In *obelix*, encoding the inwardly rectifying potassium channel Kir7.1, melanophore stripes are enlarged, with a lower than normal density of melanophores[18,43]. This channel is specifically required in melanophores and may be responsible for their proper spacing. The gap junctions formed by the connexins encoded by the *leopard* and *luchs* genes have been suggested to mediate heterotypic as well as homotypic interactions among melanophores and xanthophores[18,22,44]. Connexins mediate intercellular communication that may lead to diverse cellular outcomes including oriented cell migration[45]. The Immunoglobulin Superfamily Member 11, mutated in *seurat*, has been reported to mediate aspects of melanophore behaviour including melanophore–melanophore interactions[46]. It is conceivable that connexins and other cell-surface molecules mediate the homotypic competition-dependent proliferation and tiling of the pigment cells. Our experimental paradigm provides an opportunity to assess the molecular regulation of the cellular outcomes of the diverse cell–cell interactions during colour pattern formation.

Methods

Zebrafish lines. The following zebrafish lines were used: wild-type (WT, Tübingen strain[47] from the Tübingen zebrafish stock centre), *albino*[25], *nacre*[13], *pfeffer*[18], *brass*[27], *shady*[16,27], *Tg*(*fms:Gal4*, *UAS:mcherry*)[48], *Tg*(*pax7:GFP*)[8,24], *Tg*(*TDL358:GFP*)[49], *Tg*(*sox10:mRFP*)[5], *Tg*(*βactin2:GFP*). Zebrafish were raised as described[50]. The staging of metamorphic fish was done as described[12,51]. All animal experiments were performed in accordance with the rules of the State of Baden-Württemberg, Germany and approved by the Regierungspräsidium Tübingen.

Blastomere transplantation. Chimeric animals were generated by transplantation of cells of appropriately labelled blastula stage embryos into wild type and mutant embryos at blastula stage[52]. The number of transplanted cells was monitored using Rhodamine dextran injected in the donor embryos at the one cell stage, and the number of transplanted cells was estimated to be in the range between 1–10 cells. Fishes were raised and analysed at different time points throughout metamorphosis until adulthood.

Pharmacological inhibition of the ErbB signalling pathway. The ErbB inhibitor-treatment was done as described previously[6]. In brief, 14 somite stage embryos were treated with 10 μM ErbB inhibitor (PD168393) dissolved in E2 for 5 h at 29 °C. The ErbB inhibitor phenotype is similar to that of *erbb3b* (*hypersensitive/picasso*) mutants[6,28]: during the early stages of metamorphosis the fish develop with regions in the prospective light and dark stripe regions without iridophores and melanophores. Wild-type animals at corresponding stages display contiguous light and dark stripes. We term the melanophore and iridophore-devoid regions as "gaps". The size of these gaps along the AP axis is variable in both, the *erbb3b* mutants and the ErbB inhibitor-treated animals.

Genetically-targeted ablation of xanthophores. Targeted ablation of xanthophores was performed as described[29]. In brief, larvae carrying *Tg*(*fms:Gal4*, *Tg*(*UAS:nfsB-mcherry*))[48] were treated with metronidazole for 24 h at 5 dpf. This results in targeted ablation of xanthophores. *Tg*(*pax7:GFP*)[8,24], a reporter line that labels xanthophores, muscles and muscle progenitors, was used for xanthophore visualization. Xanthophores can be recognized by their characteristic shape and location in the skin. The first imaging of the larvae was done immediately before the drug treatment. Subsequent imaging was done as mentioned in the text.

Image acquisition and processing. Repeated imaging of zebrafish was performed as described[5]. Images were acquired on Zeiss LSM 780 NLO confocal and Leica M205 FA stereo-microscopes. ImageJ[53], Adobe Photoshop, Adobe Illustrator and Imaris were used for image processing and analysis. Maximum intensity projections of confocal scans of the fluorescent samples were uniformly adjusted for brightness and contrast. Scans of the bright field were stacked using "stack focuser" plugin and tile scans were stitched in Fiji[54].

References

1. Singh, A. P. & Nüsslein-Volhard, C. Zebrafish stripes as a model for vertebrate colour pattern formation. *Curr. Biol.* **25,** R81–R92 (2015).
2. Irion, U, Singh, A. P. & Nüsslein-Volhard, C. The developmental genetics of vertebrate colour pattern formation: lessons from zebrafish. *Curr. Top. Dev. Biol.* **117,** 141–169 (2016).
3. Watanabe, M & Kondo, S. Is pigment patterning in fish skin determined by the Turing mechanism? *Trends Genet.* **31,** 88–96 (2015).
4. Parichy, D. M. & Spiewak, J. E.. Origins of adult pigmentation: diversity in pigment stem cell lineages and implications for pattern evolution. *Pigment Cell Melanoma Res.* **28,** 31–50 (2015).
5. Singh, A. P., Schach, U & Nüsslein-Volhard, C. Proliferation, dispersal and patterned aggregation of iridophores in the skin prefigure striped colouration of zebrafish. *Nat. Cell. Biol.* **16,** 607–614 (2014).
6. Dooley, C. M., Mongera, A, Walderich, B & Nüsslein-Volhard, C. On the embryonic origin of adult melanophores: the role of ErbB and Kit signalling in establishing melanophore stem cells in zebrafish. *Development* **140,** 1003–1013 (2013).
7. Budi, E. H., Patterson, L. B. & Parichy, D. M.. Post-embryonic nerve-associated precursors to adult pigment cells: genetic requirements and dynamics of morphogenesis and differentiation. *PLoS Genet.* **7,** e1002044 (2011).
8. Mahalwar, P, Walderich, B, Singh, A. P. & Nüsslein-Volhard, C. Local reorganization of xanthophores fine-tunes and colors the striped pattern of zebrafish. *Science* **345,** 1362–1364 (2014).
9. McMenamin, S. K. *et al.* Thyroid hormone-dependent adult pigment cell lineage and pattern in zebrafish. *Science* **345,** 1358–1361 (2014).

10. Hirata, M, Nakamura, K, Kanemaru, T, Shibata, Y & Kondo, S. Pigment cell organization in the hypodermis of zebrafish. *Dev. Dyn.* **227,** 497–503 (2003).
11. Hirata, M, Nakamura, K & Kondo, S. Pigment cell distributions in different tissues of the zebrafish, with special reference to the striped pigment pattern. *Dev. Dyn.* **234,** 293–300 (2005).
12. Frohnhöfer, H. G., Krauss, J, Maischein, H. M. & Nüsslein-Volhard, C. Iridophores and their interactions with other chromatophores are required for stripe formation in zebrafish. *Development* **140,** 2997–3007 (2013).
13. Lister, J. A., Robertson, C. P., Lepage, T, Johnson, S. L. & Raible, D. W.. nacre encodes a zebrafish microphthalmia-related protein that regulates neural-crest-derived pigment cell fate. *Development* **126,** 3757–3767 (1999).
14. Parichy, D. M. *et al.* Mutational analysis of endothelin receptor b1 (rose) during neural crest and pigment pattern development in the zebrafish *Danio rerio*. *Dev. Biol.* **227,** 294–306 (2000).
15. Parichy, D. M., Ransom, D. G., Paw, B, Zon, L. I. & Johnson, S. L.. An orthologue of the kit-related gene fms is required for development of neural crest-derived xanthophores and a subpopulation of adult melanocytes in the zebrafish, *Danio rerio*. *Development* **127,** 3031–3044 (2000).
16. Lopes, S. S. *et al.* Leukocyte tyrosine kinase functions in pigment cell development. *PLoS Genet.* **4,** e1000026 (2008).
17. Krauss, J, Astrinides, P, Frohnhöfer, H. G., Walderich, B & Nüsslein-Volhard, C. transparent, a gene affecting stripe formation in zebrafish, encodes the mitochondrial protein Mpv17 that is required for iridophore survival. *Biol. Open* **2,** 703–710 (2013).
18. Maderspacher, F & Nüsslein-Volhard, C. Formation of the adult pigment pattern in zebrafish requires leopard and obelix dependent cell interactions. *Development* **130,** 3447–3457 (2003).
19. Nakamasu, A, Takahashi, G, Kanbe, A & Kondo, S. Interactions between zebrafish pigment cells responsible for the generation of Turing patterns. *Proc. Natl Acad. Sci. USA* **106,** 8429–8434 (2009).
20. Singh, A. P., Frohnhöfer, H. G., Irion, U & Nüsslein-Volhard, C. Fish pigmentation. response to comment on "Local reorganization of xanthophores fine-tunes and colors the striped pattern of zebrafish". *Science* **348,** 297 (2015).
21. Yamanaka, H & Kondo, S. *In vitro* analysis suggests that difference in cell movement during direct interaction can generate various pigment patterns *in vivo*. *Proc. Natl Acad. Sci. USA* **111,** 1867–1872 (2014).
22. Irion, U *et al.* Gap junctions composed of connexins 41.8 and 39.4 are essential for colour pattern formation in zebrafish. *Elife* **3,** e05125 (2014).
23. Fadeev, A, Krauss, J, Fröhnhofer, H. G., Irion, U & Nüsslein-Volhard, C. Tight junction protein 1a regulates pigment cell organisation during zebrafish colour patterning. *Elife* **4,** e06545 (2015).
24. Alsheimer, S. *On Teleost Muscle Stem Cells and the Vertical Myoseptum as their Niche* 1–249 PhD Dissertation, Eberhard-Karls-Univ. (2012).
25. Dooley, C. M. *et al.* Slc45a2 and V-ATPase are regulators of melanosomal pH homeostasis in zebrafish, providing a mechanism for human pigment evolution and disease. *Pigment Cell Melanoma Res.* **26,** 205–217 (2013).
26. Kelsh, R. N. *et al.* Zebrafish pigmentation mutations and the processes of neural crest development. *Development* **123,** 369–389 (1996).
27. Haffter, P *et al.* Mutations affecting pigmentation and shape of the adult zebrafish. *Dev. Genes. Evol.* **206,** 260–276 (1996).
28. Budi, E. H., Patterson, L. B. & Parichy, D. M.. Embryonic requirements for ErbB signaling in neural crest development and adult pigment pattern formation. *Development* **135,** 2603–2614 (2008).
29. Pisharath, H & Parsons, M. J.. Nitroreductase-mediated cell ablation in transgenic zebrafish embryos. *Methods Mol. Biol.* **546,** 133–143 (2009).
30. Parichy, D. M., Rawls, J. F., Pratt, S. J., Whitfield, T. T. & Johnson, S. L.. Zebrafish sparse corresponds to an orthologue of c-kit and is required for the morphogenesis of a subpopulation of melanocytes, but is not essential for hematopoiesis or primordial germ cell development. *Development* **126,** 3425–3436 (1999).
31. Krauss, J *et al.* Endothelin signalling in iridophore development and stripe pattern formation of zebrafish. *Biol. Open* **3,** 503–509 (2014).
32. Fadeev, A, Krauss, J, Singh, A. P. & Nüsslein-Volhard, C. Zebrafish leukocyte tyrosine kinase controls iridophore establishment, proliferation and survival. *Pigment Cell Melanoma Res.* http://dx.doi.org/10.1111/pcmr.12454 (2016).
33. Panza, P, Maier, J, Schmees, C, Rothbauer, U & Sollner, C. Live imaging of endogenous protein dynamics in zebrafish using chromobodies. *Development* **142,** 1879–1884 (2015).
34. Mayor, R & Theveneau, E. The neural crest. *Development* **140,** 2247–2251 (2013).
35. Martz, E & Steinber, M.S. Role of cell–cell contact in contact inhibition of cell-division—review and new evidence. *J. Cell. Physiol.* **79,** 189–210 (1972).
36. Abercrombie, M. Contact inhibition in tissue culture. *In Vitro Cell Dev. B* **6,** 128 (1970).
37. Abercrombie, M & Heaysman, J. E.. Observations on the social behaviour of cells in tissue culture. I. Speed of movement of chick heart fibroblasts in relation to their mutual contacts. *Exp. Cell. Res.* **5,** 111–131 (1953).
38. Abercrombie, M & Heaysman, J. E.. Observations on the social behaviour of cells in tissue culture. II. Monolayering of fibroblasts. *Exp. Cell. Res.* **6,** 293–306 (1954).
39. Carmona-Fontaine, C *et al.* Contact inhibition of locomotion *in vivo* controls neural crest directional migration. *Nature* **456,** 957–961 (2008).
40. Carmona-Fontaine, C *et al.* Complement fragment C3a controls mutual cell attraction during collective cell migration. *Dev. Cell.* **21,** 1026–1037 (2011).
41. Davis, J. R. *et al.* Inter-cellular forces orchestrate contact inhibition of locomotion. *Cell* **161,** 361–373 (2015).
42. Inaba, M, Yamanaka, H & Kondo, S. Pigment pattern formation by contact-dependent depolarization. *Science* **335,** 677 (2012).
43. Iwashita, M *et al.* Pigment pattern in jaguar/obelix zebrafish is caused by a Kir7.1 mutation: implications for the regulation of melanosome movement. *PLoS Genet.* **2,** e197 (2006).
44. Watanabe, M *et al.* Spot pattern of leopard Danio is caused by mutation in the zebrafish connexin41.8 gene. *EMBO Rep.* **7,** 893–897 (2006).
45. Kotini, M & Mayor, R. Connexins in migration during development and cancer. *Dev. Biol.* **401,** 143–151 (2015).
46. Eom, D. S. *et al.* Melanophore migration and survival during zebrafish adult pigment stripe development require the immunoglobulin superfamily adhesion molecule Igsf11. *PLoS Genet.* **8,** e1002899 (2012).
47. Haffter, P *et al.* The identification of genes with unique and essential functions in the development of the zebrafish, *Danio rerio*. *Development* **123,** 1–36 (1996).
48. Gray, C *et al.* Simultaneous intravital imaging of macrophage and neutrophil behaviour during inflammation using a novel transgenic zebrafish. *Thromb. Haemost.* **105,** 811–819 (2011).
49. Levesque, M. P., Krauss, J, Koehler, C, Boden, C & Harris, M. P.. New tools for the identification of developmentally regulated enhancer regions in embryonic and adult zebrafish. *Zebrafish* **10,** 21–29 (2013).
50. Brand, M, Granato, M & Nüsslein-Volhard, C. in *Keeping and Raising Zebrafish. Zebrafish, Practical Approach*. Ch. 1, 7–37 (Oxford Univ. Press, 2002).
51. Parichy, D. M., Elizondo, M. R., Mills, M. G., Gordon, T. N. & Engeszer, R. E.. Normal table of postembryonic zebrafish development: staging by externally visible anatomy of the living fish. *Dev. Dyn.* **238,** 2975–3015 (2009).
52. Kane, D. A. & Kishimoto, Y. in *Cell Labelling And Transplantation Techniques. Zebrafish, Practical Approach*. Ch. 4, 95–119 (Oxford Univ. Press, 2002).
53. Schneider, C. A., Rasband, W. S. & Eliceiri, K. W.. NIH Image to ImageJ: 25 years of image analysis. *Nat. Methods* **9,** 671–675 (2012).
54. Preibisch, S, Saalfeld, S & Tomancak, P. Globally optimal stitching of tiled 3D microscopic image acquisitions. *Bioinformatics* **25,** 1463–1465 (2009).

Acknowledgements

We thank Darren Gilmour, Patrick Müller, Uwe Irion, Hans-Georg Frohnhöfer, April Dinwiddie, Anastasia Eskova and Andrey Fadeev for comments on the manuscript. We thank Andrey Fadeev for help with the bright-field imaging of adult fish. This work was supported by the Max Planck Society.

Author contributions

B.W., A.P.S. and C.N.V. conceived and designed the experiments; B.W. performed the blastomere transplantations; A.P.S. analysed the regeneration on depletion of stem cells and P.M. the drug-mediated xanthophore ablation experiment. A.P.S. and P.M. provided confocal images of the chimeras. C.N.V., B.W. and A.P.S. wrote the paper.

Additional information

Supplementary Information accompanies this paper at http://www.nature.com/naturecommunications

Competing financial interests: The authors declare no competing financial interests.

Reprints and permission information is available online at http://npg.nature.com/reprintsandpermissions/

How to cite this article: Walderich, B. *et al.* Homotypic cell competition regulates proliferation and tiling of zebrafish pigment cells during colour pattern formation. *Nat. Commun.* 7:11462 doi: 10.1038/ncomms11462 (2016).

Publication 3

Mahalwar P., Singh A.P., Fadeev A., Nüsslein-Volhard C, Irion U. (2016). **Connexin-mediated organization of xanthophores during color pattern formation in zebrafish**. (submitted)

Synopsis

Large-scale mutagenesis screens in zebrafish have yielded important information about a variety of genes that are involved in the formation of the stripe pattern. Mutants in which all chromatophore types develop, but in which stripe formation is impaired, are of particular interest, because they may provide insights about the molecular mechanisms of cell–cell interactions underlying stripe formation. Several mutants have been described in which dark stripes are broken into spots. Of these, spotted mutants, *leo* and *luchs* encode components of gap junctions involved in cell–cell communications (Irion et al., 2014a; Maderspacher and Nüsslein-Volhard, 2003; Watanabe et al., 2006). The functions of both connexins are required in melanophores and xanthophores, but not in iridophores. *leo* mutant melanophores show a range of spotted pattern from small melanophore spotted patches to individually distributed ones (Irion et al., 2014a), however the phenotype associated with xanthophores remains unclear. Genetic evidence suggests that in the absence of one of the two connexins homomeric channels can form that still retain some functionality and lead to the formation of spots. The complete absence of both connexins leads to the loss of all patterning, and a small number of individual melanophores appear on a continuous sheet of dense iridophores. Both *leo* and *luc* are required in xanthophores and melanophores but not in iridophores (Irion et al. 2014a). These findings strongly suggested that both connexins form heterotypic gap junctions mediating the signaling between xanthophores and melanophores and recently this has been confirmed biochemically (Watanabe et al., 2015). Iridophores, a third pigment cell type, are also important for the patterning process; however, their mechanisms of interaction with melanophores or xanthophores remain unexplored. To better

understand the communication between pigment cell types, I generated combinations of several transgenic lines in various mutant backgrounds. I analyzed xanthophore cell shape and density in mutants lacking melanophores (*nac*) and iridophores (*shd*). In the absence of iridophores (*shd*), xanthophores remain at low density and display stellate cell shapes. In contrast, in the absence of melanophores (*nac*), xanthophores in the light stripe regions show higher density and a compact shape like wild type. This indicates that the higher density of xanthophores in light stripes could be due to the presence of tight iridophores. I have confirmed these results by analyzing xanthophore densities in an iridophore stem cell mutant (*erbb3b*) with a missing patch of the iridophores, and in a complementary situation in an iridophore mutant (*rose*) with residual small patches of tight iridophores.

Further, I have analyzed xanthophores in *leo* mutants, in which all chromatophore types develop, but stripe formation is impaired (dark stripes are broken into spots). A lower density of light stripe xanthophores was observed in *leo* mutants similar to that observed in iridophore mutants (*shd*). We concluded that iridophores and xanthophores interact directly and that gap junctions composed of Cx41.8 and Cx39.4 are involved in these cell-cell communications. I also analyzed xanthophore behaviors with respect to melanophores in *leo* mutants to have a better understanding of the role of *leo* in melanophore-xanthophore interaction. These analyses showed us that the xanthophore repulsion by the appearance of early melanophores is independent of *leo*. Also, the rearrangement and stellate shape of adult xanthophores, and the appearance of more melanophores in the dark stripes, is dependent on the *leo* genotype in xanthophores. Finally, blastula transplantations confirm a cell-autonomous requirement of Cx41.8 and Cx39.4 in xanthophores to acquire a stellate and compact shape in connection with melanophores and tight iridophores respectively, and suggest the possibility of heterotypic and heteromeric gap junction with melanophore and iridophores.

In conclusion, this study showed that tight iridophores are required for xanthophores to increase in density and adopt a compact shape. The cellular interactions leading to these behaviors depend on gap junctions formed by *leo* and *luc*. We also show that melanophore-xanthophore interactions can be divided

into two phases, whereby the initial interaction is independent of *leo*/*luc* gap junctions, they are essential during later stages. These results show the importance of all three types of pigment cells in the process of pattern formation and demonstrate the complexity of their interactions.

© 2016. Published by The Company of Biologists Ltd | Biology Open (2016) 5, 1680-1690 doi:10.1242/bio.022251

RESEARCH ARTICLE

Heterotypic interactions regulate cell shape and density during color pattern formation in zebrafish

Prateek Mahalwar*,¶, Ajeet Pratap Singh‡, Andrey Fadeev§, Christiane Nüsslein-Volhard and Uwe Irion¶

ABSTRACT

The conspicuous striped coloration of zebrafish is produced by cell-cell interactions among three different types of chromatophores: black melanophores, orange/yellow xanthophores and silvery/blue iridophores. During color pattern formation xanthophores undergo dramatic cell shape transitions and acquire different densities, leading to compact and orange xanthophores at high density in the light stripes, and stellate, faintly pigmented xanthophores at low density in the dark stripes. Here, we investigate the mechanistic basis of these cell behaviors *in vivo*, and show that local, heterotypic interactions with dense iridophores regulate xanthophore cell shape transition and density. Genetic analysis reveals a cell-autonomous requirement of gap junctions composed of Cx41.8 and Cx39.4 in xanthophores for their iridophore-dependent cell shape transition and increase in density in light-stripe regions. Initial melanophore-xanthophore interactions are independent of these gap junctions; however, subsequently they are also required to induce the acquisition of stellate shapes in xanthophores of the dark stripes. In summary, we conclude that, whereas homotypic interactions regulate xanthophore coverage in the skin, their cell shape transitions and density is regulated by gap junction-mediated, heterotypic interactions with iridophores and melanophores.

KEY WORDS: Pigment pattern formation, Cell-cell interactions, Gap junctions, Xanthophores, Iridophores, Melanophores, Zebrafish

INTRODUCTION

The striped coloration of adult zebrafish has emerged as a model system to study pattern formation by cell-cell interaction *in vivo* (Irion et al., 2016; Kelsh, 2004; Parichy and Spiewak, 2015; Singh and Nüsslein-Volhard, 2015; Watanabe and Kondo, 2015). The pattern of longitudinal dark and light stripes on the flank of the fish is composed of black melanophores, orange/yellow xanthophores and silvery or bluish iridophores. This color pattern is produced during a phase called metamorphosis, by the precise arrangement and superimposition of all three cell types in the skin of the fish (Hirata et al., 2003, 2005; Parichy et al., 2009).

Max Planck Institute for Developmental Biology, Spemannstrasse 35, Tübingen 72076, Germany.
*Present address: Ernst & Young GmbH, Eschborn, Frankfurt/M 65760, Germany. ‡Present address: Novartis Institutes for BioMedical Research, 250 Massachusetts Ave, Cambridge, MA 02139, USA. §Present address: Max Planck Institute for Infection Biology, Charitéplatz 1, Berlin 10117, Germany.

¶Authors for correspondence (Prateek.mahalwar@tuebingen.mpg.de; uwe.irion@tuebingen.mpg.de)

U.I., 0000-0003-2823-5840

Received 5 October 2016; Accepted 11 October 2016

In the dark stripes, melanophores are covered by loose blue iridophores and a net of highly branched (stellate) and faintly colored xanthophores; whereas the light stripes are composed of an epithelial-like sheet of dense iridophores covered by a compact net of orange xanthophores (Fig. 1A) (Mahalwar et al., 2014; Singh et al., 2016, 2014). Homotypic interactions between cells of the same type determine their collective migration and spacing during pattern formation (Walderich et al., 2016). Although it is clear that heterotypic interactions among all three types of pigment cells are necessary to generate the striped pattern (Frohnhöfer et al., 2013; Irion et al., 2014a; Singh et al., 2015), the outcome of these heterotypic interactions at the cellular level is not understood. In mutants where one type of pigment cells is absent [for example *nacre/mitfa* lacking melanophores (Lister et al., 1999), *pfeffer/csf1ra* lacking xanthophores (Parichy et al., 2000b) or *shady/ltk* lacking iridophores (Fadeev et al., 2016; Lopes et al., 2008)], only remnants of the normal stripe pattern are formed by the remaining two types of cells (see examples in Fig. 1). Together with data from ablation experiments (Nakamasu et al., 2009; Yamaguchi et al., 2007), this indicates that a number of heterotypic interactions among the different types of pigment cells are essential for the generation of the pattern (Frohnhöfer et al., 2013; Maderspacher and Nüsslein-Volhard, 2003). At the molecular level a few components mediating these heterotypic interactions have been identified so far, including gap junctions and ion channels (Irion et al., 2014a; Iwashita et al., 2006; Watanabe et al., 2006). Gap junctions are membrane channels allowing the communication between neighboring cells, and we have previously shown that two different subunits of gap junctions, Cx41.8 and Cx39.4 encoded by the *leopard* (*leo*) (Watanabe et al., 2006) and *luchs* (*luc*) (Irion et al., 2014a) genes, respectively, are required in melanophores and xanthophores, but not in iridophores for normal pattern formation. In both *leo* and *luc* loss-of-function mutants the dark melanophore stripes are dissolved into spots, and the light stripe areas are expanded. Dominant hypermorphic alleles of both *leo* and *luc* exist, and they lead to meandering melanophore patterns or even spots in heterozygous fish. Double mutants for *leo* and *luc* loss-of-function alleles display a very severe phenotype, the pattern is completely dissolved with single melanophores scattered on a uniform light sheet of epithelial-like dense iridophores covered by a net of xanthophores. Mutants homozygous for the strongest of the dominant *leo* alleles, leo^{tK3}, show the same strong phenotype, arguing that both connexins can form heteromeric and homomeric gap junctions (Irion et al., 2014a; Maderspacher and Nüsslein-Volhard, 2003), which was confirmed by *in vitro* studies (Watanabe et al., 2015). This suggests that the communication between xanthophores and melanophores via heteromeric gap junctions provides signals to the dense iridophores to induce the transition into the loose shape required for dark stripe formation.

Biology Open

Biology Open (2016) 5, 1680-1690 doi:10.1242/bio.022251

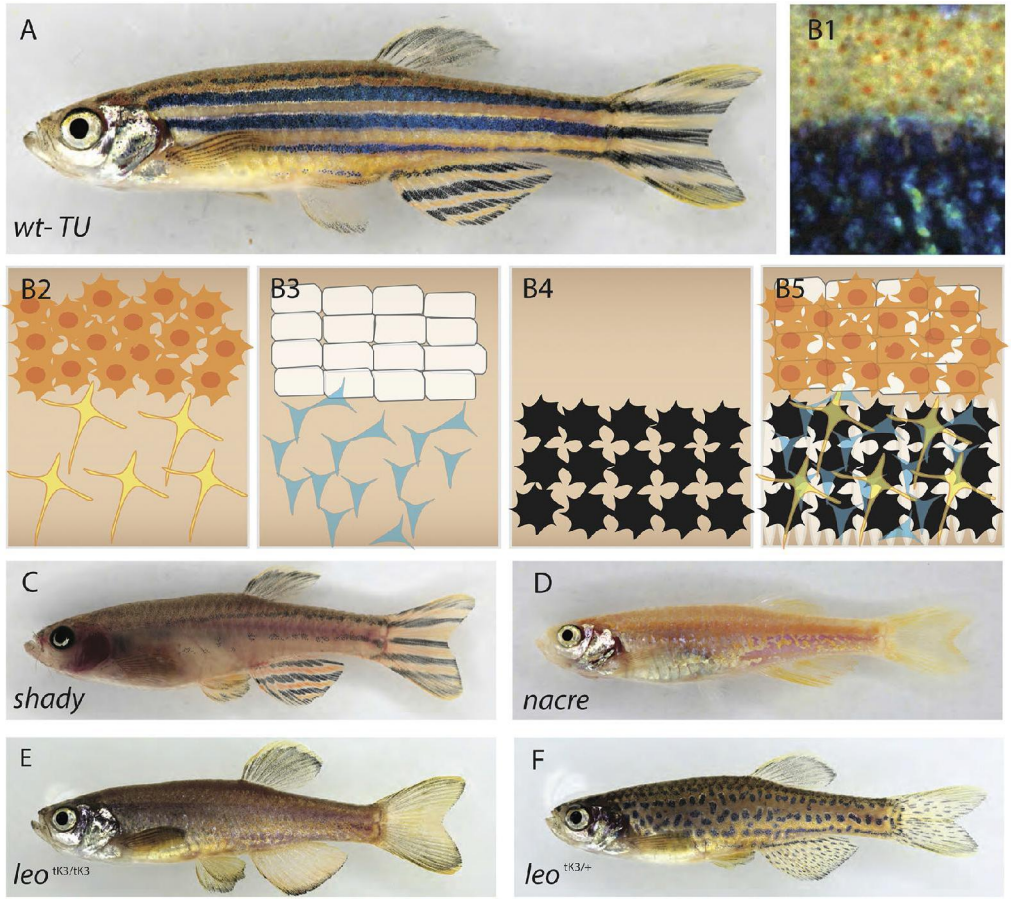

Fig. 1. Pigment cell organization in wild-type and mutant zebrafish. (A) Wild-type zebrafish, and (B1) close up view of the stripe pattern showing light and dark stripe regions. (B2-5) Schematic organization of pigment cells: (B2) xanthophores are compact and densely packed in the light stripe, loose and stellate in the dark stripe; (B3) iridophore layer beneath xanthophores – epithelial-like packing of silvery iridophores in the light stripe, loose and blue in the dark stripe; (B4) melanophores are only present in the dark stripe region; (B5) precise superimposition of all the three cell types results in golden light stripes and blue/black dark stripes. (C) *shady* lack most iridophores. (D) *nacre* lacks all the neural crest-derived melanophores. (E) Homozygous *leopard*$^{tK3/tK3}$. (F) Heterozygous *leopard*$^{tK3/+}$.

Key features of the stripe patterning process are the acquisition of precise cell shapes, as well as the correct cell density and the appropriate coloration. Xanthophores acquire their shape, density and color in a context-dependent manner, in the light stripe areas they are present at high density as compact and bright orange cells, whereas they are stellate, faintly pigmented and at lower density in the dark-stripe regions. To investigate the cellular and molecular basis of these cell behaviors, here we use fluorescently labeled xanthophores combined with long-term *in vivo* imaging in various mutants that affect pigment cell development and their interactions. We observe that heterotypic interactions with iridophores and melanophores regulate context-dependent changes in cell shape and density of xanthophores. We show that dense iridophores are required to instruct xanthophores to increase in density and adopt a compact shape. The cellular interactions leading to these behaviors depend on gap junctions formed by *leo* and *luc*. Further, we show that melanophore-xanthophore interactions can be divided into two phases: an initial phase, independent of *leo/luc* gap junctions, and a later phase, during which these junctions are essential. Our results emphasize the importance of an *in vivo* model to study heterotypic cell-cell interactions and their consequences for cell proliferation and behavior, as well as the suitability of zebrafish to investigate the role of gap junctions *in vivo*.

RESULTS

Xanthophore density is reduced in mutants lacking iridophores, and in mutants lacking functional gap junctions

In adult zebrafish xanthophores are present in light stripes and dark stripes. In the dark stripes they cover the melanophores at relatively low density, display a stellate shape and faint coloration; and in the light stripes xanthophore density is much higher, the cells are more compact and more intensely pigmented (Fig. 1A,B1-B5) (Hirata et al., 2003; Mahalwar et al., 2014). To investigate whether these differences depend upon the presence of iridophores and melanophores, and their interactions with xanthophores, we analyzed xanthophore distribution in *shady*, which lack most iridophores (Fig. 1C), in *nacre*, which lack melanophores (Fig. 1D), and in *leo*^{tK3}, in which gap junction-mediated cell-cell interactions among xanthophores and melanophores are abolished in a dose-dependent manner (*leo*^{tK3} homozygote in Fig. 1E; *leo*^{tK3}

Biology Open (2016) 5, 1680-1690 doi:10.1242/bio.022251

heterozygote in Fig. 1F). Fig. 2 shows xanthophore distribution and morphology in the skin of adult zebrafish in these mutants and in wild type (Fig. 2A1-E4, quantification in Fig. 2F; see Materials and Methods for labeling and counting of xanthophores). Dense iridophores that show an epithelial-like organization are present in the light-stripe regions of wild-type fish, in *nac* mutants and in homozygous $leo^{tK3/tK3}$ mutants, as shown by membrane localized Tjp1A (Fig. S1) (Fadeev et al., 2015).

As compared to the xanthophore density in the light-stripe regions of wild type (≈350±34 cell/mm^2; n=10 animals), we observe very low densities of xanthophores in *shady* (≈116±15 cells/mm^2; n=10 animals), and in leo^{tK3} mutants (≈168±21 cells/mm^2; n=10 animals) in heterozygotes, and (≈149±12 cells/mm^2; n=10 animals) in homozygotes. In *nacre* mutants, where no melanophores are present and dense iridophores form only a rudimentary first light stripe with irregular borders towards loose iridophores characteristic of dark stripes (Fig. 1D) (Frohnhöfer et al., 2013), we find that xanthophores covering the dense epithelial-like sheet of iridophores show roughly the same density (≈370±24 cells/mm^2; n=10 animals) as in the light stripes of wild-type fish. Thus iridophores, but not melanophores, are necessary for the high density of xanthophores in the light-stripe regions. In the regions where loose iridophores are present in *nac* mutants, corresponding to dark-stripe regions in wild type, the density of xanthophores is significantly lower (≈229±18 cells/mm^2; n=8 animals), but still higher than in wild-type dark stripes. This suggests that the reduction in the density of xanthophores in the dark stripes is dependent on melanophores. Strikingly, we find a net of xanthophores of uniform low density covering the epithelial-like dense sheet of iridophores in leo^{tK3} mutants. This low density of xanthophores, comparable to the density observed in *shd* mutants, indicates a communication defect between xanthophores and iridophores in leo^{tK3}.

Xanthophore organization depends upon the presence of epithelial-like dense iridophores and functional gap junctions

The analysis of xanthophore shape and distribution using cell type-specific markers further revealed the role of cell-cell interactions in xanthophore organization (Fig. 2A1-E4; Fig. 3). In wild-type animals, we observed a net of compact and densely packed xanthophores in the light stripe areas (arrowheads in Fig. 2A3-A4), and loose cells with a stellate appearance in the dark stripes (arrow in Fig. 2A3; Fig. S2A). In *shady* mutants, in the absence of iridophores no compact xanthophores are detectable in the light stripes, the cells display a branched morphology with thin cellular projections (Fig. 2B1-B4; arrows in Fig. 2B3-B4). In *nacre*, in the absences of melanophores xanthophores are compact in the regions with dense iridophores (Fig. 2C1-C4; arrowheads in Fig. 2C3-C4). However, in the regions devoid of dense iridophores, the xanthophores do not acquire a compact shape, they appear star-like and are loosely packed (arrows in Fig. 2C3-C4). Strikingly, we found a uniform distribution of xanthophores, albeit at low density, in the trunk along the dorso-ventral axis in homozygous leo^{tK3} mutants (Fig. 2D1-D4; arrowheads in Fig. 2D3-D4). To further investigate the consequences of non-functional gap junction channels on xanthophore behavior *in vivo*, we imaged labeled xanthophores in wild-type and leo^{tK3} mutant fish at 15 mm standard length (SL), the stage when mutants start to differ phenotypically from wild type. The uniform distribution of xanthophores was visible in leo^{tK3} mutants even at this stage, whereas wild-type animals already displayed a higher density of xanthophores in the light stripes as compared to the dark stripes (Fig. S2B). In heterozygous leo^{tK3} mutants, which produce melanophore spots, the distribution of xanthophores is different between light areas and dark spots (Fig. 2E1-E4). These data indicate that gap junction-dependent cellular interactions with the other two types of chromatophores are necessary for the acquisition of the appropriate size and shape of xanthophores in the skin of zebrafish.

Xanthophore morphology depends on iridophores

Xanthophores in leo^{tK3} mutants appear to be larger than in wild type and show a different morphology (Fig. S2). To quantify these differences, we measured the actual cellular area and the area of a simple polygon covering the cell (convex hull) for individual xanthophores from wild type and mutants (see Materials and Methods for the measurement of cell area). In wild type, compact xanthophores of the light stripe (Fig. 3A) and stellate xanthophores of the dark stripes (Fig. 3B) show distinct morphologies, reflected in the different ratios of cellular area to convex hull (Fig. 3E-F). Xanthophores in homozygous leo^{tK3} mutants show morphology that is neither identical to compact xanthophores of the light stripes nor to stellate cells of the dark stripes in wild type (Fig. 3C; quantification in Fig. 3E-F). We find that the area covered by the xanthophores in leo^{tK3} mutants is larger than for compact light stripe xanthophores in wild type; however, the ratio of cellular area to convex hull is marginally lower, indicating that the cell morphology is slightly less compact. In the absence of iridophores, in *shady* mutants, xanthophores display an intermediate phenotype, but they are clearly more branched than in leo^{tK3} mutants (Fig. 3D; quantification in Fig. 3E-F).

To confirm the role of dense iridophores in leading to a higher density and more compact organization of xanthophores, we imaged labeled xanthophores in *shady* and *rose* (Parichy et al., 2000a) mutants. They both lack iridophores, but sometimes produce random small patches of dense 'escaper' iridophores (Frohnhöfer et al., 2013). Here we observe a higher density of xanthophores associated with these patches of dense iridophores as compared to the areas outside, where no iridophores are present (Fig. 4A; Fig. S3). A similar situation is found in *erbb3b* mutants (aka *hypersensitive*, *hps* or *picasso*) (Budi et al., 2008). Due to a partial absence of dorsal root ganglia and the associated melanophore and iridophore stem cells, large portions of the body in *erbb3b* mutants are devoid of iridophores and melanophores. $erbb3b^{t21411}$ is a weak allele, which leads to variable missing patches of iridophores and melanophores (Dooley et al., 2013). However, xanthophores are unaffected in these mutants and are present in the regions lacking melanophores and iridophores. This allowed us to study the density and shapes of xanthophores in the absence of the other two pigment cell types. Consistent with our findings in *shady* and *nacre* mutants, we observed a low density of xanthophores with thin cellular projections in the patches devoid of melanophores and iridophores in *erbb3b* mutants (Fig. 4B). In these mutants iridophores divide and slowly fill the gaps (Dooley et al., 2013; Walderich et al., 2016), as this happens we also see a change in shape and compactness of xanthophores (Fig. 4B), consistent with an instructive role of dense iridophores in this process. These three independent observations confirm that the close spacing and compact organization of xanthophores depends on the interaction with the epithelial-like sheet of dense iridophores.

Taken together, these results show a direct role of iridophores in the regulation of xanthophore behavior, regarding cell shape and density. In the absence of iridophores, in *shady* mutants, xanthophores stay at low density and do not display compact cell shapes. Melanophores are not involved in the change in cell density

Biology Open (2016) 5, 1680-1690 doi:10.1242/bio.022251

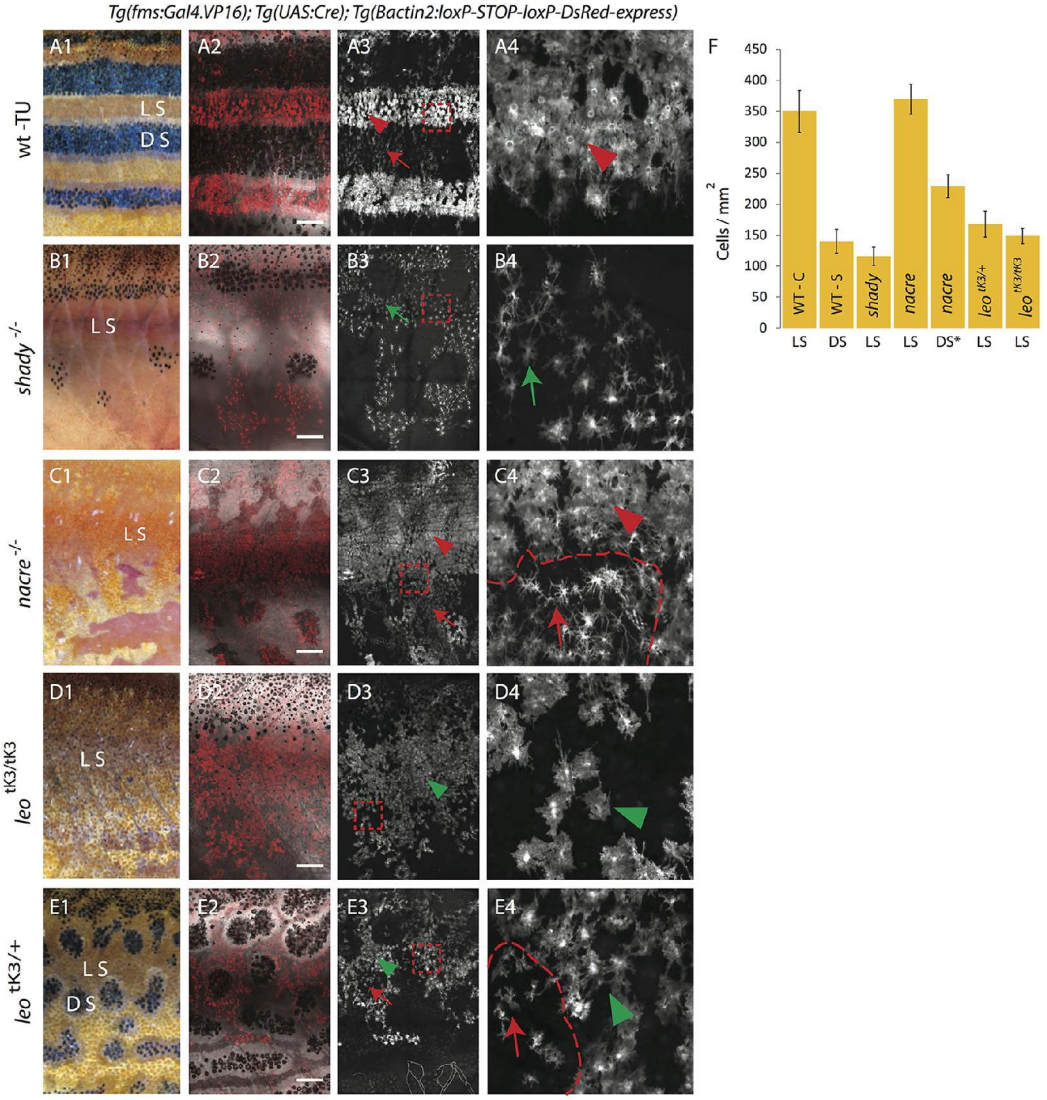

Fig. 2. Density and organization of xanthophores in various pigment cell mutants. DsRed-positive xanthophores labeled with *Tg*(*fms:Gal4.VP16*); *Tg*(*UAS:Cre*); *Tg*(*βactin2:loxP-STOP-loxP-DsRed-express*) in wild type and mutants. Due to variegated expression of the transgenes not all xanthophores are labelled. (A1-4) Wild type. (A1) Pigmentation pattern in adult wild-type fish (TU), LS, light stripe; DS, dark stripe. (A2) compact xanthophores (arrowhead) in the light stripe and loose xanthophores (arrow) the in dark stripe areas. (A3) A magnified image of the light stripe region in wild-type fish (red dotted box in A3) shows the high density of compact xanthophores (red arrowhead). (B1-4) Homozygous *shady* mutants lacking iridophores. (B1,B2) Overview showing the residual melanophore pattern in the mutant. In (B2,B3) the uniform organization of xanthophores (green arrow) is visible. (B4) Magnified image (red dotted box in B3) shows lower density and different morphology of xanthophores (green arrow). (C1-4) Homozygous *nacre* mutants lacking melanophores. (C1,C2) Overview showing irregular areas of epithelial-like dense iridophores; LS, light stripe. In (C3) the compact (arrowhead) and loose (arrow) shape of xanthophores is visible. (C4) Magnified image (red dotted box in C3) shows high (arrowhead) and low (arrow) density of xanthophores at a light stripe border area (dotted red line). (D1-4) Homozygous leo^{tK3tK3} mutant. (D1,D2) Overview showing that all three pigment cell types are present. In (D3,D4) the low density and uniform distribution of xanthophores (green arrowhead) is visible; (D4) magnified image (red dotted box in D3) shows uniform cell shape and distribution of xanthophores (green arrowhead). (E1-4) Heterozygous leo^{tK3} mutants. (E1,E2) Overview indicating the light stripe (LS) and dark stripe (DS) areas. In (E3) the low density but non-uniform distribution of xanthophores in light (green arrow head) and dark (red arrow) stripe regions is visible. (E4) Magnified image (red dotted box in E3) showing stellate (arrow) and compact (green arrowhead) xanthophores with lower density at a melanophore spot boundary (dotted red line). Scale bars: 500 µm. (F) Graph showing the density (number of xanthophores per mm^2) in light or dark stripe regions of wild type and mutants. Values are presented as mean± standard deviation. Asterisk indicate the statistical significance compared to the cell density in wild-type light stripe using Student's *t*-test. Wild-type compact (WT-C) in light stripe (LS): 349.72 cells/mm^2 ±33.67, Wild-type stellate (WT-S) in dark stripe (DS): 139.82 cells/mm^2±19.16 (P<0.0001); homozygous *shady* light stripe (*shady* -LS): 116.26 cells/mm^2±14.55 (P<0.0001), homozygous *nacre* light stripe (*nacre* -LS): 369.54 cells/mm^2±24.30, homozygous *nacre* dark stripe (*nacre* -DS): 229 cells/mm^2 ±18, heterozygous, leo^{tK3} light stripe ($leo^{tK3/+}$ - LS): 168.03 cells/mm^2±21.06 (P<0.0001), homozygous leo^{tK3} light stripe ($leo^{tK3/tK3}$ - LS): 148.71 cells/mm^2±12.28 (P<0.0001). n=10 adult (90 dpf) fish per genotype, except for *nacre* dark stripe, n=8.

Biology Open (2016) 5, 1680-1690 doi:10.1242/bio.022251

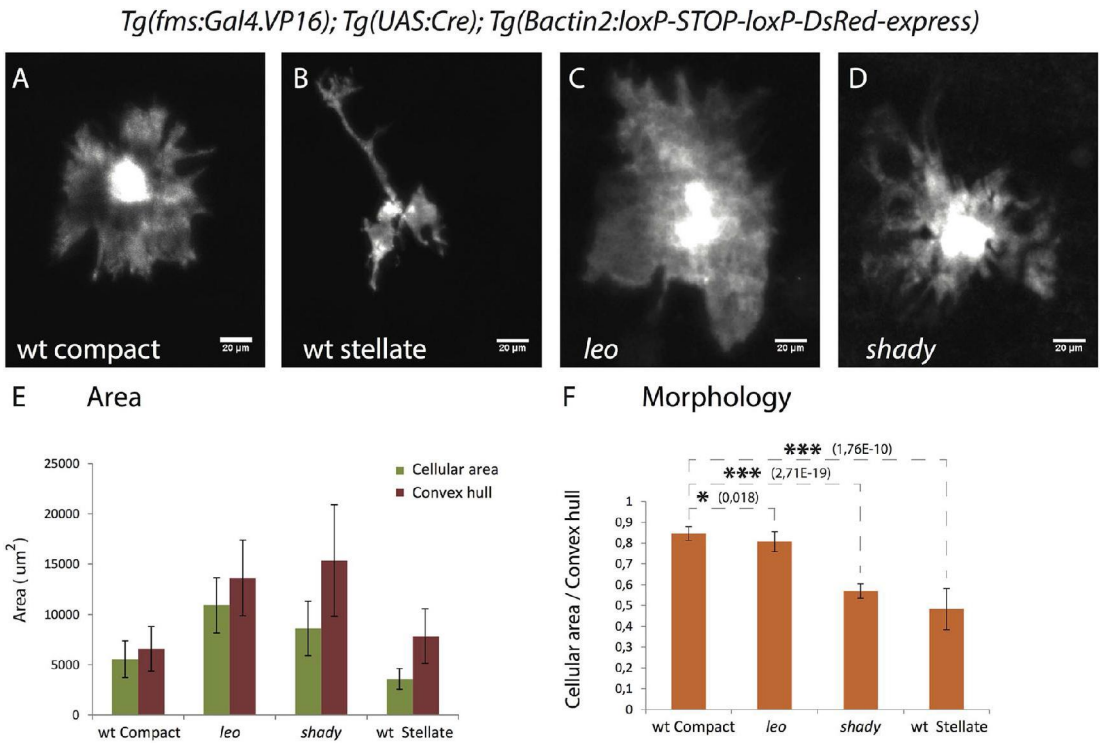

Fig. 3. Xanthophore cell morphologies. (A-D) High resolution images of xanthophores in wild type and mutants showing the different morphologies. (A) Wild-type compact xanthophore, (B) wild-type stellate xanthophore, (C) *leo*$^{tK3/tK3}$ xanthophore and (D) *shady* xanthophore, scale bar: 20 µm. (E) Graph depicting the cell areas (green bars) and the areas of a simple polygon covering the cells (convex hull, red bars) for individual xanthophores in different genotypes (n=15 adult (90 dpf) fish per genotype). (F) Graph showing the ratios of cellular areas to convex hull areas as a measure to quantify the differences in cell morphology between wild type, *leo*$^{tK3/tK3}$ and *shady* mutants. The ratio for compact xanthophores in wild type is significantly higher than for wild-type stellate xanthophores (P<0.0001), xanthophores in *leo*$^{tK3/tK3}$ (P<0.01) and *shady* (P<0.0001) mutants. Asterisks indicate the statistical significance using Student's t-test and error bars indicate standard deviations.

or morphology of the light stripe xanthophores, as these processes also happen in the absence of melanophores in *nacre* mutants. This suggests that the changes in density and shape of xanthophores are mediated by their local interactions with the epithelial-like dense iridophores of the light-stripe regions, and not by long-range interactions with the melanophores of the dark-stripe regions.

Arrival of dense iridophores at the onset of metamorphosis promotes an increase in xanthophore density

To further investigate the dynamics of the observed xanthophore behaviors, we followed fluorescently labeled xanthophores over several weeks in wild-type, *shady* and *leo*^{tK3} mutant fish during metamorphosis (Fig. 5A1-D). We found that in the beginning, before metamorphic iridophores and melanophores appear in the skin, xanthophores cover the body uniformly as a coherent net; there is no difference in the densities and organization of xanthophores in all three cases (Fig. 5A1,B1,C1,D). When iridophores appear along the horizontal myoseptum in the skin of wild-type fish the distances between neighboring xanthophores decrease (Fig. 5D), and consequently the cells become more compact and their density increases, leading to clearly distinct xanthophore populations in the dark and light stripe areas (red arrow and arrowhead in Fig. 5A2-A5; Fig. S4A) (Mahalwar et al., 2014). In *shady* mutants, where no iridophores appear during metamorphosis, distances between neighboring xanthophores do not decrease (Fig. 5D) and the cell density remains low and uniform (green arrow in Fig. 5B2-B5; Fig. S4B). Also in homozygous *leo*^{tK3} mutants the density of xanthophores remains low and uniform during the course of metamorphosis (green arrowhead in Fig. 5C1-C5,D; Fig. 4C). This analysis suggests that the cell-cell communication between xanthophores and iridophores in *leo* mutants is affected already during early stages of metamorphosis, before the appearance of melanophores. Therefore we conclude that iridophores and xanthophores interact directly and that gap junctions composed of Cx41.8 and Cx39.4 are involved in these cell-cell communications.

Multi-level melanophore–xanthophore interactions

When melanophores appear in the skin of wild-type fish during metamorphosis, xanthophores in the vicinity retract their cellular protrusions to give way (Fig. 6A1-A3; Fig. S5A). Further, with the appearance of more melanophores in the presumptive dark-stripe regions, xanthophores change their shape and become stellate (Fig. 6D1-D1′) (Mahalwar et al., 2014). To test if these behaviors are dependent on iridophores, which are present in the dark and light-stripe regions, or solely on melanophores in the dark stripes, we observed xanthophores and melanophores in *shady* mutants. We found that xanthophores reorganize their protrusions and become

Biology Open (2016) 5, 1680-1690 doi:10.1242/bio.022251

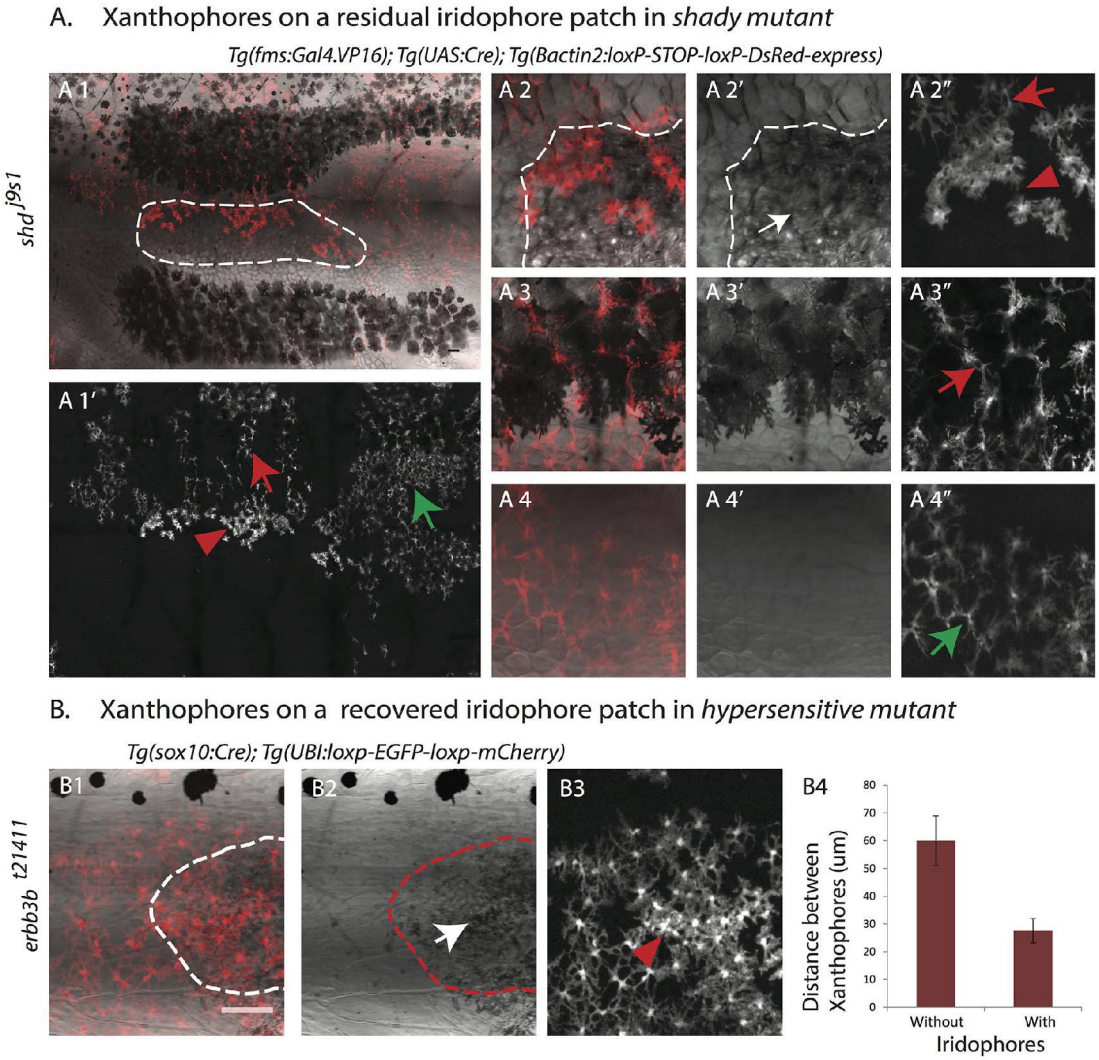

Fig. 4. Iridophores lead to a higher density and change in the organization of xanthophores. (A) Adult *shady* mutant with DsRed-positive xanthophore patches labeled with *Tg*(*fms:Gal4.VP16*); *Tg*(*UAS:Cre*); *Tg*(*βactin2:loxP-STOP-loxP-DsRed-express*). Xanthophores show a compact organization and higher density (red arrowhead in A1′ and A2″) on top of escaper iridophores (outlined in A1 and white arrow in A2′). They are stellate and loosely packed on top of the dark stripe melanophores (red arrow in A1′ and A3″). (A4-4″) Magnified image of the first light-stripe region shows the stellate shape of xanthophores in the absence of the other two pigment cell types (green arrow in A1′ and A4″). (B) *erbb3*^{bt21411} metamorphic fish showing a patch of missing iridophores and patchy clones of mCherry-positive xanthophores labeled with *Tg*(*sox10:Cre*); *Tg*(*UBI:loxp-EGFP-loxp-mCherry*). The recovery of iridophores (outlined in B1 and B2, white arrow in B2) leads to denser and more compact xanthophores (red arrowhead in B3); in the absence of iridophores xanthophores remain at lower density. Scale bar: 100 µm. (B4) Graph showing the distances (in µm) between the centers of neighboring xanthophores in the absence or presence of iridophores (*n*=15 pairs).

stellate when they encounter melanophores, even in the absence of iridophores (Fig. 6B1-B3,D2-D2′, Fig. S5B). This indicates that direct interactions between melanophores and xanthophores lead to the observed cellular behaviors and that iridophores are not involved in these processes. In homozygous *leo*^{tK3} mutants we found that xanthophores also react to newly arriving melanophores by retracting their cellular protrusions, thus making space for the melanophores (Fig. 6C1-C3, Fig. S5C). However, they do not ultimately change their shape to become stellate, like they do in the dark-stripe regions of wild-type fish (Fig. 6D4-D4′). In heterozygous *leo*^{tK3} mutants the xanthophores on top of the melanophore spots become stellate, demonstrating that some gap junction intercellular signaling activity is still present in these heterozygotes (Fig. 6D3-D3′). From this analysis, we conclude that melanophores first induce xanthophores to retract their cellular protrusions, followed later by the acquisition of the characteristic stellate morphology of the xanthophores in the dark stripe. Whereas the early aspects of this interaction are *leo*-independent, the acquisition of the final stellate shape does depend upon *leo*-mediated interactions between melanophores and xanthophores, as it does not occur in *leo*^{tk3} mutants.

Biology Open (2016) 5, 1680-1690 doi:10.1242/bio.022251

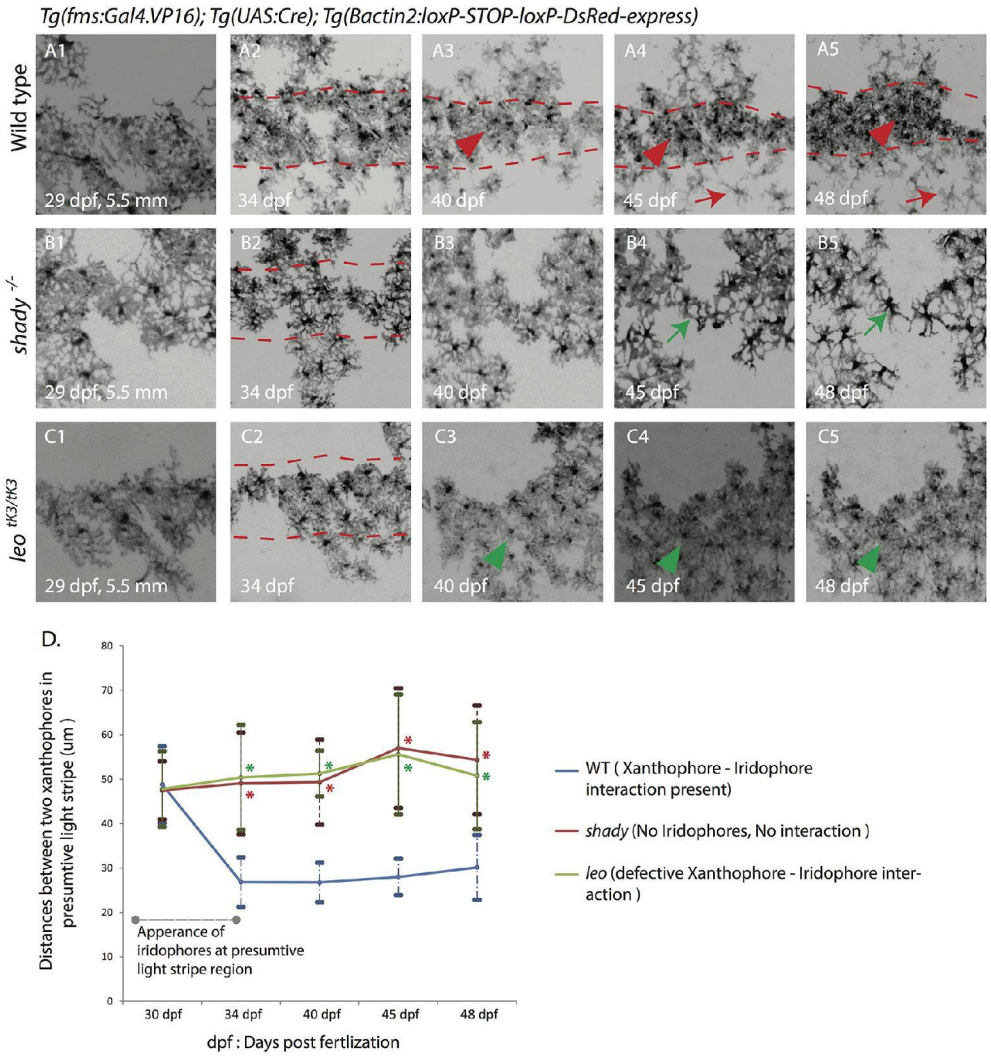

Fig. 5. Development of xanthophore distribution and organization during stripe pattern formation. Time-lapse images of DsRed-positive xanthophores labeled with *Tg*(*fms:Gal4.VP16*); *Tg*(*UAS:Cre*); *Tg*(*βactin2:loxP-STOP-loxP-DsRed-express*) in wild type and mutants during metamorphosis. (A1-5) Wild-type xanthophores reorganize upon the arrival of metamorphic iridophores and melanophores form a uniform density into two different forms: stellate and less dense (red arrowhead) in the dark-stripe areas (between the red dotted lines), and compact and dense in the light-stripe areas (red arrowheads). (B1-5) Xanthophores in *shady* mutants stay at a uniform density (green arrow) in the dark-stripe areas (between the red dotted lines). (C1-5) In homozygous *leo*^{tK3} mutants xanthophores stay at a uniform density (green arrowhead) all over the body of the fish even after the arrival of iridophores and melanophores, dark-stripe areas are shown between red dotted lines. Scale bars: 100 µm. (D) Graph showing the differences in cell densities during development of wild type, *leo*^{tK3} and *shady* mutants. The distances (in µm) between the centers of neighboring xanthophores in the prospective light-stripe regions at various developmental time points are depicted (n=25 cell pairs from 5 fish per genotype). Error bars indicate standard deviations. Asterisks indicate the statistical significance compared to wild type using Student's t-test (all P values are P<0.0001).

Gap junctions are cell-autonomously required in xanthophores for their cell shape transition

When we transplanted *Tg*(*pax7:GFP*)-labeled wild-type xanthophores into homozygous *leo*^{tK3} mutant hosts carrying *Tg* (*kita:GAL4,UAS:mCherry*), which labels xanthophores and melanophores, we found a clear difference in the density and shape between wild-type and mutant xanthophores in the resulting chimeric animals. The wild-type cells are compact and more densely organized than the mutant cells (Fig. 7A). Further, in dark-stripe regions wild-type xanthophores acquire a stellate shape even in the presence of mutant melanophores (Fig. 7B). Conversely, mutant xanthophores do not respond to the presence of wild-type melanophores; however, wild-type xanthophores do respond and show stellate shapes (Fig. 7C). This shows that gap junctions are autonomously required in xanthophores for the dense and compact organization in the light stripes and the stellate shapes in the dark stripes.

DISCUSSION

In this study we analyzed the cell-cell interactions during pigment pattern formation in zebrafish from a xanthophore perspective. The

Biology Open (2016) 5, 1680-1690 doi:10.1242/bio.022251

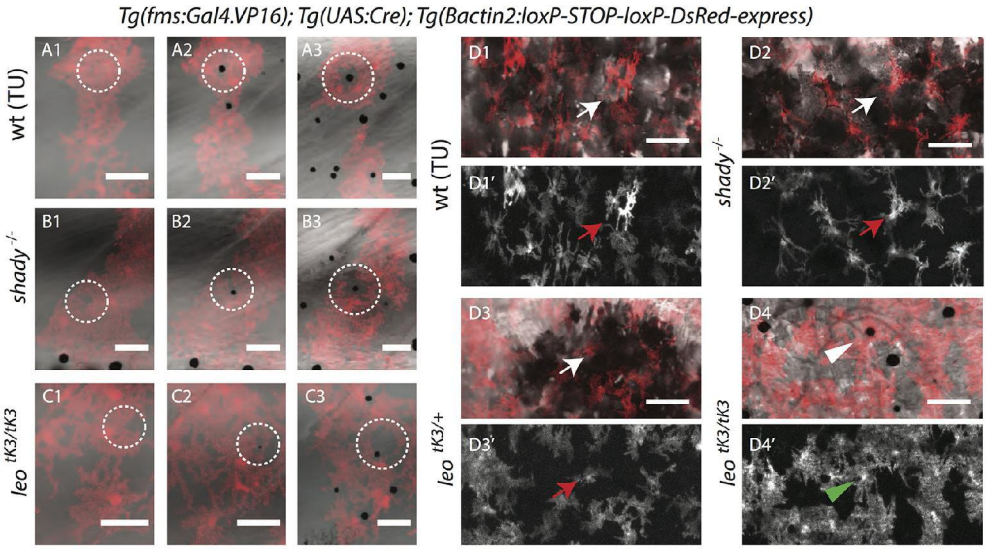

Fig. 6. Xanthophore-melanophore interactions. (A-C) Time-lapse recordings of melanophores and DsRed-labeled xanthophores during metamorphosis. (A1-3) Wild-type, (B1-3) *shady* and (C1-3) homozygous *leo*^{tK3} mutant xanthophores retract their protrusions to give space to the newly arriving melanophores (inside white dotted circles). (D1-1′) Wild-type, (D2-2′) *shady* and (D3-3′) heterozygous *leo*$^{tK3/+}$ xanthophores (white and red arrows) reorganize themselves to adopt stellate shapes upon the arrival of more melanophores in the presumptive dark-stripe regions. (D4-4′) In homozygous *leo*$^{tK3/tK3}$ mutants xanthophores (green arrowhead, xanthophore above melanophore) do not adopt a stellate shape nor loose morphology. Scale bars: 100 µm.

outcome of cell-cell interactions depends upon the chromatophore types involved. We observe that heterotypic (xanthophore-iridophore and xanthophore-melanophore) interactions regulate differential density and shape of xanthophores. It was recently shown that homotypic (xanthophore-xanthophore) interactions regulate the xanthophore coverage in the skin (Walderich et al., 2016). Taken together, we conclude that a combination of homotypic and heterotypic interactions regulate precise patterning of xanthophores during color pattern formation.

We found that heterotypic interactions with epithelial-like dense iridophores are required for xanthophores to increase their compactness in light-stripe regions. In the absence of iridophores, in *shady* mutants, xanthophore density stays low and does not increase during metamorphosis. When iridophores gradually recover in *erbb3b* mutants and start to fill in gaps previously devoid of iridophores, xanthophore density also increases. This xanthophore behavior does not depend on the presence of melanophores, as it also occurs in *nacre* mutants. Previously it was reported that iridophores act on xanthophores via Csf1, an extracellular ligand expressed in iridophores that promotes xanthophore development (Patterson and Parichy, 2013). However, the interaction we find between dense iridophores and xanthophores is likely to be more direct, as it requires functional gap junctions made from Cx41.8 and Cx39.4. In *leo*^{tK3} mutants, where these channels are non-functional, xanthophores stay at low density despite the presence of iridophores. Our transplantation experiments show that this requirement is cell-autonomous to xanthophores, which is in agreement with our previous findings that Cx41.8 and Cx39.4 are only required in xanthophores and melanophores, but not in iridophores (Irion et al., 2014a; Maderspacher and Nüsslein-Volhard, 2003). If this heterotypic interaction among iridophores and xanthophores occurs indeed via gap junctions, and not simply via hemi-channels in the xanthophore plasma membrane, a different connexin on the iridophore side must exist. Such a connexin has not yet been identified, however, our hypothesis that it exists might be corroborated by the analysis of *schachbrett* (*sbr*) mutants, where a spotted pattern is produced. It was shown that Tjp1A is affected in this mutant, the protein is specifically expressed in iridophores and known to interact with the C-termini of several connexins (Fadeev et al., 2015). This could provide the link from gap junctions to the cytoplasm in iridophores. Reverse genetic approaches may be useful in identifying novel iridophore-specific gap junction components (Irion et al., 2014b; Hwang et al., 2013a,b).

The interactions between xanthophores and melanophores, which lead to shape changes in the xanthophores, are only partially mediated by the known gap junctions, as in homozygous *leo*^{tK3} mutants we still observe that xanthophores clearly sense the appearing melanophores and rearrange their cellular protrusions; however, they do not ultimately change their shape to become stellate. This indicates that there are at least two steps in the interactions between melanophores and xanthophores and that the initial recognition is independent of *leo* and *luc* gap junctions. The signaling molecules that mediate this initial interaction are unknown; however, several molecules such as Kcnj13, an inward rectifying potassium channel (Inaba et al., 2012); spermidine, a polyamine (Frohnhöfer et al., 2016); Tetraspanin3c, a transmembrane scaffolding protein (Inoue et al., 2014); and Notch/Delta signaling (Eom et al., 2015; Hamada et al., 2014) have been identified that regulate cell-cell interactions during color pattern formation. It is possible that some of these molecules mediate gap junction-independent communication between melanophores and xanthophores.

Later steps during the interactions between melanophores and xanthophores are dependent on functional gap junctions as they don't occur in homozygous *leo*^{tK3} mutants. However, our transplantation experiments show that wild-type xanthophores can still respond to mutant melanophores, suggesting that on the melanophore side different connexins could be involved in the

Biology Open (2016) 5, 1680-1690 doi:10.1242/bio.022251

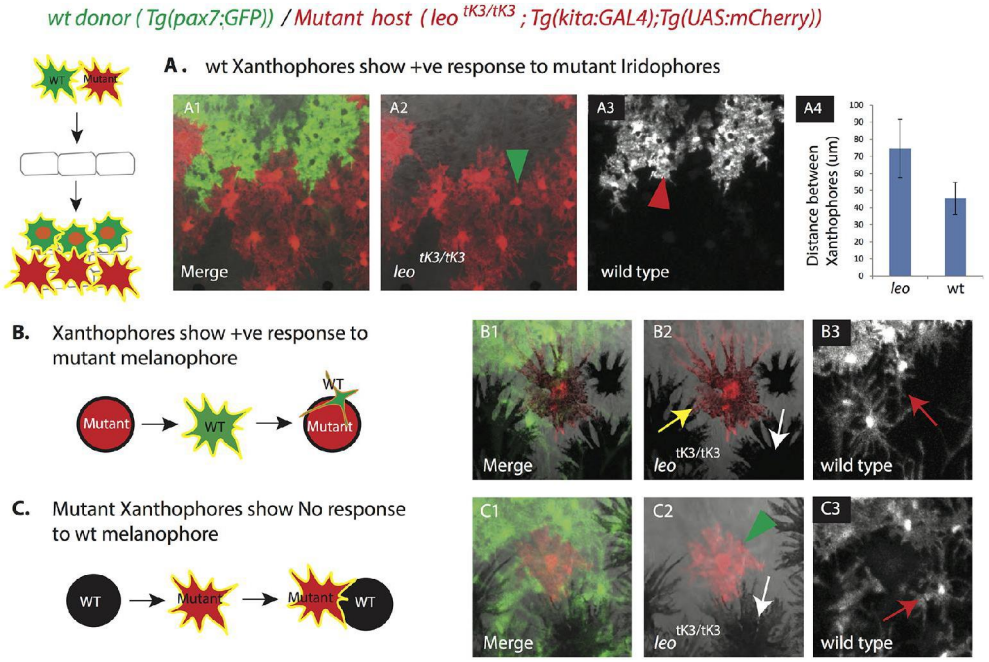

Fig. 7. Transplantation of wild-type xanthophores labeled with *Tg*(*pax7:GFP*) into *leo*$^{tK3/tK3}$ mutants carrying *Tg*(*kita:GAL4*);*Tg*(*UAS:mCherry*). (A1) Different density of wild-type (green cells, red arrow head in A3) and mutant xanthophores (red cells, green arrow head in A2) in an adult chimeric animal. (A4) Graph showing the distances (in µm) between the centers of neighboring wild-type and mutant xanthophore pairs in the chimera, error bars indicate standard deviation (n=15 pairs). (B) A wild-type xanthophore (labeled with GFP) becomes stellate (red arrow in B3) in response to a mutant melanophore (labeled with mCherry, yellow arrow in B2). White arrow in B2 points to wild-type melanophores. (C) No response and change in shape of mutant xanthophores (labeled with mCherry, green arrowhead in C2) in response to wild-type melanophores (no fluorescent label, white arrow in C2). Red arrow in C3 points to wild-type xanthophores (labeled with GFP) showing wild-type morphology in response to wild-type melanophores.

generation of heterotypic and heteromeric gap junctions. Due to its amenability to genetic and cell biological investigation pigment pattern formation, the zebrafish is an attractive model system to study the formation and function of gap junctions *in vivo*. It will be interesting to see if other connexins, expressed in iridophores or melanophores, can be identified and how they might affect the gating properties of gap junctions.

In summary, we demonstrate that gap junctions are required in xanthophores for the cell shape transitions in response to other chromatophores. We also show that iridophores are an integral part of the cell-cell interaction network responsible for generating the striped pattern. Our previous study suggested that xanthophores and melanophores together instruct the patterning of iridophores, here we show that iridophores, in turn, are required to organize xanthophores, suggesting that ultimately a feed-back mechanism involving contact-based interactions between all three types of pigment cells is the basis of stripe pattern formation in the body of zebrafish. We suggest that color pattern formation in zebrafish involves a novel mechanism of patterning dependent on cell shape transitions of xanthophores and iridophores. These shape transitions are dependent on local cell-cell interactions mediated by gap junctions.

MATERIALS AND METHODS

Zebrafish lines

The following zebrafish lines were used: wild type (WT) (TU strain from the Tübingen zebrafish stock center), *nacre*^{w2} (Lister et al., 1999), *shady*^{i9s1} (Lopes et al., 2008), *leo*^{tK3} (Irion et al., 2014a), *rose*^{tAN17X} (Krauss et al., 2014), *hps/erbb3b*^{t21411} (Dooley et al., 2013), *Tg*(*fms*:*GAL4*) (Gray et al., 2011), *Tg*(*UAS:Cre*) (Mahalwar et al., 2014), *Tg*(*βactin2:loxP-STOP-loxP-DsRed-express*) (Bertrand et al., 2010), *Tg*(*kita:GAL4,UAS:mCherry*) (Anelli et al., 2009), *Tg*(*sox10:Cre*) (Rodrigues et al., 2012) and *Tg*(*UBI:loxp-gfp-loxp-mcherry*) (Mosimann et al., 2011), *Tg*(*UAS:EGFP-CAAX*) (Fernandes et al., 2012), *Tg*(*pax7:GFP*) (Alsheimer, 2012).

Zebrafish were raised as described previously (Brand et al., 2002). The staging of metamorphic fish was done as described (Parichy, 2006). All animal experiments were performed in accordance with the rules of the State of Baden-Württemberg, Germany and approved by the Regierungspräsidium Tübingen (Aktenzeichen: 35/9185.46-5 and 35/9185.82-7).

Different methods of labeling xanthophores

Different transgenic lines labeling xanthophores were used in various combinations. All of them are stable transgenic lines, which were crossed into various mutant backgrounds. They label xanthophores using three different promoters: neural crest-specific, *sox 10*; pigment cell-specific, *kitA*; and xanthophore-specific, *fms*. These promoters have been shown to label xanthophores (Anelli et al., 2009; Gray et al., 2011; Mongera et al., 2013). *Tg*(*sox10:Cre*) was used in combination with *Tg*(*UBI:loxp-EGFP-loxp-mCherry*) for the analysis of xanthophores in the *hps* mutant background. *Tg*(*kita:GAL4*) was used in combination with *Tg*(*UAS:mCherry*) to visualize adult xanthophores in *rse* mutants. *Tg*(*fms:Gal4.VP16*) fish were crossed with the following reporter lines to drive fluorophore expression exclusively in xanthophores: *Tg*(*UAS:EGFP-CAAX*), *Tg*(*UAS:Cre*) and *Tg*(*βactin:loxp-STOP-loxp-DsRed*). This combination of four transgenes labels only xanthophores, and was used for the follow-up studies of clusters as well as individual xanthophores. In most of cases not all xanthophores are fluorescently labeled, due to the variegation/patchiness created by the combination of the GAL4, UAS and

responder transgenic lines. Variegated labeling allows us to see individual cells, and follow them during the course of development and distinguish between different morphologies.

Counting of xanthophores

Xanthophore numbers were counted using the scans with multiple channels: transgenic marker (variegation), auto-fluorescence (no variegation) and bright field. Auto-fluorescence marks all the xanthophores; however, double labeling was performed to confirm the presence of xanthophores. Only regions corresponding to the first light stripe were used for counting in all the mutants. Xanthophore counting was done using the 'cell counter' plugin in Fiji (Schindelin et al., 2012). Ten readings from ten fish per genetic background were used to obtain the densities and respective standard deviations.

Area, distance and density of xanthophores

High resolution images were taken to resolve differences between different morphologies of xanthophores in various backgrounds. To calculate the cellular areas, image thresholds were set using the mean algorithm and the values were calculated using the measure option in ImageJ. To obtain a quantitative measure for the different cell morphologies, the convex hull area value of the corresponding cell was also calculated. The final values shown in Fig. 1 were calculated as the ratios between the total cellular areas and the areas of the convex hull. 15 individual cells per genetic background were used to calculate the areas and standard deviation values in Fig. 1. Distances between the centers of neighboring xanthophores were measured using ImageJ.

Image acquisition and processing

Repeated imaging of zebrafish was performed as described in Singh et al. (2014). Images were acquired on a Zeiss LSM 780 NLO confocal microscope. Fiji (Schindelin et al., 2012) and Adobe Illustrator were used for image processing and analysis. Maximum intensity projections of confocal scans of the fluorescent samples were uniformly adjusted for brightness and contrast. Scans of the bright field were stacked using the 'stack focuser' plugin and tile scans.

Blastomere transplantations

Chimeric animals were generated by transplantation of few cells from wild-type embryos carrying *Tg*(*pax7:GFP*) into *leo*$^{tK3/tk3}$ mutant embryos carrying *Tg*(*kita:GAL4,UAS:mCherry*) at blastula stage (Kane and Kishimoto, 2002).

Immunohistochemistry

Antibody stainings were performed as described previously (Fadeev et al., 2015). anti-Tjp1aC was used 1:100, as secondary antibody Alexa Fluor 488 goat anti-mouse (Invitrogen/Molecular Probes, A11008) was used 1:400.

Acknowledgements

We thank Hans-Georg Frohnhöfer for many insightful discussions, and Katherine Rogers, April Dinwiddie and Patrick Müller for comments on the manuscript. We also thank Heike Heth, Tübingen fish facility members and Christian Liebig from light microscopy facility for great support.

Competing interests

The authors declare no competing or financial interests.

Author contributions

P.M., C.N.-V. and U.I. conceived the project; P.M. performed the experiments, U.I. performed the blastula transplantations; A.P.S. provided data for rose mutant and A.F. performed antibody staining. P.M., A.P.S., C.N.V. and U.I. wrote the manuscript.

Funding

This work was funded by the Max-Planck Society.

Supplementary information

Supplementary information available online at
http://bio.biologists.org/lookup/doi/10.1242/bio.022251.supplemental

References

Alsheimer, S. (2012). On Telost muscle stem cell and the vertical myoseptum as their niche. *PhD Disseration*, Eberhard-Karls-Univ. 1-249.

Anelli, V., Santoriello, C., Distel, M., Köster, R. W., Ciccarelli, F. D. and Mione, M. (2009). Global repression of cancer gene expression in a zebrafish model of melanoma is linked to epigenetic regulation. *Zebrafish* **6**, 417-424.

Bertrand, J. Y., Chi, N. C., Santoso, B., Teng, S., Stainier, D. Y. R. and Traver, D. (2010). Haematopoietic stem cells derive directly from aortic endothelium during development. *Nature* **464**, 108-111.

Brand, M., Granato, M. and Nüsslein-Volhard, C. (2002). Keeping and raising zebrafish. In *Zebrafish: A Practical Approach* (ed. C. Nüsslein-Volhard and R. Dahm) pp. 7-37. New York: Oxford University Press.

Budi, E. H., Patterson, L. B. and Parichy, D. M. (2008). Embryonic requirements for ErbB signaling in neural crest development and adult pigment pattern formation. *Development* **135**, 2603-2614.

Dooley, C. M., Mongera, A., Walderich, B. and Nüsslein-Volhard, C. (2013). On the embryonic origin of adult melanophores: the role of ErbB and Kit signalling in establishing melanophore stem cells in zebrafish. *Development* **140**, 1003-1013.

Eom, D. S., Bain, E. J., Patterson, L. B., Grout, M. E. and Parichy, D. M. (2015). Long-distance communication by specialized cellular projections during pigment pattern development and evolution. *eLife* **4**, e12401.

Fadeev, A., Krauss, J., Fröhnhofer, H. G., Irion, U. and Nüsslein-Volhard, C. (2015). Tight junction protein 1a regulates pigment cell organisation during zebrafish colour patterning. *eLife* **4**, 1711.

Fadeev, A., Krauss, J., Singh, A. P. and Nüsslein-Volhard, C. (2016). Zebrafish Leucocyte tyrosine kinase controls iridophore establishment, proliferation and survival. *Pigment Cell Melanoma Res.* **29**, 284-296.

Fernandes, A. M., Fero, K., Arrenberg, A. B., Bergeron, S. A., Driever, W. and Burgess, H. A. (2012). Deep brain photoreceptors control light-seeking behavior in zebrafish larvae. *Curr. Biol.* **22**, 2042-2047.

Frohnhöfer, H. G., Krauss, J., Maischein, H.-M. and Nüsslein-Volhard, C. (2013). Iridophores and their interactions with other chromatophores are required for stripe formation in zebrafish. *Development* **140**, 2997-3007.

Frohnhöfer, H. G., Geiger-Rudolph, S., Pattky, M., Meixner, M., Huhn, C., Maischein, H.-M., Geisler, R., Gehring, I., Maderspacher, F., Nüsslein-Volhard, C. et al. (2016). Spermidine, but not spermine, is essential for pigment pattern formation in zebrafish. *Biol. Open* **5**, 736-744.

Gray, C., Loynes, C. A., Whyte, M. K. B., Crossman, D. C., Renshaw, S. A. and Chico, T. J. A. (2011). Simultaneous intravital imaging of macrophage and neutrophil behaviour during inflammation using a novel transgenic zebrafish. *Thromb. Haemost.* **105**, 811-819.

Hamada, H., Watanabe, M., Lau, H. E., Nishida, T., Hasegawa, T., Parichy, D. M. and Kondo, S. (2014). Involvement of Delta/Notch signaling in zebrafish adult pigment stripe patterning. *Development* **141**, 318-324.

Hirata, M., Nakamura, K., Kanemaru, T., Shibata, Y. and Kondo, S. (2003). Pigment cell organization in the hypodermis of zebrafish. *Dev. Dyn.* **227**, 497-503.

Hirata, M., Nakamura, K.-I. and Kondo, S. (2005). Pigment cell distributions in different tissues of the zebrafish, with special reference to the striped pigment pattern. *Dev. Dyn.* **234**, 293-300.

Hwang, W. Y., Fu, Y., Reyon, D., Maeder, M. L., Kaini, P., Sander, J. D., Joung, J. K., Peterson, R. T. and Yeh, J.-R. J. (2013a). Heritable and precise zebrafish genome editing using a CRISPR-Cas system. *PLoS ONE* **8**, e68708.

Hwang, W. Y., Fu, Y., Reyon, D., Maeder, M. L., Tsai, S. Q., Sander, J. D., Peterson, R. T., Yeh, J.-R. J. and Joung, J. K. (2013b). Efficient genome editing in zebrafish using a CRISPR-Cas system. *Nat. Biotechnol.* **31**, 227-229.

Inaba, M., Yamanaka, H. and Kondo, S. (2012). Pigment pattern formation by contact-dependent depolarization. *Science* **335**, 677.

Inoue, S., Kondo, S., Parichy, D. M. and Watanabe, M. (2014). Tetraspanin 3c requirement for pigment cell interactions and boundary formation in zebrafish adult pigment stripes. *Pigment Cell Melanoma Res.* **27**, 190-200.

Irion, U., Frohnhöfer, H. G., Krauss, J., Çolak Champollion, T., Maischein, H.-M., Geiger-Rudolph, S., Weiler, C. and Nüsslein-Volhard, C. (2014a). Gap junctions composed of connexins 41.8 and 39.4 are essential for colour pattern formation in zebrafish. *eLife* **3**, e05125.

Irion, U., Krauss, J. and Nüsslein-Volhard, C. (2014b). Precise and efficient genome editing in zebrafish using the CRISPR/Cas9 system. *Development* **141**, 4827-4830.

Irion, U., Singh, A. P. and Nüsslein-Volhard, C. (2016). The Developmental Genetics of Vertebrate Color Pattern Formation: Lessons from Zebrafish. *Curr. Top. Dev. Biol.* **117**, 141-169.

Iwashita, M., Watanabe, M., Ishii, M., Chen, T., Johnson, S. L., Kurachi, Y., Okada, N. and Kondo, S. (2006). Pigment pattern in jaguar/obelix zebrafish is caused by a Kir7.1 mutation: implications for the regulation of melanosome movement. *PLoS Genet.* **2**, e197.

Kane, D. A. and Kishimoto, T. (2002). Cell labeling and transplantation techniques. In *Zebrafish: A Practical Approach* (ed. C. Nüsslein-Volhard and R. Dahm), pp. 95-119. New York: Oxford University Press.

Kelsh, R. N. (2004). Genetics and evolution of pigment patterns in fish. *Pigment Cell Res.* **17**, 326-336.

Krauss, J., Frohnhöfer, H. G., Walderich, B., Maischein, H.-M., Weiler, C., Irion, U. and Nüsslein-Volhard, C. (2014). Endothelin signalling in iridophore development and stripe pattern formation of zebrafish. *Biol. Open* **3**, 503-509.

Lister, J. A., Robertson, C. P., Lepage, T., Johnson, S. L. and Raible, D. W. (1999). nacre encodes a zebrafish microphthalmia-related protein that regulates neural-crest-derived pigment cell fate. *Development* **126**, 3757-3767.

Lopes, S. S., Yang, X., Müller, J., Carney, T. J., McAdow, A. R., Rauch, G.-J., Jacoby, A. S., Hurst, L. D., Delfino-Machín, M., Haffter, P. et al. (2008). Leukocyte tyrosine kinase functions in pigment cell development. *PLoS Genet.* **4**, e1000026.

Maderspacher, F. and Nüsslein-Volhard, C. (2003). Formation of the adult pigment pattern in zebrafish requires leopard and obelix dependent cell interactions. *Development* **130**, 3447-3457.

Mahalwar, P., Walderich, B., Singh, A. P. and Nüsslein-Volhard, C. (2014). Local reorganization of xanthophores fine-tunes and colors the striped pattern of zebrafish. *Science* **345**, 1362-1364.

Mongera, A., Singh, A. P., Levesque, M. P., Chen, Y.-Y., Konstantinidis, P. and Nüsslein-Volhard, C. (2013). Genetic lineage labeling in zebrafish uncovers novel neural crest contributions to the head, including gill pillar cells. *Development* **140**, 916-925.

Mosimann, C., Kaufman, C. K., Li, P., Pugach, E. K., Tamplin, O. J. and Zon, L. I. (2011). Ubiquitous transgene expression and Cre-based recombination driven by the ubiquitin promoter in zebrafish. *Development* **138**, 169-177.

Nakamasu, A., Takahashi, G., Kanbe, A. and Kondo, S. (2009). Interactions between zebrafish pigment cells responsible for the generation of Turing patterns. *Proc. Natl. Acad. Sci. USA* **106**, 8429-8434.

Parichy, D. M. (2006). Evolution of danio pigment pattern development. *Heredity (Edinb)* **97**, 200-210.

Parichy, D. M. and Spiewak, J. E. (2015). Origins of adult pigmentation: diversity in pigment stem cell lineages and implications for pattern evolution. *Pigment Cell Melanoma Res.* **28**, 31-50.

Parichy, D. M., Mellgren, E. M., Rawls, J. F., Lopes, S. S., Kelsh, R. N. and Johnson, S. L. (2000a). Mutational analysis of endothelin receptor b1 (rose) during neural crest and pigment pattern development in the zebrafish Danio rerio. *Dev. Biol.* **227**, 294-306.

Parichy, D. M., Ransom, D. G., Paw, B., Zon, L. I. and Johnson, S. L. (2000b). An orthologue of the kit-related gene fms is required for development of neural crest-derived xanthophores and a subpopulation of adult melanocytes in the zebrafish, Danio rerio. *Development* **127**, 3031-3044.

Parichy, D. M., Elizondo, M. R., Mills, M. G., Gordon, T. N. and Engeszer, R. E. (2009). Normal table of postembryonic zebrafish development: staging by externally visible anatomy of the living fish. *Dev. Dyn.* **238**, 2975-3015.

Patterson, L. B. and Parichy, D. M. (2013). Interactions with iridophores and the tissue environment required for patterning melanophores and xanthophores during zebrafish adult pigment stripe formation. *PLoS Genet.* **9**, e1003561.

Rodrigues, F. S. L. M., Doughton, G., Yang, B. and Kelsh, R. N. (2012). A novel transgenic line using the Cre-lox system to allow permanent lineage-labeling of the zebrafish neural crest. *Genesis* **50**, 750-757.

Schindelin, J., Arganda-Carreras, I., Frise, E., Kaynig, V., Longair, M., Pietzsch, T., Preibisch, S., Rueden, C., Saalfeld, S., Schmid, B. et al. (2012). Fiji: an open-source platform for biological-image analysis. *Nat. Methods* **9**, 676-682.

Singh, A. P. and Nüsslein-Volhard, C. (2015). Zebrafish stripes as a model for vertebrate colour pattern formation. *Curr. Biol.* **25**, R81-R92.

Singh, A. P., Schach, U. and Nüsslein-Volhard, C. (2014). Proliferation, dispersal and patterned aggregation of iridophores in the skin prefigure striped colouration of zebrafish. *Nat. Cell Biol.* **16**, 607-614.

Singh, A. P., Fröhnhofer, H. G., Irion, U. and Nüsslein-Volhard, C. (2015). Fish pigmentation. Response to Comment on "Local reorganization of xanthophores fine-tunes and colors the striped pattern of zebrafish". *Science* **348**, 297.

Singh, A. P., Dinwiddie, A., Mahalwar, P., Schach, U., Linker, C., Irion, U. and Nüsslein-Volhard, C. (2016). Pigment cell progenitors in Zebrafish remain multipotent through metamorphosis. *Dev. Cell* **38**, 316-330.

Walderich, B., Singh, A. P., Mahalwar, P. and Nüsslein-Volhard, C. (2016). Homotypic cell competition regulates proliferation and tiling of zebrafish pigment cells during colour pattern formation. *Nat. Commun.* **7**, 11462.

Watanabe, M. and Kondo, S. (2015). Is pigment patterning in fish skin determined by the Turing mechanism? *Trends Genet.* **31**, 88-96.

Watanabe, M., Iwashita, M., Ishii, M., Kurachi, Y., Kawakami, A., Kondo, S. and Okada, N. (2006). Spot pattern of leopard Danio is caused by mutation in the zebrafish connexin41.8 gene. *EMBO Rep.* **7**, 893-897.

Watanabe, M., Sawada, R., Aramaki, T., Skerrett, I. M. and Kondo, S. (2015). The physiological characterization of Connexin41.8 and Connexin39.4, which are involved in the stripe pattern formation of zebrafish. *J. Biol. Chem.* **291**, 1053-1063.

Yamaguchi, M., Yoshimoto, E. and Kondo, S. (2007). Pattern regulation in the stripe of zebrafish suggests an underlying dynamic and autonomous mechanism. *Proc. Natl. Acad. Sci. USA* **104**, 4790-4793.

CHAPTER 3

Discussion

The striped pattern of adult zebrafish is composed of three types of pigment cells - melanophores, iridophores and xanthophores. These cells are arranged in superimposed layers in the skin (Hirata et al., 2005; Singh and Nüsslein-Volhard, 2015). *In vitro* and ablation studies, in combination with mathematical modeling, have postulated that Turing-type mechanisms can lead to the global self-organization of individual cells into stripes (Kondo and Miura, 2010). During my doctoral study, I employed live imaging of larval fish, genetic lineage tracing, and long-term *in vivo* imaging of metamorphic fish to uncover the lineage and mechanism of pigment pattern in zebrafish. In particular, I focused on xanthophores and showed that color pattern formation in zebrafish involves the proliferation of larval xanthophores, migration and cell shape transition of xanthophores, and the requirement of gap junctions for the cell shape transitions that occur in response to the other two pigment cell types - melanophores and iridophores.

3.1 Origin and lineage of larval and adult xanthophores

The larvae of all the *Danio* species have similar and comparatively simple patterns composed of neural-crest derived xanthophores, melanophores and iridophores (Kelsh, 2004; Singh and Nüsslein-Volhard, 2015). It is known that different pigment cell-specific genes are initially widely expressed in NC cells, and subsequently preferentially restricted to a particular pigment cell type. For example, *mitfa*, a gene that is primarily required in melanophores shows NC-wide expression during embryogenesis (Dooley et al., 2013; Lister et al., 1999). Similar observations have been made for the progressive restriction of expression of *ltk* and *csf1ra* in iridophores and xanthophores, respectively (Lopes et al., 2008;

Parichy et al., 2000b). Moreover, some of the pigment cell-specific genes, such as *mitfa* and *ltk*, overlap in their expression pattern in NC cells, which develop directly into either melanophores or iridophores depending upon the expression level of *foxd3*. In contrast, antibody staining of early larva demonstrates the existence of few *mitfa/fms* double-positive cells (Curran et al., 2010). This evidently indicates the existence of potential bipotent melanophore and xanthophore precursors. This hypothesis is supported by the increase in the number of melanophores in *pax7a*/*pax7b* double-mutant larvae, lacking xanthophores (Nord et al., 2016). However, how *pax7* directly or indirectly affects *mitfa* expression levels has yet to be investigated. We have shown that NC-derived xanthophore precursors migrate dorso-laterally and mature into xanthophores in the skin. Less is known about the molecular signals in the dorso-lateral migration of these precursor cells. Moreover, a xanthophore mutant (*pfeffer/csfr1)* and morpholino screens have indicated that *csf1*-signalling could be involved in the migration of the xanthophore precursor in the early larval stages (Alsheimer, 2012).

We found that, upon reaching the skin, larval xanthophores show limited movement, but exhibit extensive filopodial extensions. These filopodia are highly dynamic, actin-rich thin cellular protrusions also called airinemes (Eom et al., 2015; Panza et al., 2015), which may allow xanthophores to probe their environment and contact neighboring pigment cells. Live-imaging the behavior of xanthophores in wild-type, and transplanted wild-type xanthophores in *pfeffer* mutant larvae shows that xanthophores maintain a dynamic contact with one another. In the absence of competing cells within a layer in the skin, donor-derived clusters of xanthophores proliferate at a faster rate than in their normal surrounding. This suggests that during normal development, growth is constrained by competitive interactions between cells of the same type. However, mutant analysis indicates that specification, proliferation and maintenance of pigment cells depend on individual receptor signaling systems - *fms/pfeffer/csfr*- for xanthophores. While the pigment cells express the respective receptor, the ligands are presumably functioning as trophic factors produced by surrounding connective tissue. Competition for the ligands may in part be responsible for the regulation of pigment cell proliferation in normal development.

The adult chromatophores are NC-derived, but appear after the NC has long disappeared. The postembryonic origin of metamorphic pigment cells has remained a mystery for a long time. Recently, *Kitalg* dependent MitfA-positive stem cells were discovered, located at the dorsal-root ganglia. Deletion of dorsal-root ganglia in the hypersensitive/ *erb3b* mutation or laser ablation of dorsal-root ganglia led to a defect in the adult stripe formation (Budi et al., 2008; Dooley et al., 2013). These studies suggest that the dorsal-root ganglia serve as niches for adult melanophore stem cells. Temporal Cre-mediated recombination and long-term imaging have also clearly shown that the dorsal-root ganglia serve as a pool of adult stem cell not only for melanophore but also for iridophores. However, iridophores and melanophores arrive and distribute in the skin along different routes (Singh et al., 2014).

In contrast, the origin of adult xanthophores had remained obscure. Our findings have shown that most of the metamorphic xanthophores arise from larval ones, which persist and begin to proliferate in the skin at the onset of metamorphosis. Moreover, the proliferation and differentiation is dependent on global thyroid hormone signaling and local Csfr1a–Csf1-dependent interactions with iridophores (Mahalwar et al., 2014; McMenamin et al., 2014; Patterson and Parichy, 2013). Interestingly, we discovered that adult xanthophores can develop even after the ablation of larval xanthophores, indicating that a second source of adult xanthophores must exist. Long-term imaging of labeled NC clones during metamorphosis showed that multipotent progenitors that develop neural cells, iridophores, and melanophores during metamorphosis, also produce few xanthophores (Singh et al., 2014; Walderich et al., 2016). This strongly indicates that xanthophores have a dual cellular origin: mostly from existing larval xanthophores, but also from multipotent postembryonic progenitors.

3.2 Role of xanthophores in pigment pattern formation

During metamorphosis pigment cell types appeared sequentially to form the striped pattern. Based on the appearance of pigment content, other studies have reported that the xanthophores appear and mature long after the arrival of melanophores and iridophores (Takahashi and Kondo, 2008). However, our long-term, pigment-independent analysis shows that xanthophores, albeit barely

visible by pigment content, are the first cell type to cover the trunk before the appearance of other metamorphic pigment cell types in the skin. Subsequently, metamorphic iridophores appear along the horizontal myoseptum and organize the first interstripe and lastly, metamorphic melanophores emerge amongst the xanthophores in the dark stripe region flanking the light stripe. The appearance of iridophores and melanophores leads to changes in xanthophore behavior and shape throughout metamorphosis. Eventually with iridophores, they show more compact and highly dense organization in the light stripe and a stellate and loosely packed net in the dark stripe.

Several mathematicians have shown interest in zebrafish color pattern (Nakamasu et al., 2009; Volkening and Sandstede, 2015; Yamaguchi et al., 2007; Yamanaka and Kondo, 2014). The mathematical models do not explain many of these cell behaviors and cellular interactions observed *in vivo*. Color pattern formation is modeled on the basis of melanophore and xanthophore-interactions only, these models generate self-organization via Turing-equations with one factor acting as a long-range and another as a short-range. The predictive outcome of most of these models is based on the initial condition of the two pigment cell types. These models not only ignore the presence of the third cell type (iridophores), but also the presence of xanthophores in the dark stripe area, and describe stripe formation as simply the self-sorting of melanophores and xanthophores with global reorganization (Singh et al., 2015); Watanabe and Kondo 2015). There is hardly any evidence that such a sorting takes place at a global scale during stripe pattern formation, except along the boundaries between light and dark stripes. Interestingly, our analysis of long-term imaging showed that clonal xanthophores maintain their relative positions and can be identified by their location during the formation of the stripes. This indicates that there is only a very limited global reorganization of xanthophores during stripe morphogenesis.

These models are over-simplifications of the stripe formation process and do not explain the dynamic changes in pigment cell shapes that occur during stripe formation. For example: the iridophores and xanthophores exist in loose and dense states. In particular, two types of iridophores can differ in their motility and shape, which has implications for the formation of new light stripes. Tight iridophores lead to compact and dense formations of metamorphic xanthophores

near the horizontal myoseptum and loose iridophores proliferate and migrate bidirectional in the body of the zebrafish. The first light stripe is formed by tightly packed and dense iridophores along the horizontal myoseptum serving as a morphological prepattern (Singh et al., 2014). Analysis of mutants that lack one or two of the three cell types have indicated that iridophores play a leading role in stripe formation (Frohnhöfer et al., 2013). Evidently, long-term cell imaging confirms that iridophores are the first pigment cell type to start the process of patterning by adding compact xanthophores to the first light stripe parallel to the horizontal myoseptum. However, xanthophore mutants (*pfe*) have irregular dark stripes in the body, and the fins are not striped. The melanophore stripes break up into spots, dense iridophores invade the stripes, and further, ectopic melanophores are observed in the light stripe regions giving an irregular appearance to the spotted pattern (Parichy and Turner, 2003). Blastula transplantations of xanthophore progenitor cells into *pfe* mutant embryos restore a normal pattern indicating the important role of xanthophores in stripe sharpening and coloration (Walderich et al., 2016). Mutants defective for iridophores such as *shady*, *rose* and *transparent* do not add stripes to a basic pattern, whereas mutants lacking xanthophores (*pfe*) or melanophores (*nac*) form a rudimentary first light stripe. Mutant lacking iridophores (*shd*) form normal stripes in the anal- and tail fins. Analysis of the mutant phenotypes indicates that a number of long and short range interactions are involved in organizing the striped pattern. Iridophores promote and sustain melanophores, furthermore, iridophores attract xanthophores, whereas between xanthophores and melanophores long-range activation and short-range inhibition has been observed (Frohnhöfer et al., 2013; Singh et al., 2014).

Recent studies involving *in vitro* observations of fin-derived pigment cells have suggested that xanthophores repel melanophores in a run and chase manner leading to melanophore aggregation and thereby stripe pattern formation (Inaba et al., 2012). These and previous studies based on pattern regeneration and theoretical modeling proposed that xanthophores and melanophores act as ‘diffusible factors’ in a Turing-type model; according to this model, differences in the cell movement of melanophores and xanthophores during their contact-based interactions would lead to a striped organization of pigment cells (Nakamasu et

al., 2009; Yamaguchi et al., 2007; Yamanaka and Kondo, 2014). These models may hold true for patterning in the fins, but not for the body as they are not compatible with the *pfeffer* mutant phenotype nor do they take iridophores into account (Singh et al., 2015). Iridophores are absent in the fin stripes and these stripes are only formed of melanophores and xanthophores. This strongly supports two different mechanisms of stripe formation involving three cell types in the trunk skin as compared to two in the fins.

Stripe pattern mutants such as *mau* (Eskova et al, submitted) and *npm* (Frohnhöfer et al, unpublished) which are non-cell autonomous to pigment cells indicate a crucial role of the tissue environment in the formation of the stripe pattern. However, very little is known about the molecular and cellular events that take place during the development of stripe formation. An analysis of mutants missing a single pigment cell type, where rudimentary stripes are formed in one or another form, could be instructive. These observations strongly suggest that the tissue contribute to the stripe formation. In other animals, careful analysis has shown that color patterning mechanisms are most likely based on a pre-pattern (Kaelin et al., 2012; Weiner et al., 2007). In summary, these findings challenge the previously proposed reaction-diffusion theoretical models of color pattern formation in zebrafish based on two cells and call for a new approach to mathematical modeling of color pattern formation (Bullara and De Decker, 2015; Morales et al., 2015; Painter et al., 2015; Singh et al., 2015; Volkening and Sandstede, 2015; Watanabe and Kondo, 2015).

3.3 Connexin mediated reorganization of xanthophores.

Color pattern in zebrafish involves the combination of homotypic and heterotypic interactions regulating precise patterning of xanthophores during color pattern formation. We found that the heterotypic (xanthophore-iridophore and xanthophore-melanophore) interactions regulate differential density and shape of xanthophores, whereas homotypic (xanthophore-xanthophore) interactions regulate the xanthophore coverage across the skin (Walderich et al., 2016). Heterotypic interactions with iridophores are required for xanthophores to increase their density in light stripes regions. In the absence of iridophores (*shady* mutants*),* xanthophore density stays low and does not increase during

metamorphosis. When iridophores gradually recover (*erbb3b* mutant) and start to fill in gaps previously devoid of iridophores, xanthophore density also increases. This xanthophore behavior does not depend on the presence of melanophores, as it also occurs in *nacre* mutants. Previously, it was shown that iridophores act on xanthophores via *Csf1*, an extracellular ligand expressed in iridophores that promotes xanthophore development (Patterson and Parichy, 2013). However, the interaction we find between iridophores and xanthophores is likely to be more direct, as it requires functional gap junctions made from Cx41.8 and Cx39.4. In *leo*^{tK3} mutants, where these channels are non-functional, xanthophores stay at low density despite the presence of iridophores. The transplantation experiments show that this requirement is cell-autonomous to xanthophores, which is in agreement with our previous findings that Cx41.8 and Cx39.4 are only required in xanthophores and melanophores, but not in iridophores (Irion et al., 2014a; Maderspacher and Nüsslein-Volhard, 2003). If this heterotypic interaction among iridophores and xanthophores occurs via gap junctions, and not simply via hemi-channels in the xanthophore plasma membrane, a different connexin on the iridophore side must exist. Such a connexin has not yet been identified, however, the hypothesis that it exists might be corroborated by the analysis of *schachbrett* (*sbr*) mutants. In *sbr* a spotted pattern is produced; it was shown that Tjp1A is affected in this mutant. This protein is specifically expressed in iridophores and known to interact with the C-termini of several connexins (Fadeev et al., 2015). This could provide the link from gap junctions to the cytoplasm in iridophores. Reverse genetic approaches may also be useful in identifying novel iridophore-specific gap junction components (Hwang et al., 2013a; Hwang et al., 2013b; Irion et al., 2014b).

The interactions between xanthophores and melanophores, which lead to shape changes in the xanthophores, are only partially mediated by the known gap junctions, homozygous *leo*^{tK3} mutants show that xanthophores clearly sense the appearing melanophores and rearrange their cellular protrusions; however, they do not ultimately change their shape to become stellate. This indicates that there are at least two steps in the interaction between melanophores and xanthophores and that the initial recognition is independent of *leo* and *luc* gap junctions. The signaling molecules that mediate this initial interaction are unknown; however,

several molecules, such as Kcnj13, an inward rectifying potassium channel (Inaba et al., 2012), Spermidine, a polyamine (Frohnhofer et al., 2016), Tetraspanin3c, a transmembrane scaffolding protein (Inoue et al., 2014) and Notch/Delta signaling (Eom et al., 2015; Hamada et al., 2014) have been shown to regulate cell-cell interactions during color pattern formation. It is possible that some of these molecules mediate gap junction-independent communication between melanophores and xanthophores. Introduction of wild type xanthophores into *leo*^{kt3} mutants by blastula transplantation shows that the stellate shape changes in response to mutant *leo*^{kt3} melanophores. This indicates that Cx41.8 and Cx39.4 are only required in xanthophores for the stellate shape. In turn, this suggests that there could be heterotypic and heteromeric gap junctions between xanthophores and melanophores employing Cx41.8 and Cx39.4, where multiple connexins other than Cx41.8 and Cx39.4 form the functional hemichannel on the melanophore side.

Current analysis of xanthophores in *leo* mutants indicates that xanthophores and melanophores not only instruct the patterning of iridophores but that iridophores are also required to organize xanthophores, suggesting that ultimately a feedback mechanism involving contact-based interactions between all three types of pigment cells is the basis of stripe pattern formation in the body of zebrafish. The color pattern formation in zebrafish involves a novel mechanism of patterning, dependent on cell shape transitions of xanthophores and iridophores. These shape transitions are dependent on local cell-cell interactions mediated by gap junctions. In summary, the gap junctions are required in xanthophores for the cell shape transitions in response to other chromatophores.

3.4 Zebrafish pigment cell system – a model system to study gap junctions

Little is known about the cellular and molecular events underlying the cell-cell interactions involving connexin-dependent heterotypic and heteromeric gap junctions. One question in particular is how functional heterotypic and heteromeric gap junctions work. Evidence for heterotypic channels has been largely based on the electrophysiological analysis of paired *Xenopus* oocytes or transfected cell lines expressing different sets of connexins (Cao et al., 1998; Dahl et al., 1996; Hennemann et al., 1992; Werner et al., 1989; White et al.,

1994a; White et al., 1994b). The pigment cell system in zebrafish is a beautiful model system to study the heterotypic and heteromeric gap junctions *in vivo*. The cell-autonomous requirement of Cx41.8 and Cx39.4 in xanthophores for stellate and compact shape indicates the possibility of heterotypic and heteromeric functional gap junctions. In the future, xanthophore shapes could be used as functional phenotype for forward genetic screens. Finally transplanting cells into various mutant combinations could greatly improve our understanding of how these gap junctions are rectified, and function *in vivo*.

CHAPTER 4

Bibliography

Alsheimer, S. (2012). on Telost muscle stem cell and the vertical myoseptum as their niche. *PhD Disseration*, 1-249.

Bennett, D. C. and Lamoreux, M. L. (2003). The color loci of mice--a genetic century. *Pigment Cell Res* **16**, 333-344.

Budi, E. H., Patterson, L. B. and Parichy, D. M. (2008). Embryonic requirements for ErbB signaling in neural crest development and adult pigment pattern formation. *Development* **135**, 2603-2614.

Budi, E. H., Patterson, L. B. and Parichy, D. M. (2011). Post-embryonic nerve-associated precursors to adult pigment cells: genetic requirements and dynamics of morphogenesis and differentiation. *PLoS Genet* **7**, e1002044.

Bullara, D. and De Decker, Y. (2015). Pigment cell movement is not required for generation of Turing patterns in zebrafish skin. *Nat Commun* **6**, 6971.

Cao, F., Eckert, R., Elfgang, C., Nitsche, J. M., Snyder, S. A., DF, H. u., Willecke, K. and Nicholson, B. J. (1998). A quantitative analysis of connexin-specific permeability differences of gap junctions expressed in HeLa transfectants and Xenopus oocytes. *Journal of cell science* **111 (Pt 1)**, 31-43.

Curran, K., Lister, J. A., Kunkel, G. R., Prendergast, A., Parichy, D. M. and Raible, D. W. (2010). Interplay between Foxd3 and Mitf regulates cell fate plasticity in the zebrafish neural crest. *Dev Biol* **344**, 107-118.

Dahl, E., Manthey, D., Chen, Y., Schwarz, H. J., Chang, Y. S., Lalley, P. A., Nicholson, B. J. and Willecke, K. (1996). Molecular cloning and functional expression of mouse connexin-30,a gap junction gene highly expressed in adult brain and skin. *J Biol Chem* **271**, 17903-17910.

Dooley, C. M., Mongera, A., Walderich, B. and Nüsslein-Volhard, C. (2013). On the embryonic origin of adult melanophores: the role of ErbB and Kit

signalling in establishing melanophore stem cells in zebrafish. *Development* **140**, 1003-1013.

Driever, W., Solnica-Krezel, L., Schier, A. F., Neuhauss, S. C., Malicki, J., Stemple, D. L., Stainier, D. Y., Zwartkruis, F., Abdelilah, S., Rangini, Z., et al. (1996). A genetic screen for mutations affecting embryogenesis in zebrafish. *Development* **123**, 37-46.

Eom, D. S., Bain, E. J., Patterson, L. B., Grout, M. E. and Parichy, D. M. (2015). Long-distance communication by specialized cellular projections during pigment pattern development and evolution. *Elife* **4**.

Eom, D. S., Inoue, S., Patterson, L. B., Gordon, T. N., Slingwine, R., Kondo, S., Watanabe, M. and Parichy, D. M. (2012). Melanophore migration and survival during zebrafish adult pigment stripe development require the immunoglobulin superfamily adhesion molecule Igsf11. *PLoS Genet* **8**, e1002899.

Fadeev, A., Krauss, J., Fröhnhofer, H. G., Irion, U. and Nüsslein-Volhard, C. (2015). Tight junction protein 1a regulates pigment cell organisation during zebrafish colour patterning. *Elife* **4**.

Frankel, J. S. (1979). Inheritance of spotting in the leopard danio. *J Hered* **70**, 287-288.

Frohnhofer, H. G., Geiger-Rudolph, S., Pattky, M., Meixner, M., Huhn, C., Maischein, H. M., Geisler, R., Gehring, I., Maderspacher, F., Nusslein-Volhard, C., et al. (2016). Spermidine, but not spermine, is essential for pigment pattern formation in zebrafish. *Biol Open* **5**, 736-744.

Frohnhöfer, H. G., Krauss, J., Maischein, H. M. and Nüsslein-Volhard, C. (2013). Iridophores and their interactions with other chromatophores are required for stripe formation in zebrafish. *Development* **140**, 2997-3007.

Gans, C. and Northcutt, R. G. (1983). Neural crest and the origin of vertebrates: a new head. *Science* **220**, 268-273.

Gray, C., Loynes, C. A., Whyte, M. K., Crossman, D. C., Renshaw, S. A. and Chico, T. J. (2011). Simultaneous intravital imaging of macrophage and neutrophil behaviour during inflammation using a novel transgenic zebrafish. *Thromb Haemost* **105**, 811-819.

Green, S. A., Simoes-Costa, M. and Bronner, M. E. (2015). Evolution of vertebrates as viewed from the crest. *Nature* **520**, 474-482.

Haffter, P., Granato, M., Brand, M., Mullins, M. C., Hammerschmidt, M., Kane, D. A., Odenthal, J., van Eeden, F. J., Jiang, Y. J., Heisenberg, C. P., et al. (1996a). The identification of genes with unique and essential functions in the development of the zebrafish, Danio rerio. *Development* **123**, 1-36.

Haffter, P., Odenthal, J., Mullins, M. C., Lin, S., Farrell, M. J., Vogelsang, E., Haas, F., Brand, M., vanEeden, F. J. M., FurutaniSeiki, M., et al. (1996b). Mutations affecting pigmentation and shape of the adult zebrafish. *Dev Genes Evol* **206**, 260-276.

Hamada, H., Watanabe, M., Lau, H. E., Nishida, T., Hasegawa, T., Parichy, D. M. and Kondo, S. (2014). Involvement of Delta/Notch signaling in zebrafish adult pigment stripe patterning. *Development* **141**, 318-324.

Hamilton, W. D. (1964). The genetical evolution of social behaviour. I. *J Theor Biol* **7**, 1-16.

Henion, P. D. and Weston, J. A. (1997). Timing and pattern of cell fate restrictions in the neural crest lineage. *Development* **124**, 4351-4359.

Hennemann, H., Suchyna, T., Lichtenberg-Frate, H., Jungbluth, S., Dahl, E., Schwarz, J., Nicholson, B. J. and Willecke, K. (1992). Molecular cloning and functional expression of mouse connexin40, a second gap junction gene preferentially expressed in lung. *J Cell Biol* **117**, 1299-1310.

Hirata, M., Nakamura, K., Kanemaru, T., Shibata, Y. and Kondo, S. (2003). Pigment cell organization in the hypodermis of zebrafish. *Dev Dyn* **227**, 497-503.

Hirata, M., Nakamura, K. and Kondo, S. (2005). Pigment cell distributions in different tissues of the zebrafish, with special reference to the striped pigment pattern. *Dev Dyn* **234**, 293-300.

Hwang, W. Y., Fu, Y., Reyon, D., Maeder, M. L., Kaini, P., Sander, J. D., Joung, J. K., Peterson, R. T. and Yeh, J. R. (2013a). Heritable and precise zebrafish genome editing using a CRISPR-Cas system. *PLoS One* **8**, e68708.

Hwang, W. Y., Fu, Y., Reyon, D., Maeder, M. L., Tsai, S. Q., Sander, J. D., Peterson, R. T., Yeh, J. R. and Joung, J. K. (2013b). Efficient genome editing in zebrafish using a CRISPR-Cas system. *Nat Biotechnol* **31**, 227-229.

Inaba, M., Yamanaka, H. and Kondo, S. (2012). Pigment pattern formation by contact-dependent depolarization. *Science* **335**, 677.

Inoue, S., Kondo, S., Parichy, D. M. and Watanabe, M. (2014). Tetraspanin 3c requirement for pigment cell interactions and boundary formation in zebrafish adult pigment stripes. *Pigment Cell Melanoma Res* **27**, 190-200.

Irion, U., Frohnhöfer, H. G., Krauss, J., Colak Champollion, T., Maischein, H. M., Geiger-Rudolph, S., Weiler, C. and Nüsslein-Volhard, C. (2014a). Gap junctions composed of connexins 41.8 and 39.4 are essential for colour pattern formation in zebrafish. *Elife* **3**, e05125.

Irion, U., Krauss, J. and Nüsslein-Volhard, C. (2014b). Precise and efficient genome editing in zebrafish using the CRISPR/Cas9 system. *Development* **141**, 4827-4830.

Irion, U., Singh, A. P. and Nusslein-Volhard, C. (2016). The Developmental Genetics of Vertebrate Color Pattern Formation: Lessons from Zebrafish. *Current topics in developmental biology* **117**, 141-169.

Iwashita, M., Watanabe, M., Ishii, M., Chen, T., Johnson, S. L., Kurachi, Y., Okada, N. and Kondo, S. (2006). Pigment pattern in jaguar/obelix zebrafish is caused by a Kir7.1 mutation: implications for the regulation of melanosome movement. *PLoS Genet* **2**, e197.

Kaelin, C. B., Xu, X., Hong, L. Z., David, V. A., McGowan, K. A., Schmidt-Kuntzel, A., Roelke, M. E., Pino, J., Pontius, J., Cooper, G. M., et al. (2012). Specifying and sustaining pigmentation patterns in domestic and wild cats. *Science* **337**, 1536-1541.

Kar, R., Batra, N., Riquelme, M. A. and Jiang, J. X. (2012). Biological role of connexin intercellular channels and hemichannels. *Archives of biochemistry and biophysics* **524**, 2-15.

Kelsh, R. N. (2004). Genetics and evolution of pigment patterns in fish. *Pigment Cell Res* **17**, 326-336.

Kirschbaum, F. (1975). Untersuchungen über das Farbmuster der Zebrabarbe 'Brachydanio reio' (Cyprinidae, Teleostei). *Wilhelm Roux's Archives* **177**, 129-152.

Kirschbaum, F. (1977). Zur Genetik einiger Farbmustermutanten der zebrabarbe 'Brachydanio rerio' (Cyprinidae, Teleostei) und zum Phänotyp von Artbastarden der Gattung 'Brachydanio'. *Biol Zbl.* **96**, 211-222.

Kondo, S. and Miura, T. (2010). Reaction-diffusion model as a framework for understanding biological pattern formation. *Science* **329**, 1616-1620.

Krauss, J., Frohnhöfer, H. G., Walderich, B., Maischein, H. M., Weiler, C., Irion, U. and Nüsslein-Volhard, C. (2014). Endothelin signalling in iridophore development and stripe pattern formation of zebrafish. *Biol Open* **3**, 503-509.

Lister, J. A., Robertson, C. P., Lepage, T., Johnson, S. L. and Raible, D. W. (1999). nacre encodes a zebrafish microphthalmia-related protein that regulates neural-crest-derived pigment cell fate. *Development* **126**, 3757-3767.

Lopes, S. S., Yang, X., Muller, J., Carney, T. J., McAdow, A. R., Rauch, G. J., Jacoby, A. S., Hurst, L. D., Delfino-Machin, M., Haffter, P., et al. (2008). Leukocyte tyrosine kinase functions in pigment cell development. *PLoS Genet* **4**, e1000026.

Maderspacher, F. and Nüsslein-Volhard, C. (2003). Formation of the adult pigment pattern in zebrafish requires leopard and obelix dependent cell interactions. *Development* **130**, 3447-3457.

Mahalwar, P., Walderich, B., Singh, A. P. and Nüsslein-Volhard, C. (2014). Local reorganization of xanthophores fine-tunes and colors the striped pattern of zebrafish. *Science* **345**, 1362-1364.

McMenamin, S. K., Bain, E. J., McCann, A. E., Patterson, L. B., Eom, D. S., Waller, Z. P., Hamill, J. C., Kuhlman, J. A., Eisen, J. S. and Parichy, D. M. (2014). Thyroid hormone-dependent adult pigment cell lineage and pattern in zebrafish. *Science*.

Milks, L. C., Kumar, N. M., Houghten, R., Unwin, N. and Gilula, N. B. (1988). Topology of the 32-kd liver gap junction protein determined by site-directed antibody localizations. *The EMBO journal* **7**, 2967-2975.

Mongera, A., Singh, A. P., Levesque, M. P., Chen, Y. Y., Konstantinidis, P. and Nüsslein-Volhard, C. (2013). Genetic lineage labeling in zebrafish uncovers novel neural crest contributions to the head, including gill pillar cells. *Development* **140**, 916-925.

Morales, M. A., Rojas, J. F., Oliveros, J. and Hernandez, S. A. (2015). A new mechanochemical model: coupled Ginzburg-Landau and Swift-Hohenberg

equations in biological patterns of marine animals. *J Theor Biol* **368**, 37-54.

Nakamasu, A., Takahashi, G., Kanbe, A. and Kondo, S. (2009). Interactions between zebrafish pigment cells responsible for the generation of Turing patterns. *Proc Natl Acad Sci U S A* **106**, 8429-8434.

Noden, D. M. (1983). The role of the neural crest in patterning of avian cranial skeletal, connective, and muscle tissues. *Dev Biol* **96**, 144-165.

Nord, H., Dennhag, N., Muck, J. and von Hofsten, J. (2016). Pax7 is required for establishment of the xanthophore lineage in zebrafish embryos. *Mol Biol Cell*.

Painter, K. J., Bloomfield, J. M., Sherratt, J. A. and Gerisch, A. (2015). A Nonlocal Model for Contact Attraction and Repulsion in Heterogeneous Cell Populations. *Bull Math Biol*.

Panza, P., Maier, J., Schmees, C., Rothbauer, U. and Sollner, C. (2015). Live imaging of endogenous protein dynamics in zebrafish using chromobodies. *Development* **142**, 1879-1884.

Parichy, D. M., Mellgren, E. M., Rawls, J. F., Lopes, S. S., Kelsh, R. N. and Johnson, S. L. (2000a). Mutational analysis of endothelin receptor b1 (rose) during neural crest and pigment pattern development in the zebrafish Danio rerio. *Dev Biol* **227**, 294-306.

Parichy, D. M., Ransom, D. G., Paw, B., Zon, L. I. and Johnson, S. L. (2000b). An orthologue of the kit-related gene fms is required for development of neural crest-derived xanthophores and a subpopulation of adult melanocytes in the zebrafish, Danio rerio. *Development* **127**, 3031-3044.

Parichy, D. M. and Turner, J. M. (2003). Temporal and cellular requirements for Fms signaling during zebrafish adult pigment pattern development. *Development* **130**, 817-833.

Patterson, L. B. and Parichy, D. M. (2013). Interactions with iridophores and the tissue environment required for patterning melanophores and xanthophores during zebrafish adult pigment stripe formation. *PLoS Genet* **9**, e1003561.

Roulin, A. (2004). Proximate basis of the covariation between a melanin-based female ornament and offspring quality. *Oecologia* **140**, 668-675.

Singh, A. P., Fröhnhofer, H. G., Irion, U. and Nüsslein-Volhard, C. (2015). Fish pigmentation. Response to Comment on "Local reorganization of xanthophores fine-tunes and colors the striped pattern of zebrafish". *Science* **348**, 297.

Singh, A. P. and Nüsslein-Volhard, C. (2015). Zebrafish stripes as a model for vertebrate colour pattern formation. *Curr Biol* **25**, R81-92.

Singh, A. P., Schach, U. and Nüsslein-Volhard, C. (2014). Proliferation, dispersal and patterned aggregation of iridophores in the skin prefigure striped colouration of zebrafish. *Nat Cell Biol* **16**, 607-614.

Spence, R., Gerlach, G., Lawrence, C. and Smith, C. (2008). The behaviour and ecology of the zebrafish, Danio rerio. *Biol Rev Camb Philos Soc* **83**, 13-34.

Takahashi, G. and Kondo, S. (2008). Melanophores in the stripes of adult zebrafish do not have the nature to gather, but disperse when they have the space to move. *Pigment Cell Melanoma Res* **21**, 677-686.

Thevenin, A. F., Kowal, T. J., Fong, J. T., Kells, R. M., Fisher, C. G. and Falk, M. M. (2013). Proteins and mechanisms regulating gap-junction assembly, internalization, and degradation. *Physiology* **28**, 93-116.

Unwin, P. N. and Zampighi, G. (1980). Structure of the junction between communicating cells. *Nature* **283**, 545-549.

Volkening, A. and Sandstede, B. (2015). Modelling stripe formation in zebrafish: an agent-based approach. *Journal of the Royal Society, Interface / the Royal Society* **12**.

Walderich, B., Singh, A. P., Mahalwar, P. and Nusslein-Volhard, C. (2016). Homotypic cell competition regulates proliferation and tiling of zebrafish pigment cells during colour pattern formation. *Nat Commun* **7**, 11462.

Watanabe, M., Iwashita, M., Ishii, M., Kurachi, Y., Kawakami, A., Kondo, S. and Okada, N. (2006). Spot pattern of leopard Danio is caused by mutation in the zebrafish connexin41.8 gene. *EMBO Rep* **7**, 893-897.

Watanabe, M. and Kondo, S. (2015). Is pigment patterning in fish skin determined by the Turing mechanism? *Trends Genet* **31**, 88-96.

Watanabe, M., Sawada, R., Aramaki, T., Skerrett, I. M. and Kondo, S. (2015). The physiological characterization of Connexin41.8 and Connexin39.4,

which are involved in the stripe pattern formation of zebrafish. *J Biol Chem*.

Weiner, L., Han, R., Scicchitano, B. M., Li, J., Hasegawa, K., Grossi, M., Lee, D. and Brissette, J. L. (2007). Dedicated epithelial recipient cells determine pigmentation patterns. *Cell* **130**, 932-942.

Werner, R., Levine, E., Rabadan-Diehl, C. and Dahl, G. (1989). Formation of hybrid cell-cell channels. *Proc Natl Acad Sci U S A* **86**, 5380-5384.

White, T. W., Bruzzone, R., Goodenough, D. A. and Paul, D. L. (1994a). Voltage gating of connexins. *Nature* **371**, 208-209.

White, T. W., Bruzzone, R., Wolfram, S., Paul, D. L. and Goodenough, D. A. (1994b). Selective interactions among the multiple connexin proteins expressed in the vertebrate lens: the second extracellular domain is a determinant of compatibility between connexins. *J Cell Biol* **125**, 879-892.

Wittkopp, P. J., Williams, B. L., Selegue, J. E. and Carroll, S. B. (2003). Drosophila pigmentation evolution: divergent genotypes underlying convergent phenotypes. *Proc Natl Acad Sci U S A* **100**, 1808-1813.

Yamaguchi, M., Yoshimoto, E. and Kondo, S. (2007). Pattern regulation in the stripe of zebrafish suggests an underlying dynamic and autonomous mechanism. *Proc Natl Acad Sci U S A* **104**, 4790-4793.

Yamanaka, H. and Kondo, S. (2014). In vitro analysis suggests that difference in cell movement during direct interaction can generate various pigment patterns in vivo. *Proc Natl Acad Sci U S A* **111**, 1867-1872.

Own contribution to the manuscripts

Both lead author manuscripts were primarily written by me with the help of all the coauthors. The project leading to publication 1 & 3 has been initially designed with the help of Dr. Ajeet Singh. The experiments were designed by myself and mostly done by myself. Dr. Brigitte Walderich & Dr. Uwe Irion helped with the transplantation experiments. Dr. Ajeet Singh also contributed to some adult confocal pictures. Dr. Andrey Fadeev help with antibody staining for paper 3.

For publication 2, I performed *in vivo* live imaging in larvae and adults, and xanthophore ablations experiments. My contribution to the publication 4 is mentioned in the appendix.

Curriculum Vitae

Prateek Mahalwar

Born: Janurary20th, 1986 in Meerut (India)

11/2011 – 07/2016	**PhD student**
	MPI for Developmental Biology, Tübingen, Germany
	Supervisor : Prof. Dr. Christiane Nüsslein –Volhard
	Project: Role of Xanthophores in zebrafish pattern formation
	Institut Pasteur travel grant award (2014), France
	IMPRS Scholarship (2011-15), Max Planck Society, Germany
04/2011 – 02/2012	**Master thesis**
	MPI for Developmental Biology, Tübingen, Germany
	Supervisor : Dr. Christian Söllner
	Project: Functional role of Opticin interactions in the vertebrate developing nervous system.
10/2009 – 02/2012	**M.Sc. Integrative Neuroscience**
	Otto Von Guericke University, Magdeburg, Germany
	Leibniz Gemeinschaft and CBBS Stipendium (2009-11), Germany
10/2009 – 03/2011	**Research Assistant**
	Leibniz Institute for Neurobiology, Magdeburg, Germany
05/2008 – 10/2008	**Bachelors thesis**
	All India institute of Medical sciences, New Delhi, India
	Supervisor: Prof. N.K. Mehra
	Project: Role of minor histocompatibility antigens in HSCT
	Indian Academy of Science Research Fellowship 2008
07/2005 – 08/2009	**B.Tech. Biotechnology**
	Sardar Vallabh-Bhai Patel University, Meerut, India.
	State University scholarship (2006 - 09), India

Full publication list

Mahalwar, P.[#]**,** Singh, A.P., Fadeev, A., Nüsslein-Volhard, C., Irion, U.[#] (2016 Heterotypic interactions regulate cell shape and density during color pattern formation in zebrafish. *Biology Open*

Singh, A.P., Dinwiddie, A., **Mahalwar, P.**, Schach, U., Linker, C., Irion, U., Nüsslein-Volhard, C. (2016) Pigment cell progenitors in zebrafish remains multipotent through metamorphosis. *Developmental Cell*

Walderich, B., Singh, A. P., **Mahalwar, P.**, Nüsslein-Volhard, C. (2016). Homotypic cell competition regulates proliferation and tiling of zebrafish pigment cells during colour pattern formation. *Nature Communication*

Chopra, D., Schneider, L., Perez, C.M., Malik, A., **Mahalwar, P.**[#] (2015). What do early-career researchers think about open access? e*Life*

Gao, X., Metzger, U., Panza, P., **Mahalwar, P.**, Maischein, H.M., Geiger, H., Levesque, M. P. , Templin, M., Söllner, C. (2015). A Floor Plate Extracellular Protein-Protein Interaction Screen Identifies Draxin as a Secreted Netrin-1 Antagonist. *Cell Reports*

Mahalwar, P., Walderich, B., Singh, A. P. and Nüsslein-Volhard, C. (2014). Local reorganization of xanthophores fine-tunes and colors the striped pattern of zebrafish. *Science*

Kaur, G., Kumar, N., Nandakumar, R., Rapthap, C. C., Sharma, G., Neolia, S., Kumra, H., **Mahalwar, P**., Garg, A., Kumar, S., Kaur, J., Hakim, M., Kumar, L., Mehra, N. K. (2012). Utility of saliva and hair follicles in donor selection for hematopoietic stem cell transplantation and chimerism monitoring. *Chimerism*

Corresponding author

Acknowledgments

I would like to thank Janni for giving me this opportunity as well as great guidance and encouragement throughout my work; she was always available for questions and discussions, and gave me the prefect amount of freedom. Her constant support made this research work possible.

I am very grateful to the members of my thesis advisory committee - Prof. Dr. Alfred Nordheim and Prof. Ralf Peter Janssen, for critical evaluation and valuable advice for my project. I would also like to thank Dr. Sarah Danes, coordinator of our International Max Planck Research School - Molecules to Organism for her constant support during my thesis. Many thanks to all the members of Janni's Lab at the Max Planck Institute for Developmental Biology for creating an enjoyable atmosphere. Special thanks to Ajeet Singh, Patrick Mueller and Uwe Irion, for providing invaluable advice for my projects.

I would like to address my thanks to Swati, Ramender, Fabio, Taylor, Kathrine, Luciano, Jelena and all my other friends in Tübingen for making my stay wonderful and enjoyable during my PhD thesis. There are not enough pages in this thesis to describe the contributions I have received from my parents and grandparents over the years. Learning from their example, they have instilled in me the insatiable drive and determination to accomplish my goals. Thank you for your unconditional support. I am honored to have you as my parents. Thanks to my brother Nitin whose over-achieving nature has always forced me to aim high. Finally, I would like to thank my wife, Sadhna for her continuous support and encouragement through my studies.

Appendix

Publication 4

Singh, A.P., Dinwiddie, A., **Mahalwar, P.**, Schach, U., Linker, C., Irion, U., Nüsslein-Volhard, C. (2016). **Pigment cell progenitors in zebrafish remains multipotent through metamorphosis**. *Developmental Cell*

For this paper, which presents that the NC progenitors remain multipotent and plastic beyond embryogenesis and into metamorphosis, when the adult color pattern begins to develop. I performed the time lapse imaging of clonal pigment cells in xanthophore (*pfe*) and iridophores (*shd*) mutants and showed that dorso-ventrally restricted organization of clones persists in these mutants as well.

Article

Developmental Cell

Pigment Cell Progenitors in Zebrafish Remain Multipotent through Metamorphosis

Graphical Abstract

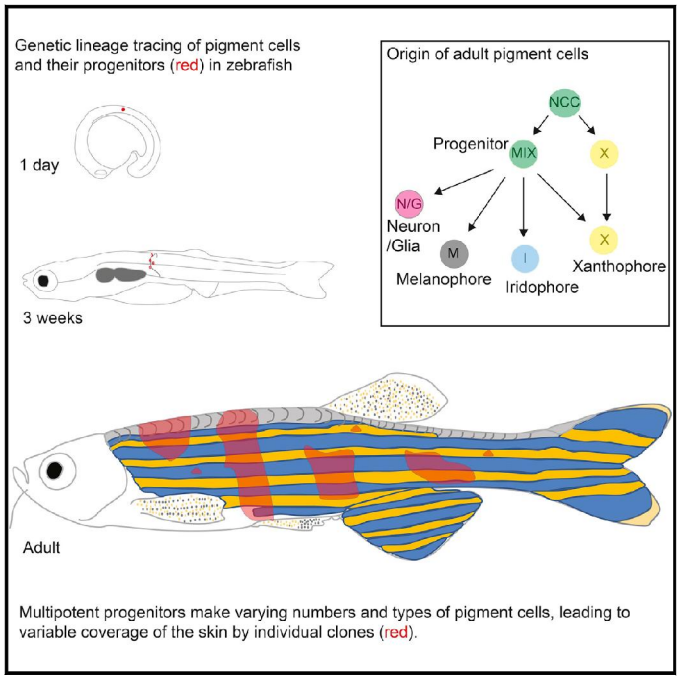

Multipotent progenitors make varying numbers and types of pigment cells, leading to variable coverage of the skin by individual clones (red).

Highlights

- Neural crest-derived progenitors of adult pigment cells remain multipotent
- The postembryonic progenitors are associated with the peripheral nervous system
- The progenitors are plastic and give rise to varying pigment cell numbers and types
- Proliferation decreases when progenitors commit to a specific pigment cell fate

Authors

Ajeet Pratap Singh, April Dinwiddie, Prateek Mahalwar, Ursula Schach, Claudia Linker, Uwe Irion, Christiane Nüsslein-Volhard

Correspondence

christiane.nuesslein-volhard@tuebingen.mpg.de

In Brief

Fish display intricate color patterns generated by specialized pigment cells. Singh et al. show that the pigment cells in zebrafish originate from neural crest-derived progenitors associated with the peripheral nervous system. These progenitors remain multipotent and plastic beyond embryogenesis and into metamorphosis, when the adult color pattern begins to develop.

Singh et al., 2016, Developmental Cell *38*, 316–330
August 8, 2016
http://dx.doi.org/10.1016/j.devcel.2016.06.020

CellPress

Developmental Cell
Article

Pigment Cell Progenitors in Zebrafish Remain Multipotent through Metamorphosis

Ajeet Pratap Singh,[1] April Dinwiddie,[1] Prateek Mahalwar,[1] Ursula Schach,[1] Claudia Linker,[2] Uwe Irion,[1] and Christiane Nüsslein-Volhard[1,*]
[1]Max Planck Institute for Developmental Biology, Spemannstraße 35, Tübingen 72076, Germany
[2]Randall Division of Cell & Molecular Biophysics, King's College, London SE1 1UL, UK
*Correspondence: christiane.nuesslein-volhard@tuebingen.mpg.de
http://dx.doi.org/10.1016/j.devcel.2016.06.020

SUMMARY

The neural crest is a transient, multipotent embryonic cell population in vertebrates giving rise to diverse cell types in adults via intermediate progenitors. The in vivo cell-fate potential and lineage segregation of these postembryonic progenitors is poorly understood, and it is unknown if and when the progenitors become fate restricted. We investigate the fate restriction in the neural crest-derived stem cells and intermediate progenitors in zebrafish, which give rise to three distinct adult pigment cell types: melanophores, iridophores, and xanthophores. By inducing clones in *sox10*-expressing cells, we trace and quantitatively compare the pigment cell progenitors at four stages, from embryogenesis to metamorphosis. At all stages, a large fraction of the progenitors are multipotent. These multipotent progenitors have a high proliferation ability, which diminishes with fate restriction. We suggest that multipotency of the nerve-associated progenitors lasting into metamorphosis may have facilitated the evolution of adult-specific traits in vertebrates.

INTRODUCTION

The neural crest is a transient, embryonic population of multipotent cells that arises from the dorsal portion of the CNS in the vertebrate embryo, and undergoes extensive migration throughout the body to give rise to diverse cell types including chondrocytes, osteocytes, gill pillar cells, neurons, glia, and pigment cells (Baggiolini et al., 2015; Dupin et al., 2007; Green et al., 2015; Mongera et al., 2013; Weston and Thiery, 2015). Some neural crest cells produce progenitors that persist and contribute to the development of adult cell types and tissues. The in vivo potential and rules of lineage segregation of these postembryonic progenitors remain poorly understood (Dupin and Sommer, 2012).

Here we use the adult color pattern of zebrafish (Figures 1A and 1A′) as a system to investigate the cell lineage and fate restrictions in the neural crest and neural crest-derived postembryonic progenitor cells. The adult coloration of zebrafish (*Danio rerio*) has emerged as a model system in which the biology of late-developing, adult-specific traits can be systematically analyzed (Irion et al., 2016; Kelsh et al., 2009; Parichy and Spiewak, 2015; Singh and Nüsslein-Volhard, 2015; Watanabe and Kondo, 2015). The layered organization of three types of neural crest-derived pigment cells—black melanophores, blue/silvery iridophores, and yellow xanthophores—generates the striped adult pattern in zebrafish, and each of these cell types can be definitively identified by its color, shape, and location in the skin (Hirata et al., 2005). The three cell types reach the skin through different routes: postembryonic progenitors associated with the peripheral nervous system (PNS) generate iridophores and melanophores (in addition to neurons and glia), and embryonic xanthophores give rise to most adult xanthophores (Budi et al., 2011; Dooley et al., 2013a; Mahalwar et al., 2014; McMenamin et al., 2014; Singh et al., 2014). The PNS-associated postembryonic progenitors in zebrafish may be comparable with the Schwann cell precursors that generate melanocytes in birds and mammals (Adameyko et al., 2009). Previously, we used Cre/loxP-mediated recombination in *sox10*-expressing, neural crest-derived progenitors in the trunk of zebrafish to induce labeled clones that allow for tracing of pigment cells through development until adulthood (Mongera et al., 2013; Singh et al., 2014). Sox10 is specifically expressed in both premigratory and migrating neural crest cells during development (Dutton et al., 2001). The pigment cell progenitors reach the skin during metamorphosis through three major routes along nerve tracts of the PNS: dorsally, laterally, and ventrally (Budi et al., 2011; Dooley et al., 2013a; Singh et al., 2014). At the onset of metamorphosis, the iridophore progenitors reach the skin along the horizontal myoseptum; they proliferate and spread dorsoventrally in the skin to contribute to most, if not all, of the light stripes along the dorsoventral axis by patterned aggregation (Singh et al., 2014). Melanophore progenitors begin to populate nerve routes to the skin at the onset of metamorphosis, and reach the skin as melanoblasts via the dorsal, horizontal, and ventral myosepta (Dooley et al., 2013a; Singh et al., 2014). Iridophores and xanthophores proliferate in the skin, whereas melanophores expand in size but rarely divide after reaching the skin. However, owing to a lack of a comprehensive lineage-tracing analysis of the pigment cell progenitors, it remains unclear if and when the pigment cell progenitors become fate restricted. Consequently, our understanding of progenitor behavior during color pattern formation and the lineage relationships between pigment cells remains ill defined.

In this study, we induced pigment cell clones at four time points from embryogenesis to early metamorphosis at 21 days

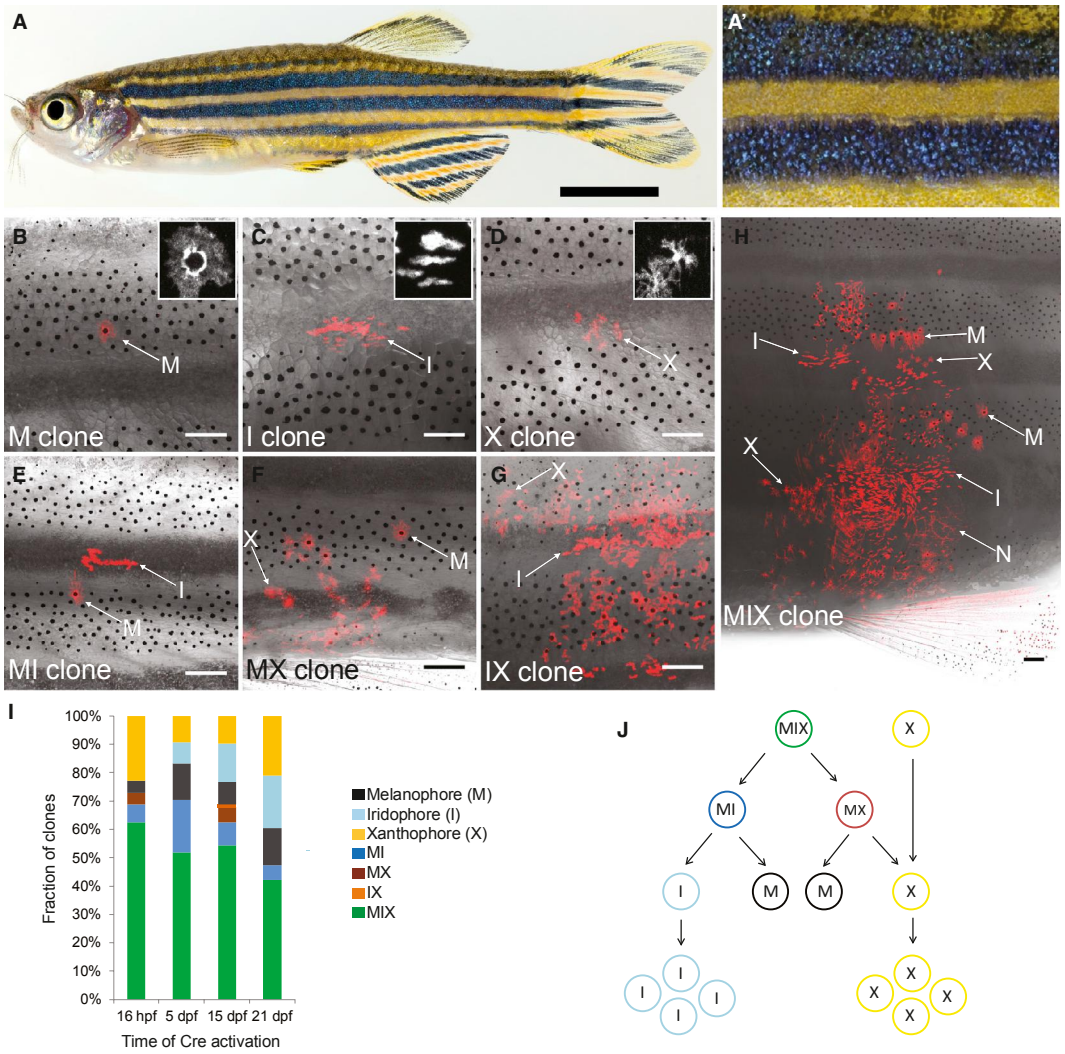

Figure 1. Clonal Association between the Three Pigment Cell Types

(A) Adult zebrafish and (A′) close-up of the striped pattern on zebrafish trunk.

(B–H) Types of pigment cell clones in young adult zebrafish carrying *Tg*(*sox10:ER*^{T2}*-Cre*) and *Tg*(*βactin2:loxP-STOP-loxP-DsRed-express*): (B) a single melanophore (M), (C) iridophores (I), (D) xanthophores (X), (E) melanophore and iridophore (MI), (F) melanophore and xanthophore (MX), (G) iridophore and xanthophore (IX; note that this is the only IX that we obtained), and (H) melanophore, iridophore, and xanthophore (MIX) clones. Representative images in (B)–(G) (DsRed/bright field) are from clones obtained from Cre activation at 15 dpf.

(I) Quantification of the clonal association between pigment cell types obtained by Cre activation at 16 hpf (n = 48 clones from 43 animals, median standard length [SL] at the time of image acquisition = 20.8 ± 1.84 mm); 5 dpf (n = 54 clones from 36 animals, median SL at the time of image acquisition = 24 ± 1.77 mm); 15 dpf (n = 112 clones from 74 animals, median SL at the time of image acquisition = 21 ± 1.77 mm); and 21 dpf (n = 38 clones from 23 animals, median SL at the time of image acquisition = 20 ± 2.07 mm).

(J) Schematic representation of the segregation of pigment cell fates.

N, neuron; M, melanophore; I, iridophore; X, xanthophore.

Insets in (B)–(D) are blow-ups. Scale bars represent 5 mm (A) and 250 μm (B–H). See also Figures S1 and S2 and Tables S1 and S2.

post fertilization (dpf), when the adult color pattern begins to develop. We analyzed clone size and composition in 2- to 3-month-old fish. We focused on the trunk region of zebrafish that includes the pigment cells forming the color pattern in the hypodermis and the scales (Figures 1A and 1A′). Our results show that neural crest-derived progenitors remain multipotent, at least until metamorphosis, and disperse in close association with nerve tracts along the dorsoventral axis. Many clones

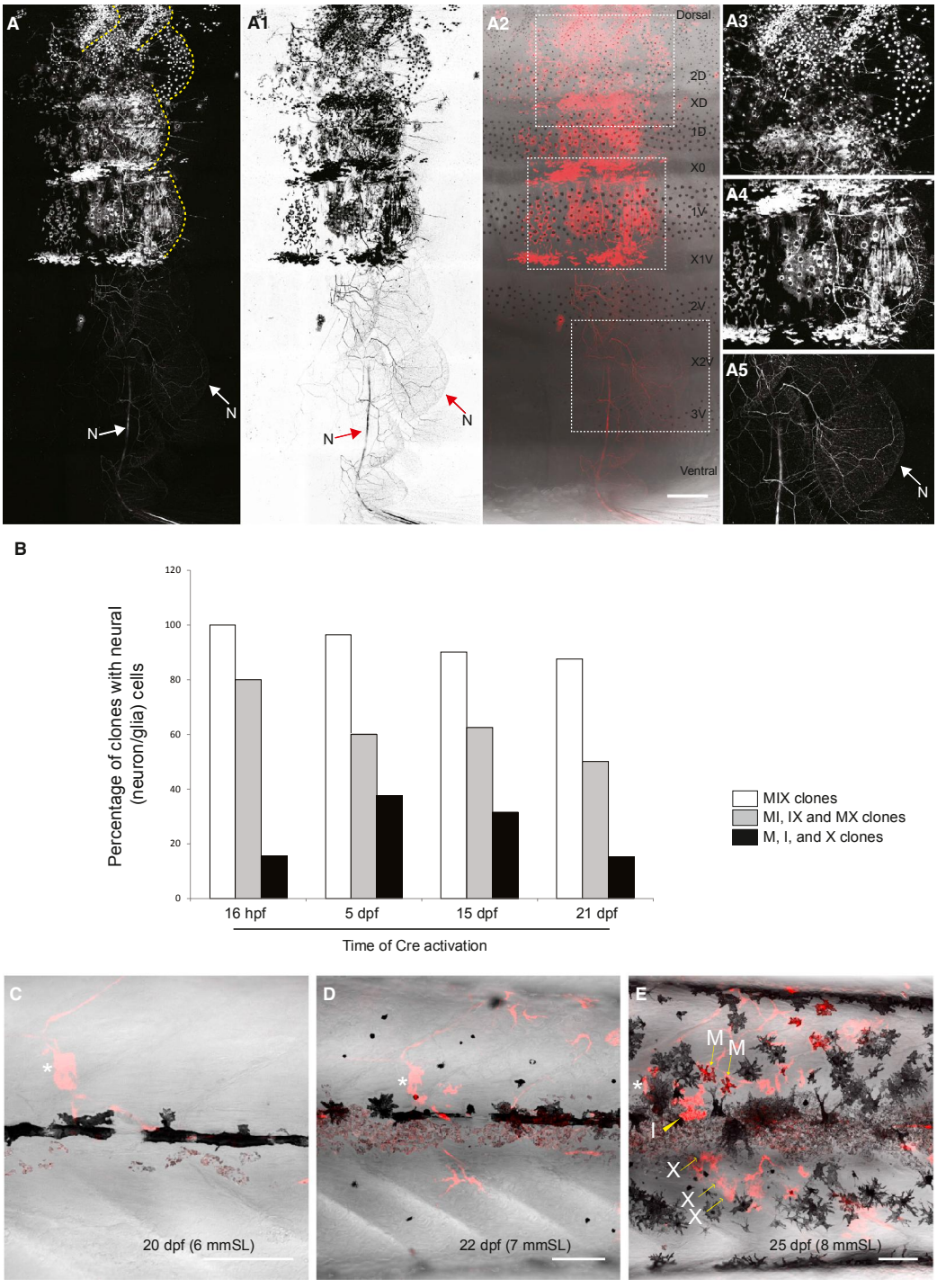

(legend on next page)

contain neurons as well as the three pigment cell types, which generate the color pattern in the skin and the scales, but clones also may be restricted to one or two cell types. Importantly, at all stages the progenitor cells are not stereotypic in terms of the types and numbers of cells that they generate: there is variability in the amount and extent of clonally derived pigment cells along the dorsoventral axis. Individual clones induced in the embryo may give rise to the entire complement of pigment cells of one hemisegment or to only a few pigment cells, suggesting that a variable number of multipotent stem cells (one to a few) are laid down in each hemisegment during embryogenesis. The stem cells produce progenitors that multiply and disperse along the branching PNS so that at later stages a single progenitor will generate a smaller number of cells. Furthermore, multipotent progenitors produce larger clones, suggesting that commitment to a specific pigment cell lineage reduces the ability to proliferate. This effect is most striking for the melanophores: clones with only labeled melanophores tend to be restricted to one or two cells, whereas iridophore-only or xanthophore-only clones are larger, yet still smaller than clones in which all three pigment cell types are labeled. In addition, analysis of clones in mutants of signaling systems that regulate the development of a single pigment cell type suggests that the establishment of multipotent progenitors along the three dorsoventral routes is not affected in the mutants, but that the activity of these genes is required in the committed precursors and differentiating pigment cells.

RESULTS

Progenitors of Adult Pigment Cells Remain Multipotent from Embryogenesis to Early Metamorphosis

To obtain DsRed-labeled clones of neural crest and their progenitor-derived cells in the trunk of zebrafish, we induced Cre/loxP-mediated recombination in fish carrying both the transgenes *Tg*(*sox10*:*ER*^{T2}-*Cre*) (Mongera et al., 2013) and *Tg*(*βactin2*:*loxP-STOP-loxP-DsRed-express*) (Bertrand et al., 2010). Cre was activated in four sets of fish at the following stages of development: embryonic migratory neural crest stage (16 hr post fertilization [hpf]); larval stage (5 dpf); prior to the onset of metamorphosis (15 dpf); and during metamorphosis (21 dpf, upon the appearance of iridophore clusters in the skin). All clones (a total of 252) that contained labeled pigment cells in the trunk of young adult fish (2–3 months post fertilization) were imaged and analyzed. All fish that were positive for pigment cell clones had, on average, fewer than two clones. For example, from Cre activation at 15 dpf, 262 fish were screened, and we obtained 74 fish carrying 112 labeled clones. In a separate experiment, imaging of clones 1 day after Cre activation revealed labeling of one cell per clone (Cre activation at 15 dpf; imaging at 16 dpf; eight clones obtained after screening 101 fish; Figure S1). This indicates that each clone arose from a single recombination event (for the exact sample sizes and methodology, see figure legends, Table S1, and Experimental Procedures). Clones varied in pigment cell composition, and a number of clones contained only one or two pigment cell types (Figures 1B–1G, quantification in Figure 1I; for pigment cell identification, see Figure S2). Significantly, each set contained a large fraction of clones with all three pigment cell types labeled: from 62% of clones obtained from Cre activation at 16 hpf, to 42% of all clones obtained from Cre activation at 21 dpf (Figure 1H, quantification in Figure 1I; Table S2). We term these clones MIX clones for melanophore-, iridophore-, and xanthophore-containing clones. Interestingly, IX clones (containing iridophores and xanthophores) were observed only once (Figure 1G), while clones containing melanophores and iridophores (MI clones, 24 clones), or melanophores and xanthophores (MX clones, eight clones) were more frequent (Figure 1I). This suggests constraints on lineage segregation, and that the multipotent progenitors differentiate into progenitors, which have the potential to generate either melanophores and iridophores, or melanophores and xanthophores (Figure 1J). The IX clones were uncommon, which suggests that progenitors for iridophores and xanthophores may split off at early time points.

Furthermore, several of the pigment cell clones labeled neural cells (Figures 2A–2A5; neurons and/or glia; 75% of clones obtained from Cre activation at 16 hpf, 72% of clones obtained from Cre activation at 5 dpf, 68% of clones obtained from Cre activation at 15 dpf, and 47% of all clones obtained from Cre activation at 21 dpf). A larger fraction of MIX clones labeled neural cells in comparison with single cell clones (histogram in Figure 2B). From these data, we conclude that neural crest-derived progenitors are multipotent, up to at least 3 weeks post fertilization, and can continue to give rise to all three pigment cell types of the body and scales, as well as peripheral nerves and glia.

Xanthophores Have a Dual Cellular Origin

It was recently shown that adult xanthophores in zebrafish originate from existing embryonic/larval xanthophores, which start to proliferate at the onset of metamorphosis (Mahalwar et al., 2014; McMenamin et al., 2014). Indeed, in agreement with these findings, we obtained a number of large, xanthophore-only clones at all stages (Figure 1I). However, adult xanthophores can develop after the ablation of embryonic/larval xanthophores (McMenamin et al., 2014; Walderich et al., 2016), indicating that a second source of adult xanthophores must exist. Our clonal analysis shows that many of the PNS-associated pigment cell progenitors are still multipotent at the onset of metamorphosis, and that the MIX and MX clones include variable numbers of xanthophores (Figure 1I). Repeated imaging of labeled clones during metamorphosis showed that clones that developed neural cells, iridophores, and melanophores during metamorphosis also produced xanthophores (Figures 2C–2E, 3, and S3; n = 11

Figure 2. Shared Multipotent Progenitors for Pigment Cells and Neural Cells

(A–A5) Example of a clone with labeled neurons and pigment cells in the trunk skin, scales, and dorsum. Dashed curves in (A) show scale pigmentation. Dashed squares in (A2) show regions enlarged in (A3)–(A5). Scale bar, 500 μm.

(B) Quantification of the clonal association between pigment cells and neural cells.

(C and D) A clone in the skin of 20-dpf zebrafish with DRG (asterisk) and neurons. Scale bar, 100 μm.

(E) Xanthophores, iridophores, and melanophores appear in this clone at 25 dpf. Asterisk indicates the DRG. Scale bar, 100 μm.

N, neuron; M, melanophore; I, iridophore; X, xanthophore.

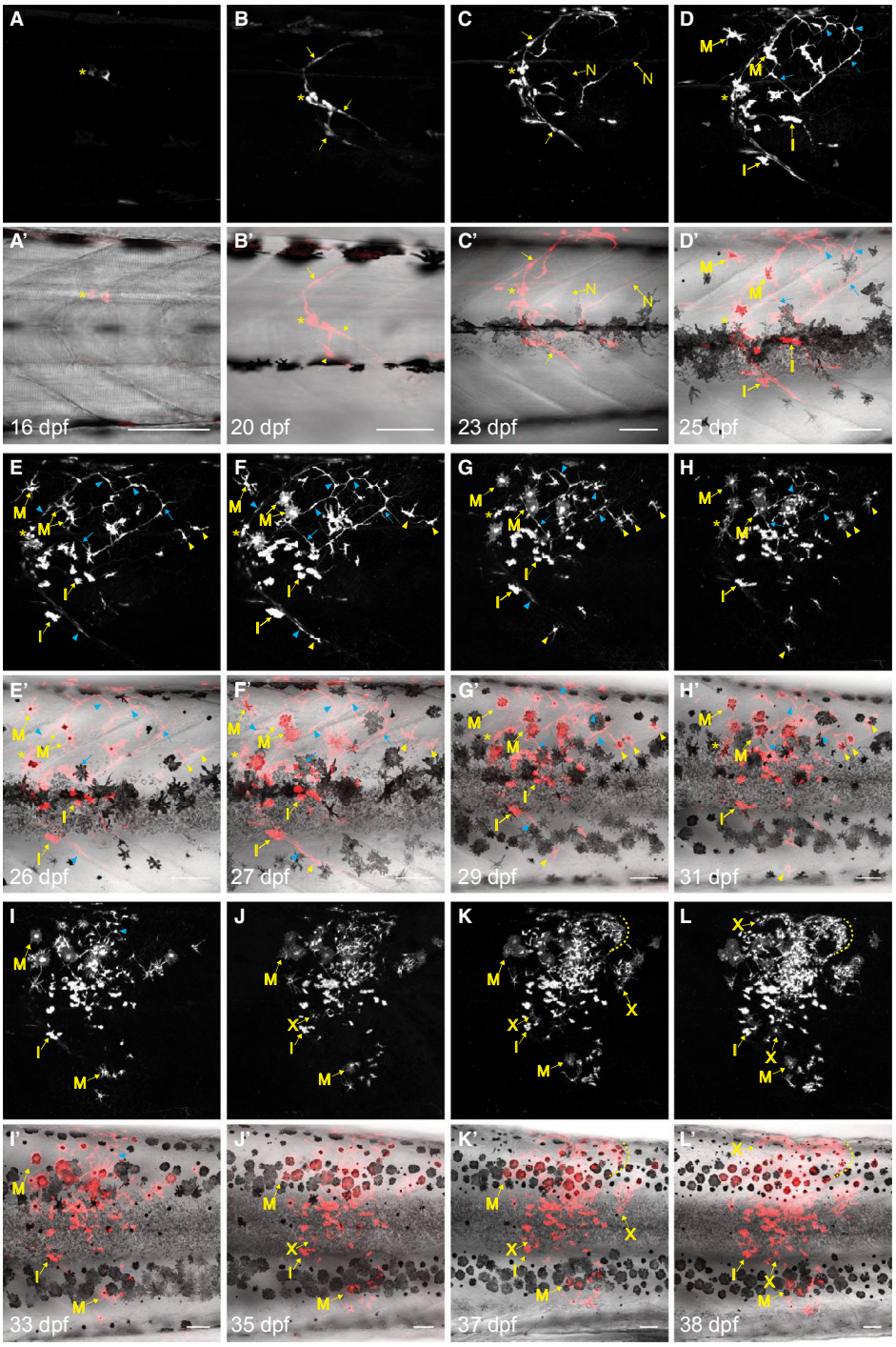

(legend on next page)

clones). Overall, we conclude that xanthophores have a dual cellular origin: initially from existing embryonic/larval xanthophores, and subsequently also from multipotent postembryonic progenitors.

Scale Pigmentation Shares a Lineage with Skin Pigmentation

Our analysis shows that scales, the mesoderm-derived dermal skeletal elements that develop during metamorphosis (Lee et al., 2013; Mongera and Nüsslein-Volhard, 2013), are populated by pigment cells originating from multipotent progenitors; in fact, nearly half of the total clones induced at 15 dpf contributed to scales, in addition to body pigmentation (59 of 112 clones; Figures 2A–2A2, close-up in Figures 2A3 and 2A4). Scale pigmentation is readily distinguished from body pigmentation by the characteristic inverted-C-shaped organization and the distinct shapes of scale pigment cells (dashed lines in Figures S3K–S3O′). Neurons derived from these progenitors innervate the skin of the trunk as well as the scales (Figures 2A–2A2, close-up in Figure 2A5). Imaging clones induced at 4–5 dpf over several days revealed events that lead to the development of the three pigment cell types on the body and scales from shared progenitors (Figures 3 and S3). Figure 3 shows progenitors located at the dorsal root ganglion (DRG) that will give rise to neurons, iridophores, and melanophores over the next several days (Figures 3A–3D′). At first, many undifferentiated cells appear along the newly developing neuronal arbors (yellow arrows in Figures 3C and 3C′ indicate thin neuronal arbors, and corresponding blue arrows in Figures 3D and 3D′ indicate cells that appear along these nerve branches). In a few cases, we were able to follow undifferentiated cells as they differentiated into pigment cells (yellow arrowheads in Figures 3E–3H′). Xanthophores and melanophores of the scales appear in this clone over the next few days (Figures 3I–3L′, dashed curves indicate newly formed scales and their pigment cells). A detailed development of scale pigmentation is presented in Figure S3, and shows the appearance of cells in close association with peripheral nerves. These cells expand in number and subsequently differentiate into melanophores, xanthophores, and iridophores of the scales. Therefore, scale and body pigment cells originate from common multipotent progenitors.

Pigment Cell Clones Are Distributed along the Dorsoventral Body Axis

Although a large fraction of pigment cell progenitors remain multipotent (Figure 1I), we observed variability of individual clones in terms of their span along the dorsoventral axis, and in terms of their cell types and cell numbers (Figures 4A–4D). Figure 4 shows the span of clones in young adult fish that were obtained from Cre activation at 15 dpf. Quantification revealed variability in the extent to which individual clones contributed to pigment cells along the dorsoventral axis: the first class of clones included the pigment cells of the dorsum and dorsal body stripes (Figure 4A), a second class primarily spanned laterally without reaching either the dorsal- or ventral-most regions of the body (Figure 4B), and a third class primarily covered ventral regions (Figure 4C, quantification in Figure 4D; n = 112 clones). Interestingly, the clones that were fate restricted to one or two pigment cell types predominantly belonged to the second class, and spanned a region along the first light stripe. Such clones, mainly of iridophores and melanophores, are presumably derived from committed precursors directly migrating through the horizontal myoseptum. By comparison, MIX clones, in which all three pigment cell types are labeled, spanned a larger area along the dorsoventral axis. This suggests that the ability of progenitors to proliferate is reduced when they become fate restricted (quantification in Figure 4D).

To refine our analysis of progenitor contribution along the dorsoventral axis, we specifically focused on melanophores, which can be easily recognized and quantified due to their distinct black pigment. In adult zebrafish, there are four to five dark stripes and four light stripes that can be identified based on their location with respect to anatomical landmarks in the body (text in Figures 4A–4C refers to standard zebrafish stripe nomenclature [Frohnhöfer et al., 2013]). We counted the number of labeled melanophores that develop in each clone in the dark stripes 1D, 1V, and 2V. Stripes 1D and 1V are the first dark stripes that appear at the dorsal and ventral side of the first light stripe, X0; stripe 2V is subsequently added ventrally. Stripes 2D and 3V were not included in this analysis as these stripes are present only in the anterior part of the trunk. Moreover, stripe 2D is masked by the melanophores of the dorsum, making it difficult to unambiguously count the number of labeled melanophores. The analysis revealed a distribution of melanophores consistent with clone span, and this suggested that there are dorsoventrally restricted multipotent progenitors. Dorsally prominent MIX clones contributed primarily to the melanophores of the dorsal stripes, whereas ventrally prominent MIX clones contributed primarily to the melanophores of the ventral stripes (quantification in Figure 4E; blue, stripe 1D; brown, stripe 1V; green, stripe 2V).

Pigment Cell Progenitors Do Not Display Stereotypic Cell-Fate Restrictions

To obtain an overview of progenitor behavior in transition from embryogenesis to metamorphosis, we performed a similar quantitative analysis of clone span and melanophore count from clones obtained by Cre activation at 16 hpf, 5 dpf, and 21 dpf (Figure 5). In clones induced at 16 hpf, a time point when the neural crest cells as such are still present and start to migrate, a large fraction of the MIX clones span the entire dorsoventral axis, and melanophores contribute to most, if not all, dark stripes. Surprisingly, however, there is considerable variability in span and pigment cell number of these clones (Figures 5A and 5A′, quantification in Figures 5D and 5G). This variability continues during the larval and metamorphic stages: clones obtained from Cre activation at 5 and 21 dpf are variable in their span, pigment

Figure 3. Long-Term Imaging of Progenitors that Make Neurons and Three Pigment Cell Types

(A–L′) Repeated imaging of a clone induced at 5 dpf in zebrafish carrying *Tg(sox10:ER^{T2}-Cre)* and *Tg(βactin2:loxP-STOP-loxP-DsRed-express)*. Grayscale in (A)–(L): clone; Red/gray scale in (A′)–(L′): clone/bright field. Asterisks indicate the DRG. Yellow arrows indicate nerve routes, unless indicated otherwise; blue arrows and arrowheads show undifferentiated progenitors; yellow arrowheads in (E)–(H′) show undifferentiated progenitors that make melanophores; dashed curves indicate pigment cells of a scale. Scale bars, 100 μm. See also Figure S3.

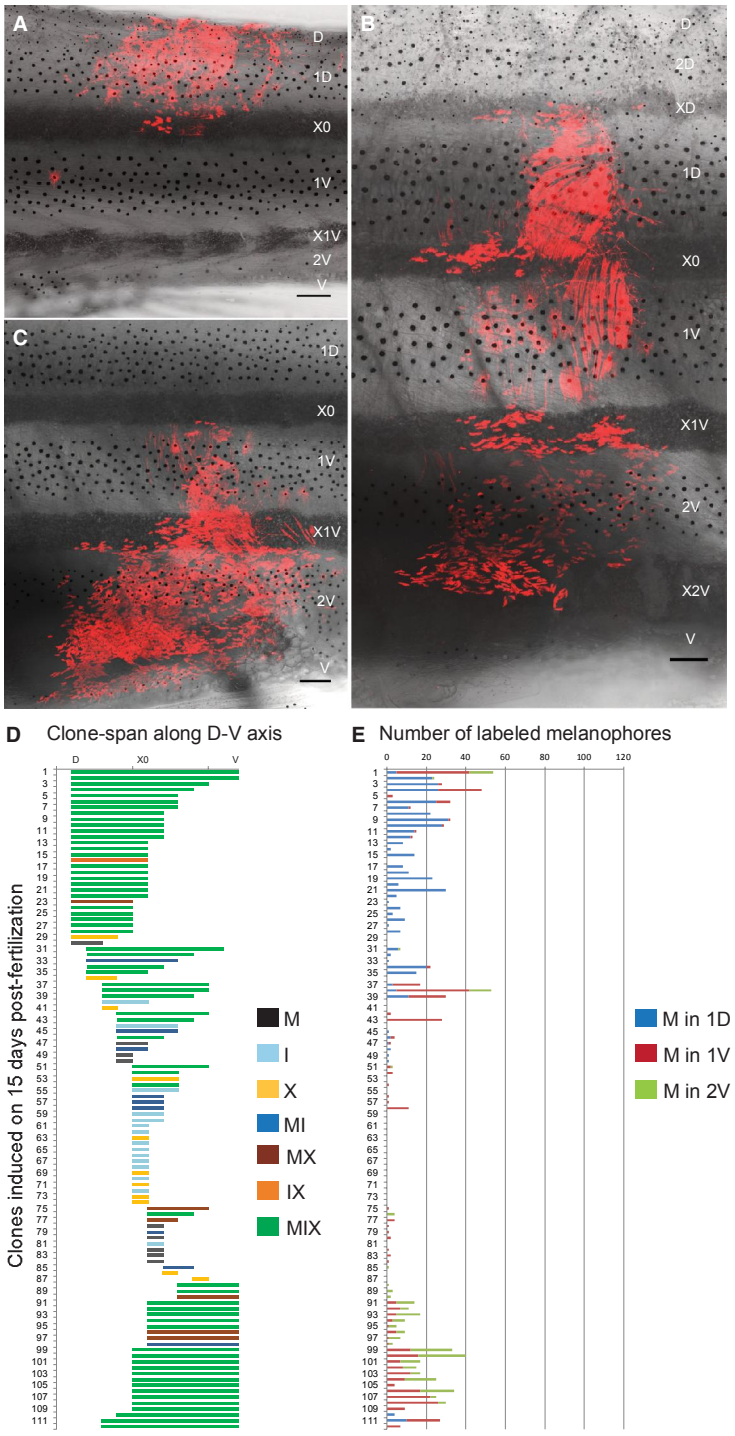

Figure 4. Regional Distribution of Clonally Derived Pigment Cells

(A–D) Clones in young adult animals obtained from Cre activation at 15 dpf (genotype *Tg*(*sox10:ER*^{T2}*-Cre*)/+; *Tg*(*βactin2:loxP-STOP-loxP-DsRed-express*)/+) show variability in clone span along the dorsoventral body axis: the clonally derived pigment cells may predominantly contribute to pigment cells of the (A) dorsal, (B) lateral, or (C) ventral regions. Scale bars represent 250 μm. (D) Quantification of the extent of the clones along the dorsoventral body axis; each line represents the dorsoventral span of a single clone. Color code indicates clone type according to pigment cell composition. MIX clones tend to be larger than clones containing only a single pigment cell type. D, dorsal; V, ventral; X0, first light stripe.

(E) Quantification of the number of labeled melanophores in each clone; each line represents the number of melanophores in an individual clone. Color code indicates the dark stripe: blue, 1D; brown, 1V; green, 2V.

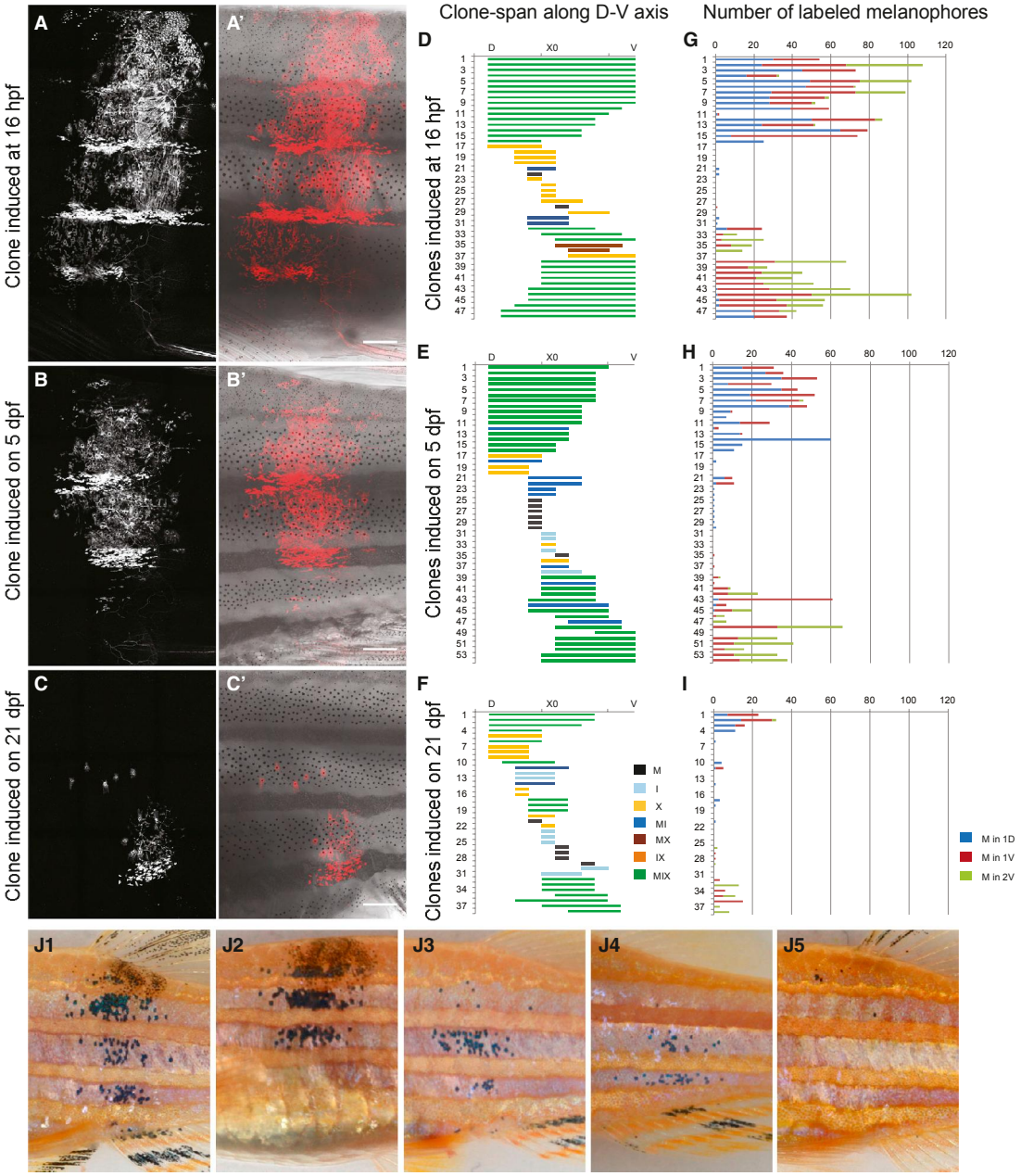

Figure 5. Neural Crest-Derived Progenitors are Multipotent but Do Not Have Stereotypic Outcome

(A–F) Clones in young adult animals obtained from Cre activation at (A, A′, D, G) 16 hpf, (B, B′, E, H) 5 dpf, and (C, C′, F, I) 21 dpf (genotype *Tg*(*sox10:ER*^{T2}*-Cre*)/+; *Tg*(*βactin2:loxP-STOP-loxP-DsRed-express*)/+) reveal a progressive reduction in the size and span of the clonally derived pigment cells, albeit several clones remain MIX, suggesting existence of multipotent progenitors at all time points. (D–F) Quantification of the extent of the clones along the dorsoventral body axis; each line represents dorsoventral span of a single clone. Color code shows clone type according to pigment cell composition.

(G–I) Quantification of the number of labeled melanophores in each clone; each line represents the number of melanophores in an individual clone. Color code indicates the dark stripe: blue, 1D; brown, 1V; green, 2V.

(J1–J5) Skin of F_0 adults from embryos injected with *albino* knockout CRISPR.

Scale bars in (A)–(C′) represent 500 μm. See also Figure S4.

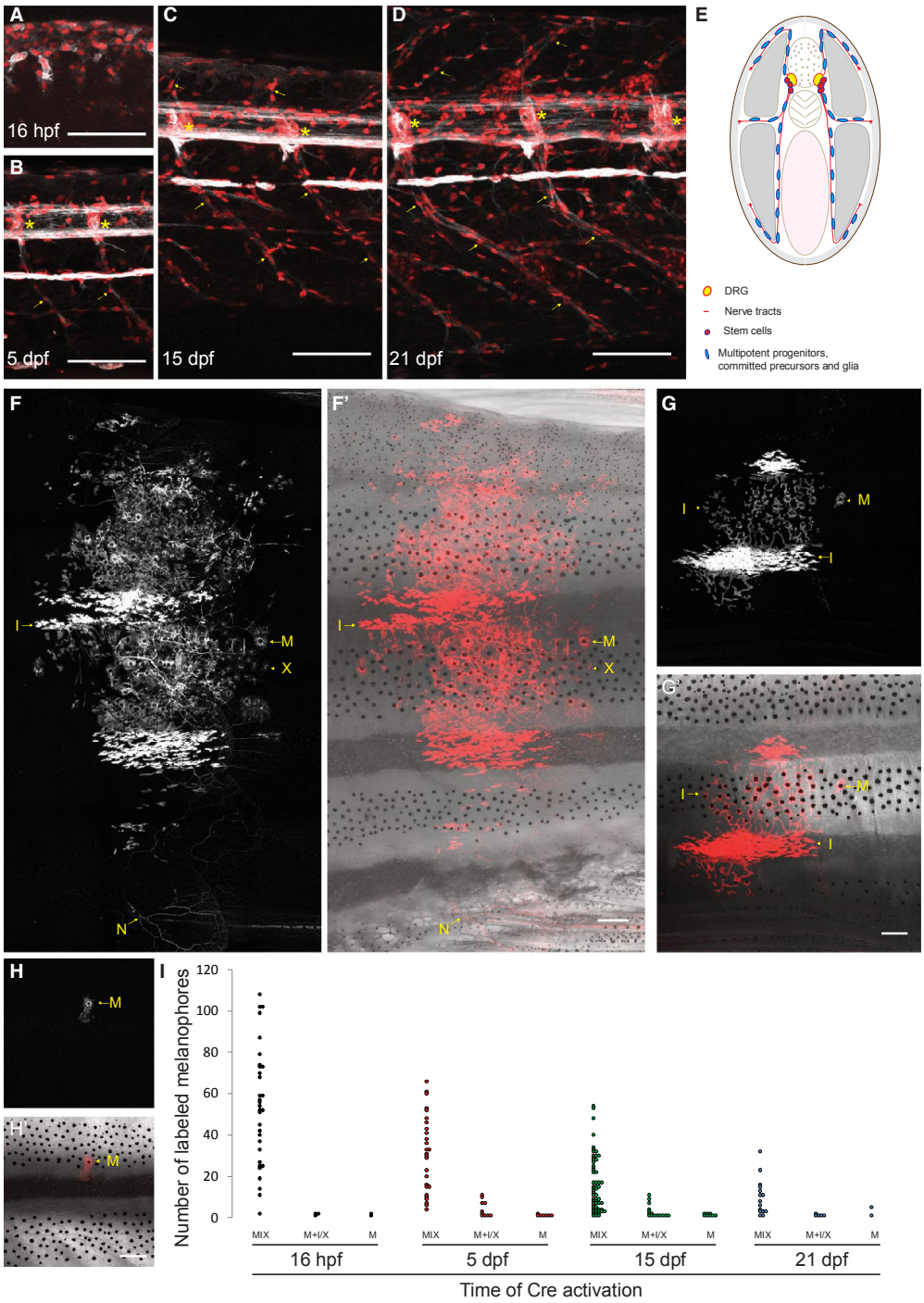

(legend on next page)

cell number, and composition, and at all time points 40%–60% are MIX clones (Figures 5B–5C′, quantification in Figures 5E–5F, bar graph in Figure 1I). This suggests that there is an inherent variability in the number and type of cells that are derived from individual progenitors, and that this variability exists in the embryonic neural crest cells as well as the neural crest-derived progenitors of larval and early metamorphic stages. An additional factor contributing to the variability is the expression of *sox10* promoter in various progenitors, which are at different stages of differentiation. In conclusion, despite some fate-restricted clones, most neural crest-derived cells remain multipotent and do not undergo stereotypic cell-fate restrictions. Quantification of the clone span shows that the fate-restricted clones are smaller than the MIX clones (Figures 5D–5F), demonstrating a link between proliferation ability and cell-fate restriction. At all time points, fate-restricted clones are predominantly laterally situated.

Pigment Cell Progenitors Increase in Number from Embryogenesis to Metamorphosis

Clones obtained from Cre activation at earlier stages can cover much larger areas in the skin and generate more pigment cells compared with clones that are obtained from Cre activation at later larval and metamorphic stages (Figures 5D–5I). The quantification of melanophore numbers in these clones also reveals a clear inverse correlation between the number of labeled cells and the timing of Cre activation; whereas 50% of the clones obtained from Cre activation at 16 hpf produced 30 or more labeled melanophores, this fraction dropped to ~28% at 5 dpf, ~10% at 15 dpf, and ~2.5% at 21 dpf (Figures 4E and 5G–5I). Furthermore, three clones obtained from Cre activation at 16 hpf generated more than 100 melanophores, nearly the full complement of the melanophores per hemisegment in stripes 1D, 1V, and 2V (quantification in Figures 5G and S4). Clones obtained by Cre activation at 16 hpf, a time when *Tg*(*sox10*:*ER*^{T2}-*Cre*) drives Cre expression in the neural crest cells (Mongera et al., 2013), indicate that a variable, very small number of neural crest cells, as few as one, can produce the complete complement of all pigment cells per hemisegment along the dorsoventral axis. Thus, a single neural crest cell can produce more than one pigment cell stem cell. The maximum clone size is the complement of one hemisegment, although pigment cells are not segmentally restricted in the adult skin, and there is lateral mixing of the pigment cells derived from the progenitors in the neighboring segments (Singh et al., 2014; Walderich et al., 2016). Proliferation of pigment cells and the dorsoventral restriction of the clones are regulated by homotypic competition between cells of neighboring segments (Fadeev et al., 2016; Walderich et al., 2016).

To confirm the observed variability, in terms of cell number and clone span, of labeled clones, we used the CRISPR/Cas9 system to knock out the *albino* locus in somatic embryonic cells and analyzed the mosaic F_0 adults; the mutations of the *albino* gene render melanophores unpigmented, and the remaining few wild-type melanophores can be recognized by their distinct black pigment (Dooley et al., 2013b; Irion et al., 2014b). This experiment offers two crucial advantages in testing our conclusions: first, there is a very high knockout efficiency (Irion et al., 2014b) and second, the CRISPR acts very early within the first few hours of embryonic development. Hence, the wild-type, black melanophores of a given cluster in this experiment must originate from rare early embryonic cells that were not affected by the *albino* CRISPR, and are most likely clonally related. Strikingly, we observe variability in the dorsoventral span and melanophore numbers similar to that in the Cre-induced clones (examples in Figures 5J1–5J5). Similar clusters were obtained when blastomeres were transplanted from wild-type donor embryos into *albino* recipients (Walderich et al., 2016).

Next, we corroborated the increase in neural crest-derived cells between 16 hpf and 21 dpf by visualizing the *sox10*-expressing nuclei in *sox10mG* transgenic fish (Richardson et al., 2016; Figures 6A–6D). In this line, expression of nuclear mCherry and membrane-bound GFP is driven by the same *sox10*-promoter as in *Tg*(*sox10*:*ER*^{T2}-*Cre*). During embryogenesis, *sox10*-positive cells are observed in migrating streams (Figure 6A), and by 5 dpf these can be seen at the DRGs and along the ventral nerve tracts; few cells are detected along the dorsal nerve tracts at this stage (Figure 6B). At 15 and 21 dpf, *sox10*-positive cells are obvious along the dorsal branches as well along the DRGs and the ventral nerve tracts (Figures 6C–6D, nerve tracts that exit via the horizontal myoseptum are not visible in this plane of view; schematic in Figure 6E). The increase in *sox10*-positive cells is evident along the entire nerve tracts. We quantified the number of *sox10*-positive nuclei in the DRGs between 5 and 21 dpf, and observed a clear increase in cell numbers (5 dpf: 10.2 ± 1.5 cells, ten DRGs from five animals; 15 dpf: 21 ± 6.4 cells, 12 DRGs from six animals; 21 dpf: 67.4 ± 15.7 cells, eight DRGs from four animals; average ± SD).

Taken together, these data confirm that a substantial number of neural crest-derived progenitors remain uncommitted. We suggest that the numbers and types of cells generated by a multipotent progenitor are not fixed. In addition, intermediate progenitors may represent a heterogeneous pool of *sox10*-positive cells. These data show that although the neural crest progenitors remain multipotent throughout embryonic, larval, and early metamorphic stages, they increase in number, and with time each progenitor gives rise to a smaller number of cells.

Most Melanophores Originate from Undifferentiated Progenitors

The analysis of clone span and melanophore numbers suggests that fate restriction is concomitant with a reduction in the

Figure 6. Progenitors Increase in Number between Embryogenesis and Metamorphosis; Proliferation Ability Diminishes with Fate Restriction

(A–D) *Tg*(*sox10mG*) expression in zebrafish trunk at (A) 16 hpf, (B) 5 dpf, (C) 15 dpf, and (D) 21 dpf. Asterisk indicates DRG; arrows point to *sox10*-positive cells along the nerve tracts. Gray, membrane-tagged GFP; red, nuclear RFP.

(E) Schematic representation of the association between pigment cell progenitors and peripheral neurons.

(F–I) Committed melanoblasts generate a small number of melanophores. Melanophore distribution in (F) MIX, (G) MI, and (H) M clones. (I) Quantification of the number of labeled melanophores; each dot represents the number of labeled melanophores in an individual clone.

Scale bars represent 100 μm in (A)–(D) and 250 μm in (F)–(H). See also Figures S5 and S6.

progenitor's ability to proliferate: MIX clones tend to be larger than the fate-restricted clones (Figures 5D–5I). To understand the quantitative differences in the potential of multipotent progenitors and committed precursors, we counted the melanophores produced in clones that generated all three pigment cell types (MIX clones), clones that generated melanophores and one additional pigment cell type (MI or MX clones), and the clones in which only melanophores were produced (M clones) (examples from Cre activation at 5 dpf in Figures 6F–6H; and at 16 hpf, 15 dpf, and 21 dpf in Figure S5). Melanophore quantification was done for the clones obtained from Cre activation at all four stages (Figure 6I). Progenitors that give rise to the MIX clones generate a large number of melanophores, whereas progenitors that give rise to the clones belonging to the other two categories (MI/MX clones or M clones) make only a small number of melanophores (Figure 6I). The clones containing only melanophores make the fewest melanophores (rarely more than two cells). This indicates that committed melanophore precursors rarely undergo cell divisions before terminal differentiation into mature melanophores.

Committed xanthophores and iridophores are known to exhibit local proliferation (Mahalwar et al., 2014; Singh et al., 2014). Consistent with this, clones containing only iridophores can extend up to two light stripes and contain many iridophores (Figures S6A1–S6C2). Similarly, the committed xanthophores can generate several xanthophores (Figures S6D–S6H). Interestingly, fate-restricted clones of iridophores frequently spanned the first light stripe, X0, and fate-restricted clones of melanophores were associated with the first two dark stripes, 1D and 1V (Figures 4D and 5D–5F). This may reflect the developmental sequence of events. During metamorphosis, iridophores initially appear along the horizontal myoseptum and organize the first light stripe. Similarly, melanophores that appear via the horizontal myoseptum during early metamorphosis are incorporated in the first two dark stripes.

The dorsoventrally restricted organization of clones persists in mutants that are compromised in a single pigment cell type (Figure 7). We analyzed the clonal organization of pigment cells in *sparse/kita* mutants (Parichy et al., 1999) that lack a subset of melanophores (Figures 7A–7C), in *shady/leukocyte tyrosine kinase* (*ltk*) mutants (Lopes et al., 2008) that lack iridophores (Figures 7D–7F), and in *pfeffer/fms/colony stimulating factor 1receptor a* (*csf1ra*) mutants (Parichy et al., 2000b) that lack xanthophores (Figures 7G–7I). We found MIX clones in *sparse*, MX clones in *shady*, and MI clones in *pfeffer*, which show a similar distribution along the dorsoventral axis as in wild-type. Furthermore, developmental profiling of clones in *shady* and *pfeffer* mutants shows qualitatively normal behavior of pigment cell progenitors in generating the remaining pigment cell types (Figure S7). This is consistent with the notion that the genes affected in these mutants do not have an influence on the organization of the multipotent progenitors but are required to promote the differentiation of a particular cell type.

DISCUSSION

Our clonal analysis of the adult pigment cell progenitors in zebrafish shows that the majority of neural crest-derived progenitors remain multipotent for several weeks after fertilization. The progenitors generate neurons contributing to the PNS, and all three pigment cell types that make up the adult color pattern on the body and scales. The progenitors may either be plastic or there may be multiple progenitors at different stages of differentiation throughout metamorphosis. This is reflected in lack of stereotypy in clones: clones of varying sizes and shapes are obtained at all four time points studied here.

Cell-Fate Plasticity and Commitment in the Pigment Cell Progenitors

In the context of the larval pigment cells that originate directly from the neural crest, it is known that several of the genes required in a pigment cell-specific manner are initially widely expressed in neural crest cells and are subsequently preferentially restricted to a particular pigment cell type. For example, *mitfa*, a gene that is primarily required in melanophores, shows neural crest-wide expression during embryogenesis (Dooley et al., 2013a; Lister et al., 1999). Similar observations have been made for the progressive restriction of expression of *ltk* and *csf1ra* in iridophores and xanthophores, respectively (Lopes et al., 2008; Parichy et al., 2000b). In fact, some of the pigment cell-specific genes, such as *mitfa* and *csf1ra*, overlap in their expression pattern in neural crest cells (Curran et al., 2010; Parichy et al., 2000b). These observations may offer an explanation for the lack of lineage commitment in neural crest cell-derived progenitors. In principle, the progenitors may express a diverse set of cell-specific factors that promote a split into separate MX and MI lineages (Figure 1J). Commitment to a given pigment cell fate would then depend upon the availability of specific ligands in the immediate environment of the undifferentiated progenitors.

The cell numbers required to generate the adult stripe pattern are not identical along the anterior-posterior body axis; in the anterior region of the trunk there are four to five dark stripes and four light stripes, and only three dark and two light stripes extend to the posterior regions. Similarly, along the dorsoventral axis, pigment cell numbers and composition varies in body, viscera, and scales (Ceinos et al., 2015; Fadeev et al., 2016). Given that the pigment cells share a lineage along the dorsoventral axis, it might be advantageous to have progenitors that are not fate restricted: this will allow an efficient local regulation of specific cell fates during development and regeneration. The progenitors may become fate restricted depending upon the environmental cues. The environment, in turn, might be defined by the ligands for pigment cell-specific signaling systems such as Kita for melanophores, Ltk and Ednrb for iridophores, and Csf1ra for xanthophores (Dooley et al., 2013a; Fadeev et al., 2016; Frohnhöfer et al., 2013; Lopes et al., 2008; Parichy et al., 1999, 2000a, 2000b). Consistent with a role for the tissue environment, other genes have been identified that affect pigment cell fate non-cell autonomously, and in a body region-specific manner (Ceinos et al., 2015; Krauss et al., 2014a; Lang et al., 2009). Expression of the ligands may lead to a specific pigment cell fate by interactions between specific ligand-receptor systems, although it is also possible that there are other mechanisms that prime the progenitors toward specific cell fates. During metamorphosis, the three pigment cell types depend upon one another for differentiation, migration, proliferation, and survival, and in

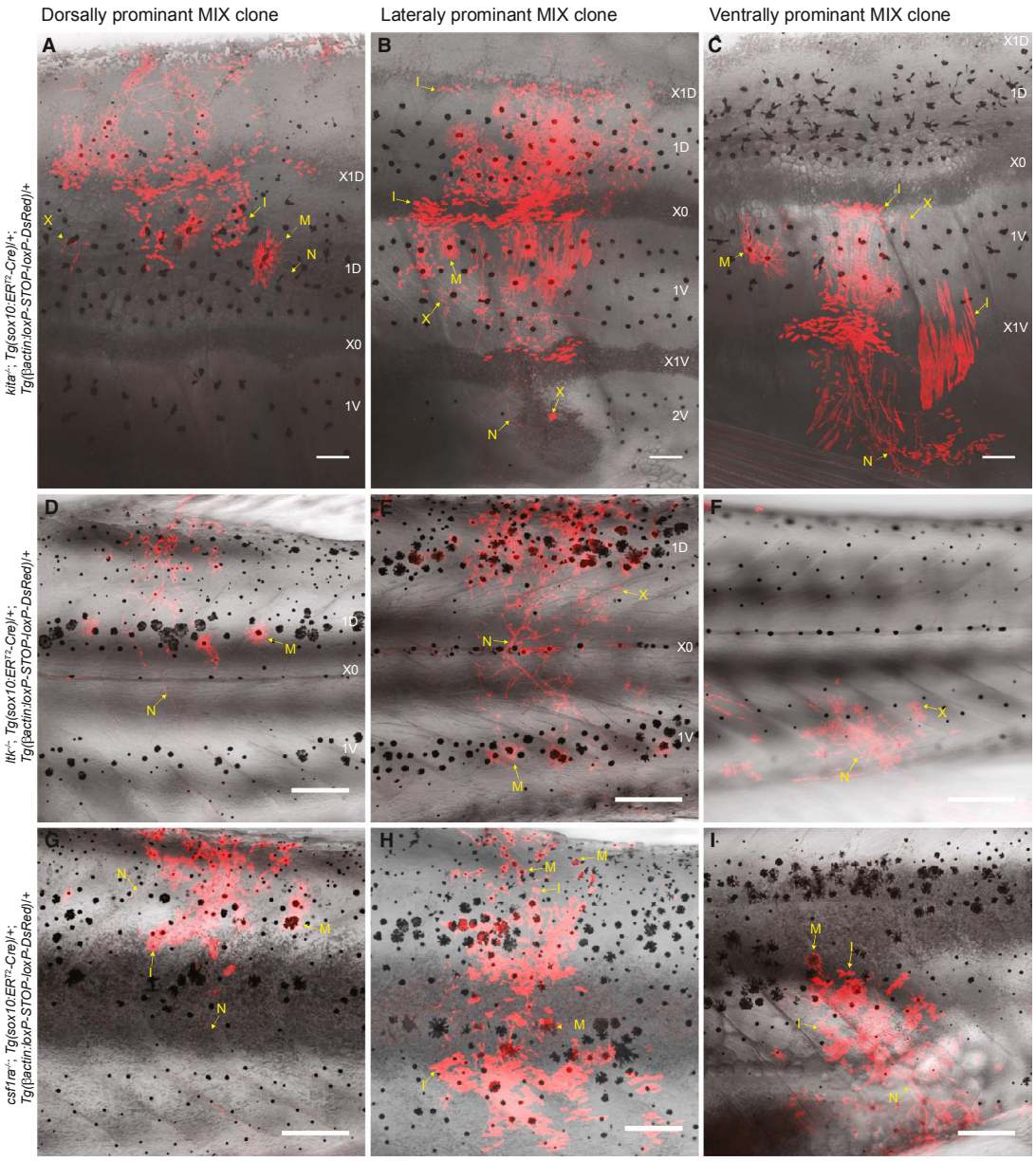

Figure 7. Dorsoventral Organization of Clones in Pigmentation Mutants

(A–I) Clones in the background of (A–C) *sparse/kita* lacking a subset of melanophores (n = 18 clones), (D–F) *shady/ltk* lacking iridophores (n = 20 clones), and (G–I) *pfeffer/csf1ra* lacking xanthophores (n = 20 clones). Scale bars, 250 μm. See also Figure S7.

the absence of any two given pigment cell types, the remaining third cell type tends to cover the entire skin (Fadeev et al., 2015; Frohnhöfer et al., 2013; Irion et al., 2014a). Thus, cross-communication between pigment cells, their precursors, and the environment are important in determining the pigment cell fate.

Multipotent Progenitors as Stem Cells for Postembryonic Neurons and Pigment Cells

Following work in birds and mammals (Adameyko et al., 2009), several studies highlighted a close association between neuronal arbors and pigment cell progenitors, and suggested that they play an important role in pigment cell development

(Budi et al., 2011; Dooley et al., 2013a; Singh et al., 2014). At the level of the progenitors, restriction to a given cell fate may occur as the progenitors move toward the skin along the peripheral nerves. The progenitors associated with the DRG remain multipotent and are the adult stem cells that give rise to pigment cells and neurons during metamorphosis. Neurons are continuously added to the fish DRG: the larval DRG contains five to six neurons at 5 dpf, and this number increases many fold by 22 dpf (McGraw et al., 2012). The new neurons are added by proliferating, non-neuronal, *sox10*-positive cells that reside within the DRG (McGraw et al., 2012). We show that the DRG-associated cells generate neurons as well as pigment cells beyond the larval stages, indicating that these cells remain multipotent. It has been observed that the DRG-associated cells regenerate new melanophores upon depletion of existing melanophores (Dooley et al., 2013a). This indicates that some, if not all, *sox10*-positive multipotent progenitors at the DRG behave like stem cells. Consistent with this, pigment cells regenerate after several rounds of targeted ablation, or after pigment cell death due to genetic mutations as in *tyrp1A* (Krauss et al., 2014b; O'Reilly-Pol and Johnson, 2009). Between embryogenesis to early metamorphic stages, the multipotent progenitors proliferate and increase their pool size. The increase in the number of progenitors leads to a progressive reduction in the size of clones that nevertheless generate all three pigment cell types.

It was recently suggested that the emergence of peripheral nerve-associated multipotent progenitors allowed vertebrates to afford faster growth rate and bigger bodies: the nerves serve as a niche for the progenitors and facilitate their long-distance transport throughout the body (Dyachuk et al., 2014; Ivashkin et al., 2014). Taken together, our data indicate a general role of peripheral nerves in the development and transport of multipotent progenitors. Our clonal analysis and long-term imaging provide the in vivo dynamics of progenitor behavior and suggest that the progenitors for adult pigment cells reside in several locations in proximity to nerve arbors along the dorsoventral axis (schematic in Figure 6E). Consistent with this, we observe three classes of MIX clones that are anatomically associated with the three major nerve routes along the dorsal, horizontal, and ventral myosepta. The neuronal arbors might act as a niche as well as supply routes for pigment cell precursors to different locations in the skin along the dorsoventral axis. It is known that melanoblasts populate the spinal nerves during metamorphosis and travel along these nerves to reach the skin (Budi et al., 2011; Dooley et al., 2013a). It is possible that as the progenitors migrate along the spinal nerves, they become partially fate restricted depending upon the route of exit to the skin, as has been observed for the neural crest cells: in the embryo, neural crest cells that migrate along the dorsolateral route generate larval xanthophores and melanophores, whereas cells migrating along the medial route generate iridophores, melanophores, neurons, and glia (Kelsh et al., 2009). It is noteworthy that the stripe iridophores are primarily produced by progenitors that exit via the horizontal myoseptum, whereas most melanophores are produced by progenitors that use dorsal and ventral routes to reach the skin. Also, MX clones are primarily associated with the ventral routes (Figures 4D, 5D, and S5A2).

In summary, we describe the cell-fate potential of neural crest-derived progenitors between larval stages and early metamorphosis, and identify key features of the pigment cell progenitors during color pattern formation in zebrafish. Our data imply multipotency of nerve-associated progenitors, a feature that may have facilitated rapid divergence of color patterns during the evolution of *Danio* species.

EXPERIMENTAL PROCEDURES

Zebrafish Lines

Wild-type (WT, Tü strain from the Tübingen zebrafish stock center), *Tg(sox10:ER^{T2}-Cre)* (Mongera et al., 2013), *Tg(βactin2:loxP-STOP-loxP-DsRed-express)* (Bertrand et al., 2010), *Tg(sox10:H2BmCherry-2A-GPIGFP)*, abbreviated as *Tg(sox10mG)* (Richardson et al., 2016), *sparse* (Kelsh et al., 1996), *shady* (Lopes et al., 2008), and *pfeffer* (Maderspacher and Nüsslein-Volhard, 2003). All animal experiments were performed in accordance with the rules of the State of Baden-Württemberg, Germany, and approved by the Regierungspräsidium Tübingen (Aktenzeichen: 35/9185.46-5 and 35/9185.82-7).

Cre Induction

Zebrafish of appropriate stage (16 hpf, 5 dpf, 15 dpf, and 21 dpf), carrying a single copy of *Tg(sox10:ER^{T2}-Cre)* and *Tg(βactin2:loxP-STOP-loxP-DsRed-express)*, were treated with 5 μM 4-hydroxytamoxifen (4-OHT; Sigma, H7904) for 1–2 hr at 28°C. Cre activation was carried out for 3 hr for animals on 21 dpf. 5 mM stock solution of 4-OHT was prepared by dissolving it in absolute ethanol, and stored at −20°C. For 4-OHT treatment, batches of ~40 larvae were transferred to plastic Petri dishes (Greiner Bio-one) containing 40 ml of embryonic medium and 4-OHT was added to a final concentration of 5 μM. For Cre activation at 16 hpf, embryos were dechorionated in Pronase prior to 4-OHT treatment. Subsequently, fish were washed three times in E2 and transferred to fresh medium. Larvae and young adult fish (2–3 months post fertilization) were screened for DsRed-labeled clones under a Zeiss LSM 5Live confocal microscope equipped with a Plan-Apochromat 10× objective (0.45 NA; air; 2 mm working distance).

Imaging

Confocal scans were acquired using a Zeiss LSM 780 NLO microscope equipped with 488-Argon laser and 561-diode laser, C-Apochromat 10× objective (0.45 NA; water immersion; 1.8 mm working distance), and LD LCI Plan-apochromat 25× objective (0.8 NA; water, glycerol, oil immersion; 0.57 mm working distance). For the repeated imaging of zebrafish, fish at appropriate developmental stage were anesthetized by adding 30 μl of 0.4% Tricaine (MS-222, Sigma) per 1 ml of embryonic medium 2. Anesthetized animals that were in early stages of metamorphosis (~6.5 mm standard length) were mounted in 0.5% low-melting agarose (NuSieve GTG Agarose, catalog number 50080, Lonza) dissolved in Tricaine-containing embryonic medium on 35 mm glass bottom dishes (MatTek Cultureware). Older animals were mounted in a minimum amount of Tricaine-containing embryonic medium such that animals do not desiccate and yet remain still. Older animals do not survive well if mounted in low-melting agarose, possibly due to blockade of the gills. On the other hand, younger individuals tend to desiccate quickly and hence it is important to mount these in low concentrations of low-melting agarose. After imaging, animals were transferred to fresh fish water or embryonic medium, and their breathing was facilitated by gently flowing water across the operculum with a small plastic pipette. On average, it takes 15–20 min per animal from anesthetization to recovery after imaging. Recovered fish were transferred to and raised in mouse cages (1–1.5 l of running fish water) with each mouse cage housing a single fish.

Generation of Melanophore Mosaics by *Albino* Knockout

Albino mutant F_0 mosaics were generated as described by Irion et al. (2014b). Adult zebrafish were anesthetized with Tricaine and treated with epinephrine hydrochloride (E4642, Sigma) prior to photograph acquisition using Canon 5D Mark II.

SUPPLEMENTAL INFORMATION

Supplemental Information includes Supplemental Experimental Procedures, seven figures and two tables and can be found with this article online at http://dx.doi.org/10.1016/j.devcel.2016.06.020.

AUTHOR CONTRIBUTIONS

Conceptualization, A.P.S. and C.N.-V.; A.P.S. performed experiments; A.D. was responsible for additional clones induced at 16 hpf; P.M. collected *shady* and *pfeffer* mutant data; U.S. helped with crosses and genotyping; C.L. was responsible for *Tg*(*sox10mG*) line and U.I. for *albino* knockouts; Analysis, A.P.S. and C.N-V.; Writing, A.P.S. and C.N-V., with input from A.D. and U.I.

ACKNOWLEDGMENTS

We thank Hans-Georg Frohnhöfer, Anastasia Eskova, Andrey Fadeev, and Darren Gilmour for comments on the manuscript. We thank Heike Heth, Brigitte Walderich, Horst Geiger, Silke Geiger-Rudolph and the Tübingen zebrafish facility, Christian Liebig, Aurora Panzera, and the light microscopy facility for support. This work was supported by funding to C.N.-V. from the Max Planck Society.

Received: March 7, 2016
Revised: May 24, 2016
Accepted: June 15, 2016
Published: July 21, 2016

REFERENCES

Adameyko, I., Lallemend, F., Aquino, J.B., Pereira, J.A., Topilko, P., Muller, T., Fritz, N., Beljajeva, A., Mochii, M., Liste, I., et al. (2009). Schwann cell precursors from nerve innervation are a cellular origin of melanocytes in skin. Cell *139*, 366–379.

Baggiolini, A., Varum, S., Mateos, J.M., Bettosini, D., John, N., Bonalli, M., Ziegler, U., Dimou, L., Clevers, H., Furrer, R., et al. (2015). Premigratory and migratory neural crest cells are multipotent in vivo. Cell Stem Cell *16*, 314–322.

Bertrand, J.Y., Chi, N.C., Santoso, B., Teng, S., Stainier, D.Y., and Traver, D. (2010). Haematopoietic stem cells derive directly from aortic endothelium during development. Nature *464*, 108–111.

Budi, E.H., Patterson, L.B., and Parichy, D.M. (2011). Post-embryonic nerve-associated precursors to adult pigment cells: genetic requirements and dynamics of morphogenesis and differentiation. PLoS Genet. *7*, e1002044.

Ceinos, R.M., Guillot, R., Kelsh, R.N., Cerda-Reverter, J.M., and Rotllant, J. (2015). Pigment patterns in adult fish result from superimposition of two largely independent pigmentation mechanisms. Pigment Cell Melanoma Res. *28*, 196–209.

Curran, K., Lister, J.A., Kunkel, G.R., Prendergast, A., Parichy, D.M., and Raible, D.W. (2010). Interplay between Foxd3 and Mitf regulates cell fate plasticity in the zebrafish neural crest. Dev. Biol. *344*, 107–118.

Dooley, C.M., Mongera, A., Walderich, B., and Nüsslein-Volhard, C. (2013a). On the embryonic origin of adult melanophores: the role of ErbB and Kit signalling in establishing melanophore stem cells in zebrafish. Development *140*, 1003–1013.

Dooley, C.M., Schwarz, H., Mueller, K.P., Mongera, A., Konantz, M., Neuhauss, S.C., Nüsslein-Volhard, C., and Geisler, R. (2013b). Slc45a2 and V-ATPase are regulators of melanosomal pH homeostasis in zebrafish, providing a mechanism for human pigment evolution and disease. Pigment Cell Melanoma Res. *26*, 205–217.

Dupin, E., and Sommer, L. (2012). Neural crest progenitors and stem cells: from early development to adulthood. Dev. Biol. *366*, 83–95.

Dupin, E., Calloni, G., Real, C., Gongalves-Trentin, A., and Le Douarin, N.M. (2007). Neural crest progenitors and stem cells. C R Biol. *330*, 521–529.

Dutton, K.A., Pauliny, A., Lopes, S.S., Elworthy, S., Carney, T.J., Rauch, J., Geisler, R., Haffter, P., and Kelsh, R.N. (2001). Zebrafish colourless encodes sox10 and specifies non-ectomesenchymal neural crest fates. Development *128*, 4113–4125.

Dyachuk, V., Furlan, A., Shahidi, M.K., Giovenco, M., Kaukua, N., Konstantinidou, C., Pachnis, V., Memic, F., Marklund, U., Muller, T., et al. (2014). Neurodevelopment. Parasympathetic neurons originate from nerve-associated peripheral glial progenitors. Science *345*, 82–87.

Fadeev, A., Krauss, J., Fröhnhofer, H.G., Irion, U., and Nüsslein-Volhard, C. (2015). Tight Junction Protein 1a regulates pigment cell organisation during zebrafish colour patterning. Elife *4*, e06545.

Fadeev, A., Krauss, J., Singh, A.P., and Nüsslein-Volhard, C. (2016). Zebrafish leukocyte tyrosine kinase controls iridophore establishment, proliferation and survival. Pigment Cell Melanoma Res. *29*, 284–296.

Frohnhöfer, H.G., Krauss, J., Maischein, H.M., and Nüsslein-Volhard, C. (2013). Iridophores and their interactions with other chromatophores are required for stripe formation in zebrafish. Development *140*, 2997–3007.

Green, S.A., Simoes-Costa, M., and Bronner, M.E. (2015). Evolution of vertebrates as viewed from the crest. Nature *520*, 474–482.

Hirata, M., Nakamura, K., and Kondo, S. (2005). Pigment cell distributions in different tissues of the zebrafish, with special reference to the striped pigment pattern. Dev. Dyn. *234*, 293–300.

Irion, U., Frohnhofer, H.G., Krauss, J., Colak Champollion, T., Maischein, H.M., Geiger-Rudolph, S., Weiler, C., and Nüsslein-Volhard, C. (2014a). Gap junctions composed of connexins 41.8 and 39.4 are essential for colour pattern formation in zebrafish. Elife *3*, e05125.

Irion, U., Krauss, J., and Nüsslein-Volhard, C. (2014b). Precise and efficient genome editing in zebrafish using the CRISPR/Cas9 system. Development *141*, 4827–4830.

Irion, U., Singh, A.P., and Nüsslein-Volhard, C. (2016). The developmental genetics of vertebrate colour pattern formation: lessons from zebrafish. Curr. Top. Dev. Biol. *117*, 141–169.

Ivashkin, E., Voronezhskaya, E.E., and Adameyko, I. (2014). A paradigm shift in neurobiology: peripheral nerves deliver cellular material and control development. Zoology (Jena) *117*, 293–294.

Kelsh, R.N., Brand, M., Jiang, Y.J., Heisenberg, C.P., Lin, S., Haffter, P., Odenthal, J., Mullins, M.C., van Eeden, F.J., Furutani-Seiki, M., et al. (1996). Zebrafish pigmentation mutations and the processes of neural crest development. Development *123*, 369–389.

Kelsh, R.N., Harris, M.L., Colanesi, S., and Erickson, C.A. (2009). Stripes and belly-spots—a review of pigment cell morphogenesis in vertebrates. Semin. Cell Dev. Biol. *20*, 90–104.

Krauss, J., Frohnhöfer, H.G., Walderich, B., Weiler, C., Irion, U., and Nüsslein-Volhard, C. (2014a). Endothelin signalling in iridophore development and stripe pattern formation of zebrafish. Biol. Open *3*, 503–509.

Krauss, J., Geiger-Rudolph, S., Koch, I., Nüsslein-Volhard, C., and Irion, U. (2014b). A dominant mutation in tyrp1A leads to melanophore death in zebrafish. Pigment Cell Melanoma Res. *27*, 827–830.

Lang, M.R., Patterson, L.B., Gordon, T.N., Johnson, S.L., and Parichy, D.M. (2009). Basonuclin-2 requirements for zebrafish adult pigment pattern development and female fertility. PLoS Genet. *5*, e1000744.

Lee, R.T., Thiery, J.P., and Carney, T.J. (2013). Dermal fin rays and scales derive from mesoderm, not neural crest. Curr. Biol. *23*, R336–R337.

Lister, J.A., Robertson, C.P., Lepage, T., Johnson, S.L., and Raible, D.W. (1999). Nacre encodes a zebrafish microphthalmia-related protein that regulates neural-crest-derived pigment cell fate. Development *126*, 3757–3767.

Lopes, S.S., Yang, X., Muller, J., Carney, T.J., McAdow, A.R., Rauch, G.J., Jacoby, A.S., Hurst, L.D., Delfino-Machin, M., Haffter, P., et al. (2008). Leukocyte tyrosine kinase functions in pigment cell development. PLoS Genet. *4*, e1000026.

Maderspacher, F., and Nüsslein-Volhard, C. (2003). Formation of the adult pigment pattern in zebrafish requires leopard and obelix dependent cell interactions. Development *130*, 3447–3457.

Mahalwar, P., Walderich, B., Singh, A.P., and Nüsslein-Volhard, C. (2014). Local reorganization of xanthophores fine-tunes and colors the striped pattern of zebrafish. Science *345*, 1362–1364.

McGraw, H.F., Snelson, C.D., Prendergast, A., Suli, A., and Raible, D.W. (2012). Postembryonic neuronal addition in zebrafish dorsal root ganglia is regulated by Notch signaling. Neural Dev. *7*, 23.

McMenamin, S.K., Bain, E.J., McCann, A.E., Patterson, L.B., Eom, D.S., Waller, Z.P., Hamill, J.C., Kuhlman, J.A., Eisen, J.S., and Parichy, D.M.

(2014). Thyroid hormone-dependent adult pigment cell lineage and pattern in zebrafish. Science *345*, 1358–1361.

Mongera, A., and Nüsslein-Volhard, C. (2013). Scales of fish arise from mesoderm. Curr. Biol. *23*, R338–R339.

Mongera, A., Singh, A.P., Levesque, M.P., Chen, Y.Y., Konstantinidis, P., and Nüsslein-Volhard, C. (2013). Genetic lineage labeling in zebrafish uncovers novel neural crest contributions to the head, including gill pillar cells. Development *140*, 916–925.

O'Reilly-Pol, T., and Johnson, S.L. (2009). Melanocyte regeneration reveals mechanisms of adult stem cell regulation. Semin. Cell Dev. Biol. *20*, 117–124.

Parichy, D.M., and Spiewak, J.E. (2015). Origins of adult pigmentation: diversity in pigment stem cell lineages and implications for pattern evolution. Pigment Cell Melanoma Res. *28*, 31–50.

Parichy, D.M., Rawls, J.F., Pratt, S.J., Whitfield, T.T., and Johnson, S.L. (1999). Zebrafish sparse corresponds to an orthologue of c-kit and is required for the morphogenesis of a subpopulation of melanocytes, but is not essential for hematopoiesis or primordial germ cell development. Development *126*, 3425–3436.

Parichy, D.M., Mellgren, E.M., Rawls, J.F., Lopes, S.S., Kelsh, R.N., and Johnson, S.L. (2000a). Mutational analysis of endothelin receptor b1 (rose) during neural crest and pigment pattern development in the zebrafish *Danio rerio*. Dev. Biol. *227*, 294–306.

Parichy, D.M., Ransom, D.G., Paw, B., Zon, L.I., and Johnson, S.L. (2000b). An orthologue of the kit-related gene fms is required for development of neural crest-derived xanthophores and a subpopulation of adult melanocytes in the zebrafish, *Danio rerio*. Development *127*, 3031–3044.

Richardson, J., Gauert, A., Montecinos, L.B., Escudero, L.F., Alhashem, Z., Assar, R., Marti, E., Kabla, A., Härtel, S., and Linker, C. (2016). Leader cells define directionality of trunk, but not cranial, neural crest migration. Cell Rep. *15*, 1–16.

Singh, A.P., and Nüsslein-Volhard, C. (2015). Zebrafish stripes as a model for vertebrate colour pattern formation. Curr. Biol. *25*, R81–R92.

Singh, A.P., Schach, U., and Nüsslein-Volhard, C. (2014). Proliferation, dispersal and patterned aggregation of iridophores in the skin prefigure striped colouration of zebrafish. Nat. Cell Biol. *16*, 607–614.

Walderich, B., Singh, A.P., Mahalwar, P., and Nüsslein-Volhard, C. (2016). Homotypic cell competition regulates proliferation and tiling of zebrafish pigment cells during colour pattern formation. Nat. Commun. *7*, 11462.

Watanabe, M., and Kondo, S. (2015). Is pigment patterning in fish skin determined by the Turing mechanism? Trends Genet. *31*, 88–96.

Weston, J.A., and Thiery, J.P. (2015). Pentimento: neural crest and the origin of mesectoderm. Dev. Biol. *401*, 37–61.